Yip1A structures the mammalian endoplasmic reticulum

A thesis presented by

Kaitlyn M. Dykstra

B.S., State University of New York at Fredonia

to

The Department of Biological Sciences

Carnegie Mellon University

Pittsburgh, Pennsylvania

in partial fulfillment of the requirements for the degree of

Doctor of Philosophy

in the field of

Biological Sciences

September 27, 2012

Thesis Advisor: Dr. Tina H. Lee

ABSTRACT

The mammalian endoplasmic reticulum (ER) is the largest organelle in the cell, extending from the nuclear envelope throughout the cell periphery. The ER houses a wide variety of vital cell processes within a single membrane bound organelle. In order to accommodate these functions and respond to the demands of the cell, the ER is partitioned into dynamically regulated subdomains, each with its own distinct structure. Despite the likely importance of ER structure for its functions, few proteins have been identified as having a direct role in maintaining the structure of the ER and the consequences of alteration of normal ER structure are not well understood.

Here we identify Yip1A, a conserved membrane protein that cycles between the ER and early Golgi, as a likely regulator of ER organization. Yip1A depletion led to restructuring of ER membranes into micrometer-sized, concentrically stacked whorls. These structures are reminiscent of the ER whorls found in certain specialized secretory cell types, where the regulation and functional consequence of ER whorl formation is not understood. We found that membrane stacking and whorl formation after Yip1A depletion coincided with a marked slowing of coat protein (COP) II-mediated protein export from the ER. Furthermore, whorl formation driven by exogenous expression of an ER protein with no role in COPII function also delayed cargo export. Thus, it appears that Yip1A is required to prevent ER whorl formation and that whorl formation can in turn delay protein export from the organelle. Whether this is the function of ER whorls in tissues remains to be seen, however these results make Yip1A a good candidate for playing a role in their regulation.

To obtain insight into how Yip1A regulates ER whorl formation and to determine whether the mechanism might be shared with the yeast homologue Yip1p, we carried out a systematic mutational analysis of all residues in the protein. Two discrete sites (E95 and K146) were crucial for the control of ER whorl formation by Yip1A. Notably, the same residues were previously shown to be important for Yip1p-mediated viability in yeast, indicating a shared mechanism. On the other hand, a third site (E89) also essential for yeast viability was dispensable for Yip1A function in regulating whorl formation. Thus Yip1p/Yip1A may possess at least two distinct essential functions only one of which is required for regulation of ER structure. Of note, the sites required for control of ER whorl formation by Yip1A were dispensable for the binding of Yip1p to its established binding partners Yif1p and Ypt1/31p, whereas the site required for Yip1p to bind the same partners was dispensable for ER structuring by Yip1A. Based on these observations, we speculate that the function of Yip1A in regulating whorl formation is mediated by one or more distinct and yet-to-be identified binding partners.

Collectively, these findings indicate that a dispersed ER network is important for proper COPII-mediated protein export and that Yip1A has a conserved function between yeast and humans in maintaining proper ER network dispersal through prevention of ER whorl formation. These studies set up an important framework for determining the molecular mechanism of Yip1A as an ER structuring protein.

TABLE OF CONTENTS

List of Figures

ACKNOWLEDGMENTS

I first and foremost thank my advisor Dr. Tina Lee. She has been a true mentor and I credit her for much of my success in graduate school. She trained me how to think like a scientist and to always pay close attention to detail. Her guidance kept me focused and inspired me to work hard.

I thank my thesis committee, Dr. Adam Linstedt and Dr. Jon Minden for their supervision and support throughout my thesis. I also want to thank Dr. Meir Aridor for generously agreeing to serve as my outside reader and committee member.

I thank all of the members of the Lee laboratory for being such wonderful lab mates. Simran Saini and Idil Ulengin, thank you for listening to all of my gripes about lab and life and being such smart and strong women. Nick DelRose, my undergraduate, thank you for being a test subject in my mentorship experiments. Jackie Pokusa, thank you for showing me the ropes. And Jeanne Morin-Leisk, thank you for being a constant source of support from rotation to graduation. Our lunchtime conversations kept me sane and in the lab we were always in sync. I consider myself very lucky to have had you all as friends and lab mates.

I thank all of the members and the Linstedt and Puthenveedu labs. Smita, Steve, Som, Debrup, Cas, Tim J., Tim F., Collin, Ritika, Yusong, Rachel, Amanda, Dan, and Shanna, thank you for your helpful comments during lab meetings and for sharing reagents and ideas. Also, thank you to our dishwasher, Mrs. Li, for making our lives so much easier and to all of the members of labs on the second floor of Mellon Institute for creating such a friendly environment.

I thank my family for all of their unwavering support and love. I thank my brother Danny, also in grad school, for being there to commiserate with. And thank you to my mom and dad, Anne and Bill, for their sacrifices and providing me with every opportunity to follow my dreams, but especially for helping me keep things in perspective over the course of my studies.

Finally, I thank my fiancé, Mike, for the six hours of driving he put in back and forth to Pittsburgh every weekend and sitting next to me while I worked at the bench. No one has been more understanding and reassuring throughout this process and I cannot imagine how I would have gotten through it without him.

CHAPTER 1

INTRODUCTION

The defining feature of eukaryotic cells is that they contain intracellular membrane-bound organelles, each of which has its own distinct membrane composition and structural features. The endoplasmic reticulum (ER) in mammalian cells is the largest and arguably the most complex organelle. It houses a plethora of important cellular functions including secretory and membrane protein synthesis and quality control, coat protein (COP) II-mediated secretory protein export, lipid synthesis, calcium homeostasis and drug metabolism and detoxification (Baumann and Walz, 2001). Maintenance of proper ER structure is likely of great importance to the cell, with disruptions in structure being of potentially devastating consequence on the functions of the organelle. Understanding how the ER maintains its characteristic shape and how its structure relates to its function is a fundamental question in cell biology. This thesis explores the molecular mechanisms by which the ER maintains its dispersal throughout the cell periphery through the protein Yip1A and examines the functional consequences of the loss of this dispersal on membrane trafficking through the early secretory pathway.

OVERVIEW OF THE EARLY SECRETORY PATHWAY

The early secretory pathway consists of the ER, the Golgi apparatus and the vesicular carriers that mediate both anterograde and retrograde transport to and from these compartments. Proteins and lipids are synthesized in the ER and are sorted for exit via COPII-coated vesicles (Barlowe, 1998). In yeast, these vesicles fuse directly with the Golgi. However, in mammalian

cells, these vesicles uncoat and undergo homotypic fusion, or fusion with pre-existing membranes to form the ER-Golgi Intermediate Compartment (ERGIC) or Vesiculo-Tubular Clusters (VTCs) (Schweizer et al., 1990). Proteins that have escaped the ER or are continuously cycling are sorted for retrograde trafficking back to the ER via COPI membrane vesicles (Bannykh and Balch, 1997). Multiple small Rab-GTPases and their effectors mediate the spatial and temporal regulation of these different vesicle tethering and fusion events (Zerial and McBride, 2001). Secretory proteins then travel to the Golgi apparatus where they can be further processed and sorted to their final destination of the endosome, lysosome, plasma membrane, or secretion into the extracellular space (Mellman and Warren, 2000). The structure of the ERGIC and Golgi is highly dependent on influx of membrane and proteins from the ER (Ward et al., 2001; Puri and Linstedt, 2003). This emphasizes the impact of maintaining the structural integrity and export functions of the ER in the early secretory pathway.

ENDOPLASMIC RETICULUM STRUCTURE AND FUNCTION

The mammalian endoplasmic reticulum is a membrane network that extends from the outer nuclear envelope, throughout the entire cell periphery. The membranes of the ER are continuous and enclose a singular lumen. In order to accommodate its wide variety of functions within this uninterrupted space, the ER generates subdomains, each with its own distinct structural features. These subdomains were originally classified through electron microscopy (EM) and are well characterized morphologically (Palade, 1975). They include the nuclear envelope and the peripheral ER; the peripheral ER being further subdivided into the rough ER, transitional ER and smooth ER. These subdomains are thought to adopt the structure best suited for their function, with different cell types being more enriched in specific subdomains of the

ER. Though the most energetically favorable form for a phospholipid bilayer is relatively flat and spherical, the ER adopts a complex structure that consists of highly curved tubules, cisternae and fenestrations (Voeltz and Prinz, 2007). The conserved nature of these structures throughout evolution in eukaryotes highlights the importance of maintaining these specific structures for proper function (Voeltz and Prinz, 2007).

Our early understanding of the structure of the ER and its subdomains relied on both EM and time-lapse video microscopy of ER membranes. It is now generally accepted that partitioning of subdomain specific proteins is thought to drive the division of the ER into its subdomains, though the mechanisms that facilitate this sorting are not well understood (Voeltz et al., 2002). Identification of a number of proteins critical for the maintenance of ER subdomains has given tremendous insight into how the organelle maintains its varied structure, however there are still many unknowns regarding the molecular mechanism of how these proteins function.

THE NUCLEAR ENVELOPE

The nuclear envelope (NE) is found in all eukaryotic cells. Its characteristic large, flat and double phospholipid bilayer membrane sheets consist of both the inner (INM) and outer nuclear membrane (ONM). It is continuous with the rest of the peripheral ER. The INM and ONM are separated by the ER lumen (known as the perinuclear space (PNS)) at an even distance of ~50nm (Voeltz and Prinz, 2007).

The primary role of the NE is to house the nuclear genome while allowing the selective exchange of proteins and RNA between the nucleoplasm and cytoplasm through nuclear pore complexes (NPCs) that span both the INM and ONM (Hetzer, 2010). These NPCs are found only in the NE and are excluded from the rest of the ER. Proteins that are distinctive to the INM

are proteins that interact with nuclear lamins, a type of intermediate filament protein in the nucleoplasm that confers stability to nuclear morphology (Schirmer and Gerace, 2005) in addition to playing a major role chromatin function and gene expression (Hetzer, 2010). Proteins of the ONM interact with proteins of the INM to create the PNS, as well as with the actin cytoskeleton, which serves to position the nucleus in the cell (Fridkin et al., 2009). In higher metazoans, the NE breaks down during mitosis and reforms after cell division in a phosphorylation dependent manner (Hetzer, 2010). The reconstruction of the NE is thought to be dependent on the restructuring of the peripheral ER, with ER tubules being recruited to chromatin following mitosis. The rate-limiting step for nuclear assembly and expansion appears to be the transitioning of these membrane tubules to sheets through displacement of the curvature stabilizing proteins DP1 and the reticulons (Anderson and Hetzer, 2008).

There is mounting evidence for a functional relationship between nuclear shape, structure and stiffness and cellular phenotypes seen in diseases, as well as nuclear shape changes seen in specialized cell types. Dissecting how nuclear structure influences the interplay between membrane proteins of the NE, the nuclear lamina and gene expression will be an important next step in studying nuclear membrane biology (Dahl et al., 2008).

THE ROUGH ENDOPLASMIC RETICULUM

The rough endoplasmic reticulum (RER) consists of ER sheets or cisternae. The sheets of the RER are large flattened membranes or sac-like structures, studded with ribosomes. Though ribosomes can be found on ER tubules, most RER proteins segregate to the ER sheets and this partitioning depends on membrane-bound polysomes (Shibata et al., 2010). The RER is typically perinuclear and is continuous with the NE.

The RER is the site of multiple ER functions. It is best known for being the site of protein synthesis. All of the proteins of the ER as well as those destined for secretion or insertion into the plasma membrane, as well as some proteins that reside in the lumen or membrane of other intracellular organelles, are directed to the ER from the cytosol during their translation via a signal sequence. This signal directs the ribosome to the translocon, a protein complex in the ER membrane that allows the import of proteins in the ER membrane and lumen (Johnson and van Waes, 1999), via the cytoplasmic signal recognition particle (SRP) and its ER membrane receptor (Gilmore et al., 1982). The ribosomes with the nascent polypeptide chain are brought to these sites, allowing for co-translation and translocation, creating the distinctive ribosome-studded RER.

The RER and ER generally serve to provide an environment to facilitate proper protein folding. Disulfide bonds that stabilize tertiary and quaternary structure occur almost exclusively in the ER due to it being more oxidizing than the cytoplasm (Rietsch and Beckwith, 1998). Additionally, many secretory proteins are N-glycosylated in the ER, allowing for proper protein folding and activity (Helenius and Aebi, 2001). Chaperone proteins such as BiP, protein disulfide isomerase (PDI), calnexin and calreticulin aid in folding proteins into their native conformations and are also important for protein quality control by retaining unfolded proteins in the ER (Ellgaard et al., 1999). Proteins that are determined to be terminally misfolded undergo ER-associated degradation (ERAD) and are retrotranslocated from the ER and degraded by the proteasome (Fewell et al., 2001).

The mechanism of how flattened ER sheets are formed is still not well understood. The size of the sheets varies, however the distance between the membranes is approximately the same diameter of 50nm. This luminal spacing is thought to be partially mediated by the coiled-

coil protein, Climp-63, with its depletion leading to significant reduction in the width of the lumen (Shibata et al., 2010). Curvature-stabilizing proteins, the reticulons and DP1, are found at the more highly curved sheet edges and are hypothesized to bring the two membranes of the sheet into close apposition to create the cisternae. It is thought that the relative levels of these curvature-stabilizing proteins to lipid determine the ratio of sheets to tubules (Shibata et al., 2010).

THE SMOOTH ENDOPLASMIC RETICULUM

The smooth ER (SER) consists of all ribosome-free regions of the peripheral ER. These include the transitional ER (described in more detail in the next section), as well as regions of the ER that contact other organelle membranes (Shibata et al., 2006). The SER has the most diversity of function. Many different cell types are abundant in SER. Their activities range from a primary detoxification role in liver cells, calcium release and uptake in muscle cells (known as the sarcoplasmic reticulum) and steroid-synthesizing activity in steroid producing cells such as adrenocortical cells (Voeltz et al., 2002). The most prominent structures of SER are the ER tubules that branch throughout the cell periphery. These tubules are highly curved, elongated and cylindrical in structure, providing a high surface area to volume ratio.

The microtubule (MT) cytoskeleton plays an important role in extension of the ER network (Du et al., 2004). There is a high degree of correlation between the MT network and ER tubules. The ER can be seen extending out into the cell periphery along MTs both during ER expansion in live cells and in cell-free reconstitutions of the ER network from microsomes (Terasaki et al., 1986; Dabora and Sheetz, 1988; Allan and Vale, 1991; Waterman-Storer et al., 1995). This extension occurs through a mechanism known as the tip attachment complex (TAC),

in which the ER tubules attach to the growing tip at the MT plus end. This process is dependent on the ER protein STIM1 and the MT plus-end binding protein, EB1 (Grigoriev et al., 2008). Remodeling of the ER network however primarily occurs by ER sliding bi-directionally along MTs, using the microtubule motors dynein and kinesin (Waterman-Storer and Salmon, 1998). This ER sliding occurs preferentially on stable acetylated MTs, while TAC occurs only on dynamic nonacetylated MTs (Friedman et al., 2010).

Although the MT cytoskeleton plays an important role, retraction of the ER after depolymerization of MTs does not occur immediately, which suggested additional mechanisms for maintaining the tubular ER (Terasaki et al., 1986). The reticulon (Rtn) family of proteins are a structurally related family of proteins that have been implicated in shaping and maintaining the tubular ER (Voeltz et al., 2006). In mammals, this family consists of four RTN genes and the six DP1/REEP genes. In yeast, depletion of Yop1p, the only yeast homologue of DP1, in conjunction with depletion of the two yeast RTN proteins, Rtn1p and Rtn2p, results in a loss of peripheral ER tubulation (Voeltz et al., 2006). Additionally, antibody inhibition of Rtn4a prevents network formation *in vitro* (Dreier and Rapoport, 2000; Voeltz et al., 2006). These RTN proteins share a conserved domain that consists of two long hydrophobic segments, proposed to form hairpins in the membrane, deforming the bilayer through displacement of lipids on only the outer leaflet to create curvature (Voeltz et al., 2006). In support of this, purified yeast homologs of Rtn1 and DP1 are sufficient to deform proteoliposomes into tubules (Hu et al., 2008).

The three-way junctions that characterize the polygonal ER network are dynamically created and consumed in the cell periphery through the fusion of a growing ER tubule with an existing one. This fusion is mediated by the Atlastin proteins, part of the dynamin superfamily

of GTPases. Atlastins interact with the Rtn and DP1 proteins of the tubular ER and antibody inhibition experiments show that they are required for ER network formation *in vitro*, similar to what was seen with Rtn4a (Dreier and Rapoport, 2000; Hu et al., 2009). *Drosophila* Atlastin can mediate the tethering and fusion of proteoliposomes *in vitro* in a GTPase dependent manner, demonstrating the fusogenic properties of the protein (Orso et al., 2009). Additionally, siRNA knockdown of Atlastin isoforms in HeLa cells results in a loss of ER branching, suggesting fusion of ER tubules is important for the maintenance of the ER network (Hu et al., 2009; Morin-Leisk et al., 2011).

WHORLED ENDOPLASMIC RETICULUM

One type of specialized ER structure seen often in steroid and peptide hormone producing cells but that is poorly understood is whorled ER (Nickerson and Curtis, 1969). The ER membranes in these cells are tightly stacked in concentric spirals. Most often this is seen with SER membranes, however some ribosome-studded whorls have been observed. Cell types that have been observed with whorled ER include testicular interstitial cells (Carr and Carr, 1962; Christensen and Fawcett, 1966), adrenocortical cells (Nickerson and Curtis, 1969), melanoma cells (Hu, 1971), cells of the anterior pituitary (Dubois and Girod, 1971), and hypothalamic arcuate neurons (King et al., 1974). The functional relevance of whorl formation is not well understood. Interestingly, the formation of whorls seen in gonadotropin-releasing hormone (GnRH)-secreting hypothalamic arcuate neurons seems to be regulated by the estrous cycle. It could be that this tight packing of the membranes may be a means of regulating lipid or protein export in response to physiological cues.

Whorled ER can also be seen as a consequence of drug treatments (Jones and Fawcett, 1966; Hwang et al., 1974; Singer et al., 1988), or the up-regulation of certain ER-membrane anchored proteins such as HMG-CoA reductase (Chin et al., 1982; Koning et al., 1996), microsomal aldehyde dehydrogenase (Yamamoto et al., 1996), cytochrome b_5 (Pedrazzini et al., 2000), and the inositol 1,4,5-triphosphate receptor (Takei et al., 1994). This transformation of the ER is termed organized smooth ER (OSER). The basis of this whorl formation is thought to be through low-affinity protein interactions of these ER-anchored proteins on opposing membranes in *trans* (Snapp et al., 2003), however it is not known whether this is how ER whorls are formed in the hormone producing cells.

THE TRANSITIONAL ENDOPLASMIC RETICULUM

After secretory proteins are properly folded in the RER, they are transported to the Golgi apparatus via membrane vesicles. The sorting of cargo, deformation of the membrane and formation of the vesicles that facilitate anterograde trafficking is mediated by the multi-subunit complex, coat protein II (COPII) (Barlowe et al., 1994). In higher metazoans, these vesicles form in subdomains of the RER that are devoid of ribosomes called the transitional ER (tER) (Palade, 1975), also known as ER exit sites (ERES). In mammalian cells, COPII-coated vesicles bud off from the tER and undergo homotypic fusion to form vesicular-tubular clusters (VTCs) also known as the ER-Golgi intermediate compartment (ERGIC) (Schweizer et al., 1990). ERES are found throughout the entire cell, however over half are clustered near the Golgi, which is juxtanuclear in many cell types (Budnik and Stephens, 2009).

The core components of the COPII coat (Sar1, Sec23/24 and Sec13/31) are peripheral membrane proteins that continuously cycle on and off of the membrane (Hughes and Stephens,

2008). The purified core coat proteins are sufficient to reconstitute vesicle formation *in vitro* on synthetic liposomes (Matsuoka et al., 1998). The cytoplasmic Sar1 GTPase initiates COPII assembly through insertion of an amphipathic helix into the lipid bilayer, deforming the membrane and initiating membrane curvature(Bielli et al., 2005; Lee et al., 2005). It is activated by exchange of GDP for GTP through its ER localized guanine nucleotide exchange factor (GEF), Sec12 (Nakano et al., 1988). The activated Sar1 then recruits the Sec23/24 heterodimer. Sec24 functions to bind cargo in the growing vesicle bud (Aridor et al., 1998), whereas Sec23 acts as a GTPase-activating protein (GAP) for Sar1 (Yoshihisa et al., 1993), coordinating the kinetics of proper cargo selection with GTP hydrolysis (Sato and Nakano, 2004). Recruitment of the outer coat, a heterotetrameric complex of Sec13 and Sec31 follow this. The Sec13/31 complex oligomerizes into a cage around the COPII vesicle, providing a structural scaffold (Fath et al., 2007). Sec31 also contributes to the active site of Sar1, increasing the efficiency of its GTPase activity (Bi et al., 2007). Additional protein components are also being identified in organizing ERES, the most notable being Sec16 (Espenshade et al., 1995), which is thought to be important for preventing premature COPII subunit disassembly (Bevis et al., 2002).

Lipid composition of the tER plays an important, but less well characterized role in COPII vesicle formation. Phosphatidyic acid (PA) is thought to be important for recruiting Sec23/24 after Sar1 activation (Pathre et al., 2003) based on the requirement of phospholipase D (PLD), which generates PA, in ER to Golgi transport. Cholesterol also plays a role in the mobility of cargo proteins in the ER membrane as well as the turnover rate of Sec23 (Runz et al., 2006). There is also evidence that phosphatidylinositol 4-phosphate (PI4P) may be important for COPII assembly, with expression of a PI4P binding domain blocking ER to Golgi transport (Blumental-Perry et al., 2006).

There is very little known about integral membrane factors in the ER that are important for determining and maintaining the tER and ERES. One protein that has been implicated in COPII vesicle biogenesis is Yip1p in yeast (Heidtman et al., 2003) and its mammalian homolog Yip1A (Tang et al., 2001), however the mechanism by which it facilitates vesicle formation is not known. Our studies of the Yip1A protein have revealed that the effects on COPII vesicle formation seen in genetic mutations of Yip1p may be a secondary consequence of a primary defect in maintaining the proper structure of the ER (Dykstra et al., 2010).

THE YIP1A PROTEIN

IDENTIFICATION AND CHARACTERIZATION OF YIP1P IN YEAST

Yip1p was initially discovered through a two-hybrid screen for factors that bind specifically to ER-to-Golgi vesicular transport Rab-GTPases, Ypt1 and Ypt31 (*Ypt interacting protein*) (Lazar et al., 1997; Yang et al., 1998). Yip1p is predicted to be a five-pass integral membrane protein, with the C-terminal half of the protein in the membrane and its N-terminus was shown to face the cytoplasm. It is localized to both ER and Golgi membranes (Yang et al., 1998). It is the founding member of the Yip1 family of proteins, Yip1p paralogues that are related by a common overall domain topology, interaction with Rab proteins and an ability to physically associate with other Yip1 family members (Chen and Collins, 2005). Yip1p was found to be essential for cell growth in yeast and temperature sensitive mutations resulted in a massive accumulation of multilayered ER membranes and protein transport defects in the early stages of the biosynthetic pathway, based on studies of the processing of vacuolar hydrolases in these mutants (Yang et al., 1998).

There have been conflicting studies in yeast concerning the precise step in which Yip1p functions in the early secretory pathway using antibody inhibition experiments. One study found that addition of antibodies against Yip1p or its interacting partner Yif1p prior to formation of COPII vesicles blocked fusion of ER vesicles with the Golgi *in vitro* with minor effects on vesicle budding (Barrowman et al., 2003). However, in another study, addition of anti-Yip1p antibodies also inhibited transport, however this block was found to be specific to COPII-dependent vesicle budding (Heidtman et al., 2003). This was corroborated with observations with a *yip* mutant (*yip1-4*) that blocked COPII vesicle formation both in an *in vitro* budding

assay as well as *in vivo*, without an accumulation of vesicles, a phenotype associated vesicle fusion mutants (Heidtman et al., 2003). There is also evidence from synthetic lethal genetic studies of *yip1* mutants that the interaction of Yip1p with Golgi Rab proteins Ypt1, Ypt31, Ypt32 and Ypt6 are required for its function (Chen et al., 2004), however the exact nature of how the protein is functioning the early secretory pathway is poorly understood.

YIP1A IN MAMMALIAN CELLS

Mammalian cells have two orthologs of Yip1p, Yip1A and Yip1B. Both proteins share a 31% identity to Yip1p and a 61% identity to each other (Tang et al., 2001). Yip1A is ubiquitously expressed whereas Yip1B is found specifically in heart tissue (Tang et al., 2001). Yip1A is localized to ERES, ERGIC and *cis*-Golgi and cycles between the ER and Golgi apparatus (Yoshida et al., 2008; Dykstra et al., 2010). Like the studies of Yip1p in yeast, studies of Yip1A in mammalian cells have also been contradictory. Initial studies of Yip1A also suggested a possible role in COPII vesicle formation. The cytoplasmic domain of Yip1A was shown to bind the Sec23/24 subunit of the COPII vesicle coat and over-expression of the cytoplasmic domain in HeLa cells inhibited ER export and resulted in fragmentation of the Golgi (Tang et al., 2001). However, while other studies of Yip1A in HeLa cells using siRNA knockdown also resulted in Golgi fragmentation into mini-stacks, no effect on anterograde protein transport from the ER was observed using a temperature sensitive VSV-G export assay (Yoshida et al., 2008). Rather they observed an accumulation of β-COP, a component of the COPI coat, on ERGIC membranes (Yoshida et al., 2008).

In yet another set of Yip1A knockdown experiments, HeLa cells lacking Yip1A showed no observable defect in organelle structure, yet displayed a dissociation of Rab6 from

membranes as well as a delay in the transport COPI-independent retrograde transport (Kano et al., 2009). Finally, our studies have implicated a primary role for Yip1A in maintaining proper ER network dispersal (Dykstra et al., 2010). This wide variety of defects that have been observed in Yip1A knockdowns may be a result of off target effects of the siRNAs, insufficient knockdown or perhaps indicative of Yip1A having multiple functions within the cell.

YIP1 INTERACTING PROTEINS

A number of proteins have been identified in both yeast and mammalian cells to interact with Yip1, however the functional relevance of these interactions has not yet been determined. It is possible that the spatial and temporal regulation of Yip1 interactions may contribute to multiple functions of the Yip1 protein. In addition to the Rab-GTPases (Calero et al., 2003) and COPII coat (Tang et al., 2001), Yip1 has been shown to interact with the proteins Yif1 (*Yip1 interacting factor*) (Matern et al., 2000), Yos1 (*Yip1 one suppressor*) (Heidtman et al., 2005), and Yop1/DP1 (*Yip one partner*) (Calero et al., 2001).

YPT/RAB GTPASES

The interaction of Yip1p with Ypt/Rab GTPases is essential for viability in yeast (Yang et al., 1998). Rab proteins are posttranslationally modified with two geranylgeranyl lipid moieties to associate with the membrane. The association of Yip1p with Rabs was shown to be dependent on this modification in yeast (Calero et al., 2003). Yip1p can interact promiscuously with multiple Rab proteins in detergent extracts, but genetic analyses *in vivo* have shown that only interaction with Golgi localized Rabs (Ypt1, Ypt31, Ypt32 and Ypt6) is required for yeast viability (Chen et al., 2004). While Rab6A, the human homologue of yeast Ypt6, has been

implicated in Yip1A function, no interaction either *in vitro* or *in vivo* has been detected between mammalian Yip1A and Rab proteins (Kano et al., 2009).

YIP1-YIF1-YOS1 COMPLEX

Yip1 forms a complex with the proteins Yif1 and Yos1 that cycles between the ER and Golgi (Matern et al., 2000; Heidtman et al., 2005). Yif1p was identified through a yeast two-hybrid screen for Yip1p interacting proteins (Matern et al., 2000). It has a very similar topology to Yip1p, with a cytosolic N-terminus and a transmembrane C-terminus. In yeast, depletion of Yif1p also resulted in a similar phenotype to depletion of Yip1p, with a block of ER-to-Golgi protein transport, an accumulation of ER membranes and additionally an accumulation of vesicles (Matern et al., 2000). Unlike Yip1p, Yif1p is not essential and its interaction of Yif1p with Rabs is also dispensable for yeast viability (Matern et al., 2000). Yos1p is an essential two-pass integral membrane protein that was identified as a multi copy suppressor of the mutant *yip1-4* (E70K) strain (Heidtman et al., 2005). Temperature sensitive mutations in Yos1p also lead to defects in ER-to-Golgi trafficking (Heidtman et al., 2005).

The mammalian Yip1A has also been shown to interact with the mammalian homolog of Yif1p, Yif1A (Jin et al., 2005; Yoshida et al., 2008). The localization of Yif1A to the Golgi is dependent on the proper localization of Yip1A, however Yip1A localization is not dependent on Yif1A (Jin et al., 2005). The expression of Yip1A and Yif1A are also highly dependent on one another. Depletion of Yip1A leads to a concurrent, almost equal reduction in levels of Yif1A, however depletion of Yif1A only has a minimal effect of Yip1A expression levels (Yoshida et al., 2008). The Yos1 interaction with the Yip1A/Yif1A complex has not yet been recapitulated in mammalian cells.

YIP1-YOP1/DP1

The ER localized Yop1p was also identified as a Yip1p interacting protein and a negative regulator of Yip1p (Calero et al., 2001). Overexpression of Yop1p results in cell death, accumulation of internal cell membranes and a block in membrane traffic (Calero et al., 2001). This overexpression phenotype was suppressed by concurrently overexpressing Yip1p (Calero et al., 2001). Yop1p is the yeast homologue of the mammalian DP1, a member of the reticulon family of proteins that have a proposed role in maintaining tubular ER structure (see page 7) (Voeltz et al., 2006). We have recently confirmed the Yip1A/DP1 interaction through co-immunoprecipitation in mammalian cells (Dykstra et al., 2010).

YIP1A AND THE ENDOPLASMIC RETICULUM

The existence of multiple Yip1 interacting partners, coupled with its cycling between the ER and Golgi suggests that Yip1 may have multiple functions in the early secretory pathway. Studies have shown that RNAi mediated knockdown of Yip1A in mammalian cells leads to a pleiotropic phenotype that is consistent with this hypothesis (Kano et al., 2009; Dykstra et al., 2010). This thesis characterizes a novel role for Yip1A in directly maintaining ER structure in mammalian cells and makes progress towards elucidating a molecular mechanism for this ER structuring function through a mutational analysis of the protein. Additionally, it contributes to the understanding of the relationship between the structure of the ER and its function in COPII vesicle mediated protein and lipid transport.

CHAPTER 2

YIP1A STRUCTURES THE MAMMALIAN ENDOPLASMIC RETICULUM

INTRODUCTION

The endoplasmic reticulum (ER) in most cell types is an interconnected membrane network of flattened sheet-like cisternae and narrow diameter tubules dispersed throughout the cell cytoplasm (Baumann and Walz, 2001). The network is continuous with the outer nuclear envelope and extends outwards toward the cell periphery. It is the largest membrane bound organelle in animal cells and houses a wide array of essential cellular processes including secretory and membrane protein biosynthesis and quality control, coat protein II (COPII)-mediated secretory protein export, lipid synthesis, detoxification and the regulation of intracellular Ca^{2+} (Baumann and Walz, 2001).

To accommodate its varied functions, the ER is further sub-compartmentalized into discrete sub-domains (Baumann and Walz, 2001; Voeltz et al., 2002; Borgese et al., 2006; Shibata et al., 2006). Rough ER, enriched in membrane-bound ribosomes, is the primary site of protein biosynthesis and translocation, whereas smooth ER is the major site of Ca+2 exchange, lipid synthesis and detoxification. Between rough and smooth regions, the transitional ER comprises the sub-domain where coat protein II (COPII) vesicles bud to facilitate protein and lipid export. Each ER sub-domain is generally thought to adopt the morphology most suited to its primary function. Thus the flattened sheets of the rough ER may better accommodate large

arrays of actively translating and translocating polysomes, whereas the greater surface-to-volume ratio associated with the highly curved tubules of the smooth ER may facilitate rapid transport of ions and lipids (Shibata et al., 2006).

The ER can additionally adopt wide-ranging variations in structure and organization in specialized cell types (Borgese et al., 2006). Examples include the striking tubular morphology of the sarcoplasmic reticulum in muscle (Baumann and Walz, 2001; Rossi et al., 2008), and the dense parallel arrays of flattened rough ER sheets in the liver or pancreas (Rajasekaran et al., 1993; Baumann and Walz, 2001). The ER can also undergo dramatic expansion. For instance, B-lymphocytes undergo a several-fold increase in ER volume during differentiation (Wiest et al., 1990). Another type of frequently observed ER reorganization is the formation of tightly stacked membrane arrays of distinct architectures that yet retain continuity with the rest of the network (Chin et al., 1982; Yamamoto et al., 1996). These arrays can take on the appearance of compressed bodies of sinusoidal ER (Anderson et al., 1983), ordered arrays of tubules and sheets with hexagonal or cubic symmetry (Chin et al., 1982; Yamamoto et al., 1996), or concentric membrane whorls (Koning et al., 1996). Often, membrane packing or stacking occurs as a consequence of drug treatments (Jones and Fawcett, 1966; Hwang et al., 1974; Singer et al., 1988) or of up-regulation of a variety of membrane-anchored ER proteins such as cytochrome P450 (Koning et al., 1996), HMG-CoA reductase (Chin et al., 1982), microsomal aldehyde dehydrogenase (Yamamoto et al., 1996), cytochrome b(5) (Pedrazzini et al., 2000) or the inositol 1,4,5-triphosphate receptor (Takei et al., 1994). Significantly though, tightly stacked and concentrically whorled ER membranes have also been observed in a large number of normal tissues (King et al., 1974) including testicular interstitial cells (Carr and Carr, 1962; Christensen and Fawcett, 1966) adrenocortical cells (Nickerson and Curtis, 1969), melanoma cells (Hu,

1971), cells of the anterior pituitary (Dubois and Girod, 1971) and hypothalamic arcuate neurons (King et al., 1974). In some instances the whorled ER membranes are primarily smooth while in others the whorled membranes also include ribosome-studded rough ER (King et al., 1974).

The prevalence of such large-scale ER reorganization is suggestive that form follows function. Indeed, ER membrane expansion in differentiating B-lymphocytes increases the protein folding capacity of the ER that enables massive up-regulation of antibody secretion (Wiest et al., 1990). The functional consequences of other types of ER reorganization including concentrically whorled ER is less well understood. One possibility is that the tight packing of either smooth or rough membranes provides a means of sequestration and storage of either lipid or protein cargo for later use. Of note, many of the specialized cell types that have been observed to undergo ER stacking have roles in either peptide or steroid hormone secretion (King et al., 1974). In the case of gonadotropin releasing hormone (GnRH)-secreting hypothalamic arcuate neurons, the formation of ER whorls appears to be additionally regulated by the estrous cycle (King et al., 1974). Thus large-scale ER reorganization may serve as a mechanism for regulating lipid or protein export in response to physiological cues.

Here we identify a novel ER structuring role for Yip1A, the mammalian homologue of a yeast protein implicated previously in the biogenesis of COPII transport vesicles from the ER (Heidtman et al., 2003). In its absence, the ER network is reorganized into concentrically whorled, stacked membranes. Stacked whorl formation is in turn sufficient to delay COPII-mediated ER export, consistent with the idea that whorled ER formation provides a means of delaying lipid or protein export. Together, our results suggest a role for Yip1A in the structural organization of the ER and raise the possibility that reorganization of ER membranes into whorls under certain physiological conditions may provide a means of transiently down-regulating cargo

exit without directly modifying components of the COPII machinery.

RESULTS

YIP1A KNOCK DOWN ALTERS ER NETWORK ORGANIZATION

Yip1 in yeast has been established as a cycling membrane protein required for COPII vesicle biogenesis (Heidtman et al., 2003). However, the mechanism by which it facilitates ER export remains largely unknown. There are two Yip1 isoforms in mammalian cells, Yip1A and Yip1B. Though each is 31% identical to yeast Yip1, Yip1B is expressed only in the heart, whereas Yip1A is ubiquitous (Tang et al., 2001). We therefore focused on Yip1A. Previous work suggests that both yeast Yip1 and mammalian Yip1A are ER-to-Golgi cycling proteins with a steady state pattern of localization coincident with ER exit sites and/or the ER-to-Golgi intermediate compartment (ERGIC) (Tang et al., 2001; Heidtman et al., 2003; Yoshida et al., 2008). Staining with our affinity purified Yip1A antibodies confirmed a high degree of co-localization of Yip1A with ERGIC-53, a marker for the ERGIC (Fig 2-1A,B). Further, consistent with the idea that Yip1A cycles constitutively through the ER and ERGIC compartments (Tang et al., 2001; Heidtman et al., 2003; Yoshida et al., 2008), blocking ER export using the protein kinase inhibitor H89 (Aridor and Balch, 2000; Lee and Linstedt, 2000), caused redistribution ($t1/2 \sim 10$ min) of Yip1A to the ER as observed previously (Lee and Linstedt, 2000) for the rapidly recycling ERGIC-53 (Fig 2-1C,D).

To determine the consequences of Yip1A depletion, Yip1A in HeLa cells was targeted for RNAi. Two different siRNAs targeting Yip1A yielded substantial knock down of the protein as determined by immunoblot (Fig 2-2A). By indirect immunofluorescence, siRNA-1 and -2 both reduced Yip1A to near undetectable levels (compare Fig 2-2D and 2-2F to 2-2B), though a higher percentage of cells treated with siRNA-2 lacked detectable protein. To our initial surprise, cells lacking Yip1A displayed strikingly altered ER organization as marked by antibodies against

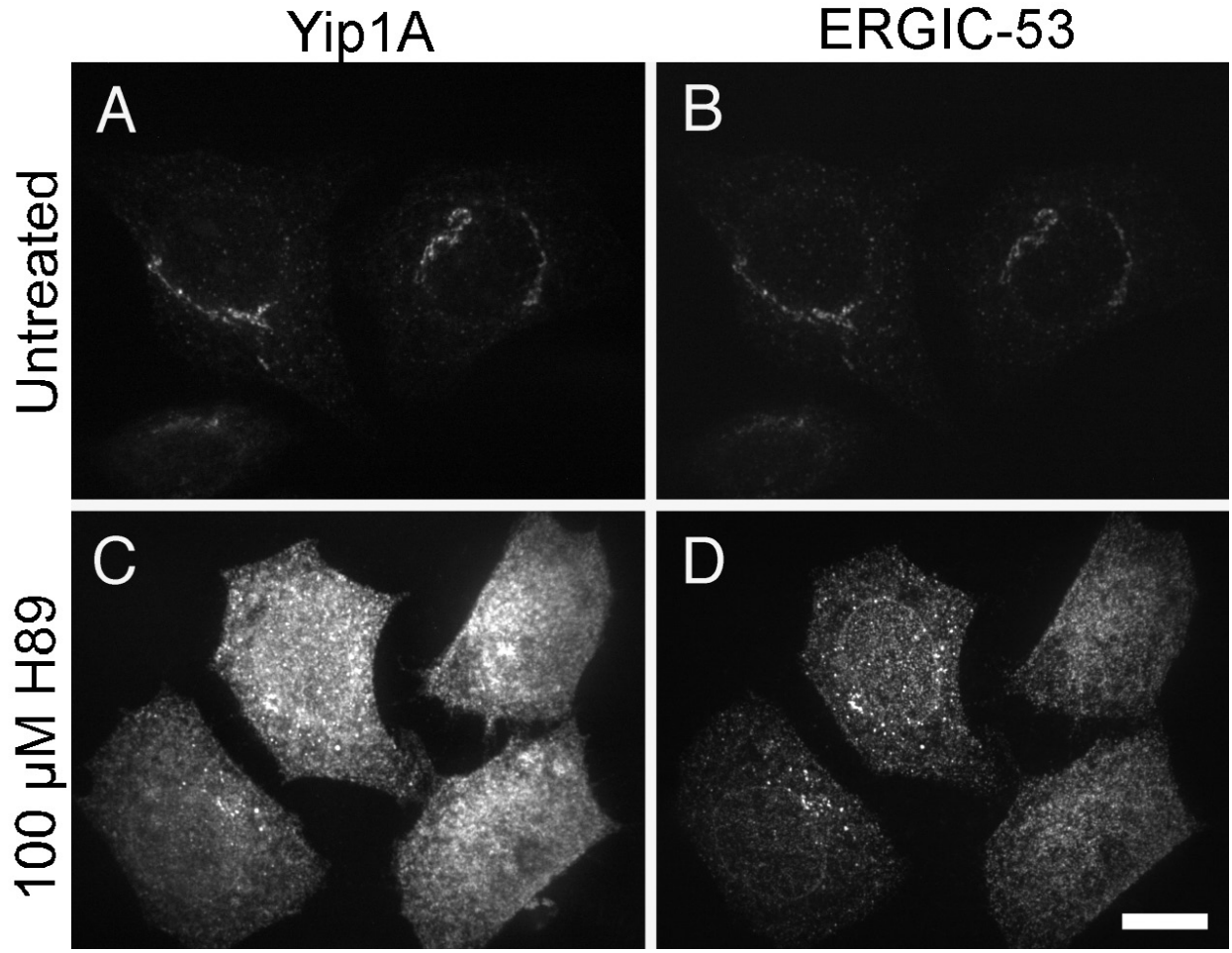

Figure 2-1: Yip1A likely achieves its steady state localization at in the ERGIC by cycling through the ER.

Cells untreated (A, B) or treated for 20 min at 37°C with 100 µM H89 (C, D) were fixed and stained with antibodies against Yip1A (A, C) or ERGIC-53 (B, D). Scale bar, 10 µm.

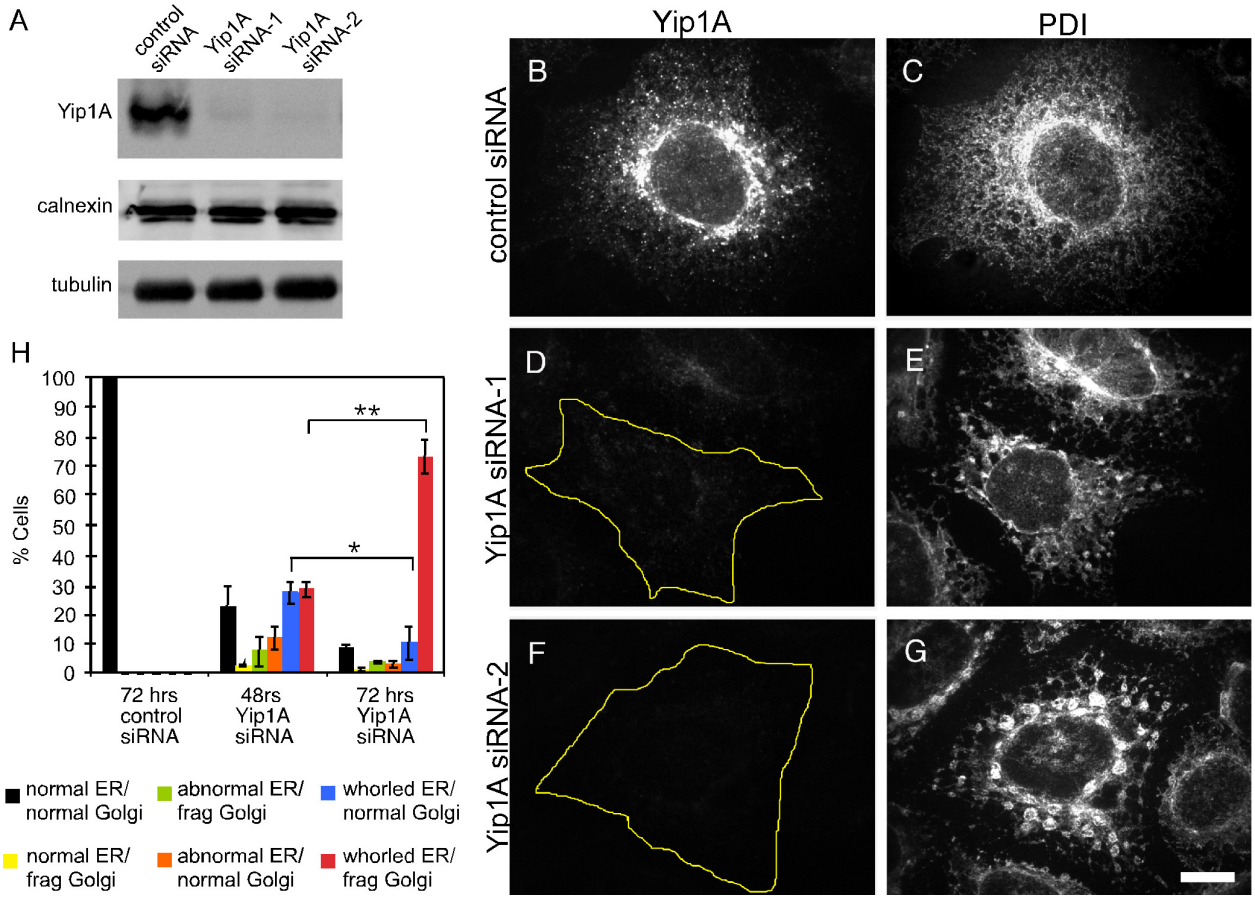

Figure 2-2: RNAi-mediated Yip1A depletion causes ER compaction.

(A) Immunoblot demonstrating loss of Yip1A by two distinct siRNAs. HeLa cells stably expressing Golgi localized GFP-GalNacT2 were transfected with a control siRNA, Yip1A siRNA-1 or Yip1A siRNA-2, harvested 72 hrs. later and probed using antibodies against Yip1A, Calnexin and Tubulin. (B-G) Yip1A loss correlates with ER morphological changes. Cells transfected with control siRNA (B, C), Yip1A siRNA-1 (D, E) or Yip1A siRNA-2 (F, G) were fixed 72 hrs. later and doubly stained with antibodies against Yip1A (B,D,F) and PDI (C,E,G). Scale bar, 10 μm. (H) ER morphological changes precede Golgi fragmentation. Cells transfected with a control siRNA or Yip1 siRNA-2 were fixed 48 or 72 hrs. later and stained with antibodies against PDI. ER and Golgi morphologies were classified as indicated (frag Golgi = fragmented Golgi; whorled ER indicates compacted ER as shown in E and F; abnormal ER indicates ER morphologies intermediate between normal and whorled). Quantitation of the average percent of cells displaying the indicated ER and Golgi morphologies from 3 independent experiments (>50 cells per condition per experiment) is shown, +/- S.D. Single asterisk indicates $p<0.05$ and double asterisk indicates $p<0.001$ (student's t-test).

the luminal ER resident protein disulfide isomerase (PDI) (Mazzarella et al., 1990). In contrast to control siRNA-treated cells with robust Yip1A staining (Fig 2-2B) and a typically dispersed tubular reticular network that extended throughout the cell cytoplasm (Fig 2-2C), cells with undetectable Yip1A protein exhibited a notable loss of the peripheral tubular ER network and an apparent clustering of ER membranes into large micron-scale sized structures (Fig 2-2E,G). The change in ER morphology was not marker specific. It was also readily observed with antibodies against the trans-membrane ER resident Calnexin (Ahluwalia et al., 1992). Moreover, the observed clustering of ER membranes appeared to reflect a reorganization of the ER as opposed to membrane proliferation, as shown by comparable levels of Calnexin in control and Yip1A siRNA-treated cells (Fig 2-2A).

In addition to alterations in ER morphology, a marked fragmentation of the Golgi apparatus into mini-stacks was observed (Fig 2-3A-F and also Fig 2-4), as previously reported (Yoshida et al., 2008). But despite extensive fragmentation of the Golgi, light level analysis revealed that Golgi marker separation was similar to that in control cells (unpublished data), and Golgi sub-compartmentalization and its overall organization seemed to be maintained in cells lacking Yip1A (Fig 2-4). Several observations suggested that the striking ER rearrangements observed upon Yip1A knockdown were unlikely to have occurred as an indirect consequence of either Golgi fragmentation or redistribution of Golgi tethering and/or stacking proteins to the ER. First, a significant number of cells with clustered ER were detected as early as 48 hrs. after Yip1A siRNA addition. At this time, ~50% of cells with clustered (or whorled, see below) ER showed as yet no noticeable Golgi fragmentation (Fig 2-2H). Second, the ER appeared normal in cells treated with siRNAs targeting either golgin160 (Yadav et al., 2009) or GRASP55 (Feinstein and Linstedt, 2008) even though the Golgi was fragmented in both cases (unpublished data).

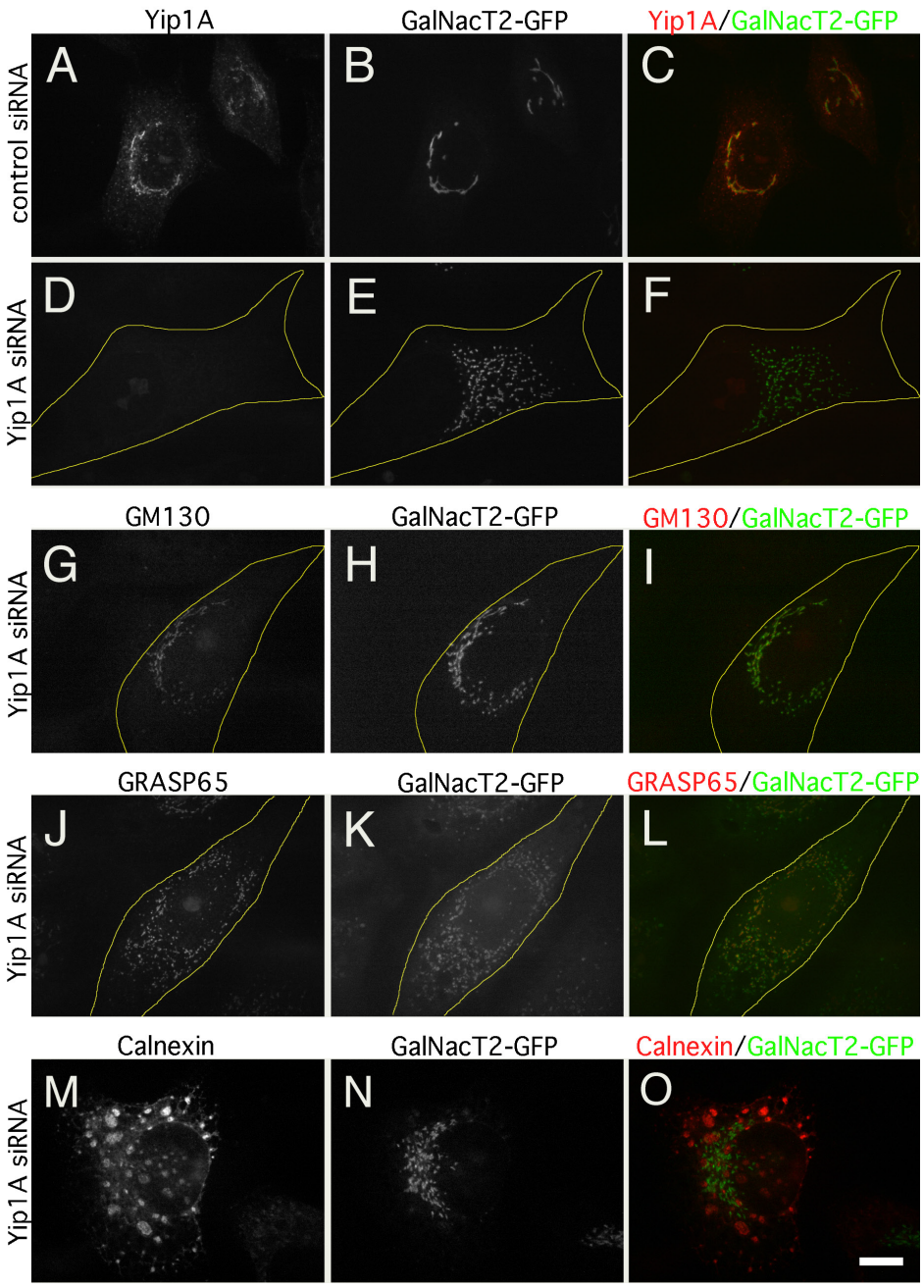

Figure 2-3: Yip1A depletion results in fragmentation of the Golgi into mini-stacks that retain both GM130 and GRASP65.

Cells stably expressing GFP-GalNacT2 and treated with a control siRNA (A-C) or Yip1A siRNA (D-O) were fixed 72 hrs. later and stained with antibodies against Yip1A (A, D), GM130 (G), GRASP65 (J) or PDI (M). The corresponding GFP-GalNacT2 patterns are shown in (B, E, H, K and N) and the merge is also shown (C, F, I, L, O). Scale bar, 10 μm. Note that both GM130 and GRASP65 are in GalNacT2-containing Golgi membranes that are separate from the whorled ER. Scale bar, 10 μm.

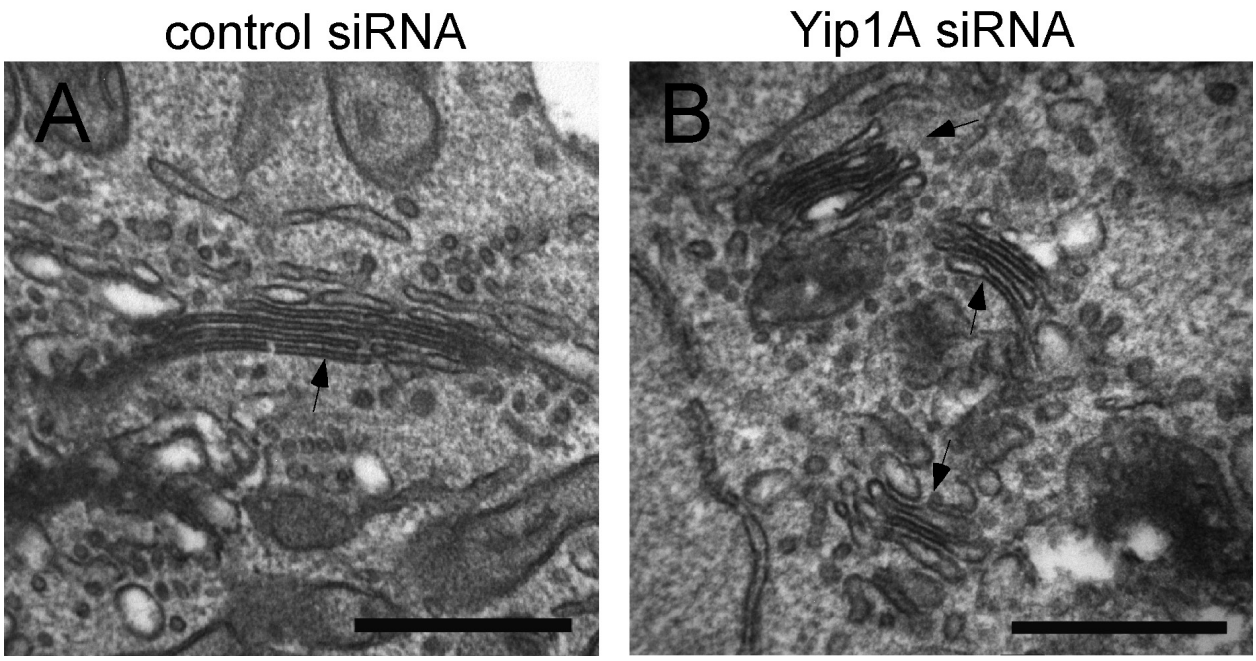

Figure 2-4: Golgi organization is largely intact in cells lacking Yip1A.

Golgi stacks in cells treated with a control (A) or Yip1A siRNA (B). Arrow (A) indicates a Golgi stack of typical length in cells treated with control siRNA. Arrows (B) indicate shorter Golgi stacks in Yip1A siRNA-2- treated cells. Scale bar (E, F), 500 nm.

Third, both components of the Golgi tethering/stacking complex GM130/GRASP65 (Barr et al., 1997; Sengupta et al., 2009) colocalized with other Golgi markers in Yip1A depleted cells (Fig 2-3G-L) in structures largely separate from the ER (Fig 2-3M-O and Fig 2-5). Finally, the ERGIC compartment was maintained mostly separate from the ER in cells lacking Yip1A, as evidenced by co-staining with Yip1A and ERGIC-53 antibodies in control siRNA- and Yip1A siRNA-treated cells (Figs 2-6 and 2-7).

YIP1A LOSS LEADS TO ER MEMBRANE STACKING

Ultra-structural analysis by thin section electron microscopy (EM) corroborated the change in ER network organization seen at the light level. In contrast to control cells with a high density of ER membrane profiles in the cell periphery (Fig 2-8A), the majority of Yip1A knock down cells were relatively devoid of identifiable peripheral ER membranes (Fig 2-8B). Instead, large densely packed membrane clusters were frequently observed (arrows in Fig 2-8B). Such densely packed ER structures were never observed in control cells. At higher magnification, the membrane clusters, clearly corresponding to the compacted ER membranes observed at the light level, were visible as stacked membranes arranged in concentric whorls ranging from 1 to 5 μm in outer diameter (Fig 2-8C, D). The whorls were ER-derived because clear connections to the nuclear envelope were frequently observed (arrows in Fig 2-8E, F). Connectivity of the whorls to the ER network was also demonstrated by relatively rapid diffusion of mGFP-Sec61γ from the general ER into bleached whorls (Fig 2-9). Moreover, as expected for ER membranes, mitochondria were frequently in close apposition either to the whorls themselves or to membranes extending from the whorls. And, as suggested by light level analysis, Golgi cisternal organization appeared relatively normal in both control (Fig 2-4) and Yip1A knock down cells (Fig 2-4), though the Golgi stacks were shorter in cells lacking Yip1A, as expected from the

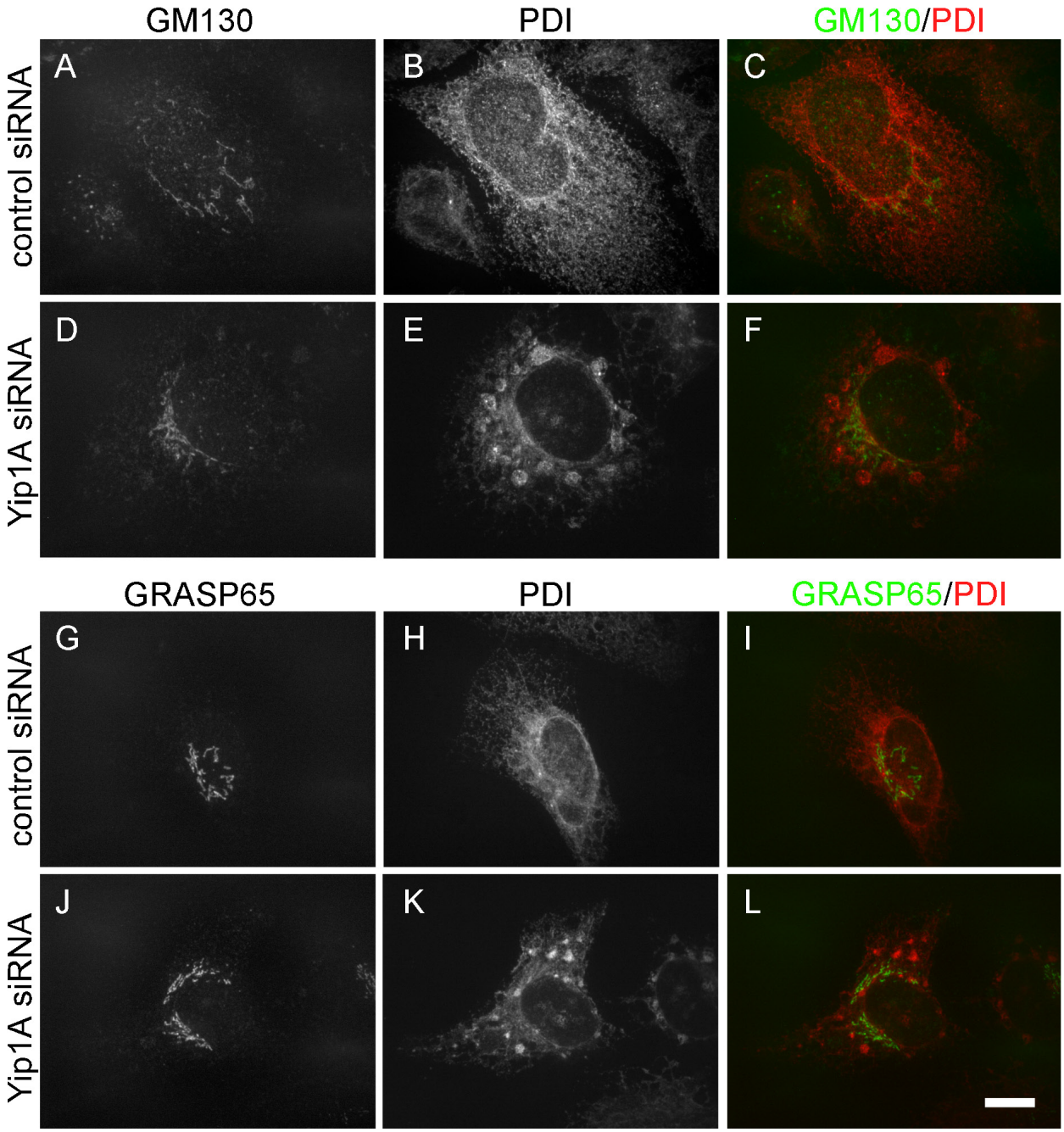

Figure 2-5: GM130 and GRASP65 remain largely separate from the whorled ER in cells lacking Yip1A.

Cells treated with a control siRNA (A-C and G-I) or Yip1A siRNA (D-F and J-L) were fixed 72 hrs. later and doubly stained using antibodies against GM130 (A, D) and PDI (B, E) or GRASP65 (G, J) and PDI (H, K). The merges are also shown (C, F, I, L). Scale bar, 10 μm.

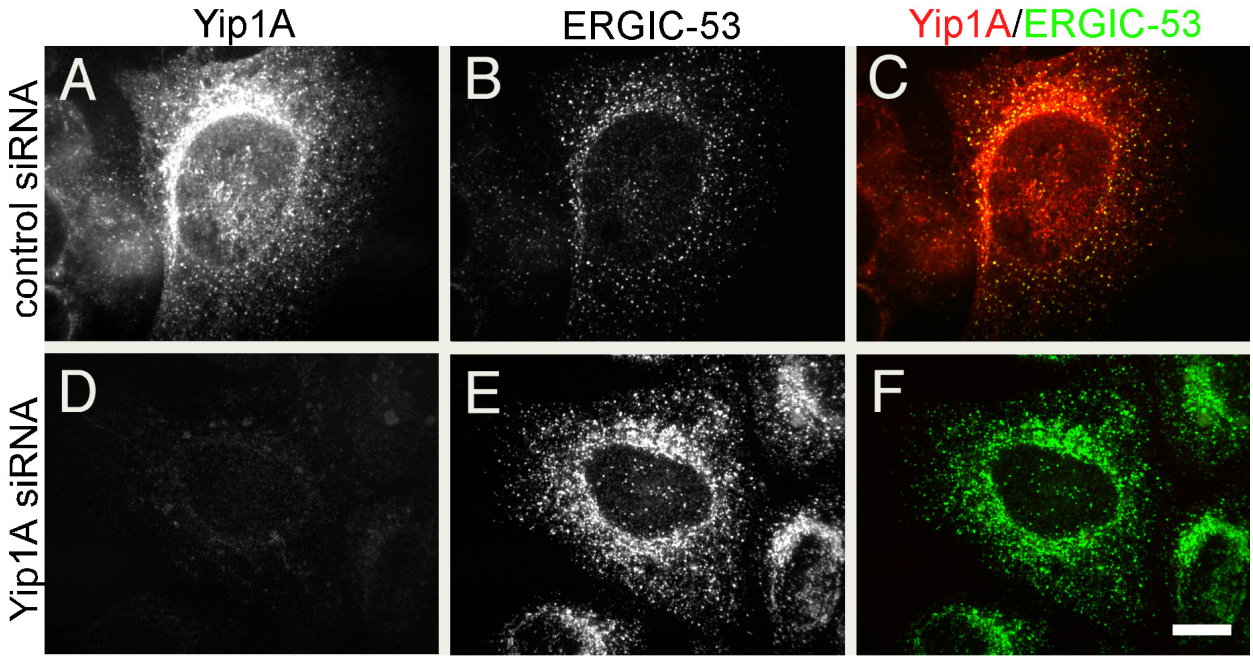

Figure 2-6: ERGIC integrity is maintained in cells lacking Yip1A.

Cells treated with a control siRNA (A-C) or Yip1A siRNA (D-F) were fixed 72 hrs. later and doubly stained using antibodies against Yip1A (A, D) and ERGIC-53 (B, E). The merge is also shown (C, F). Scale bar, 10 μm.

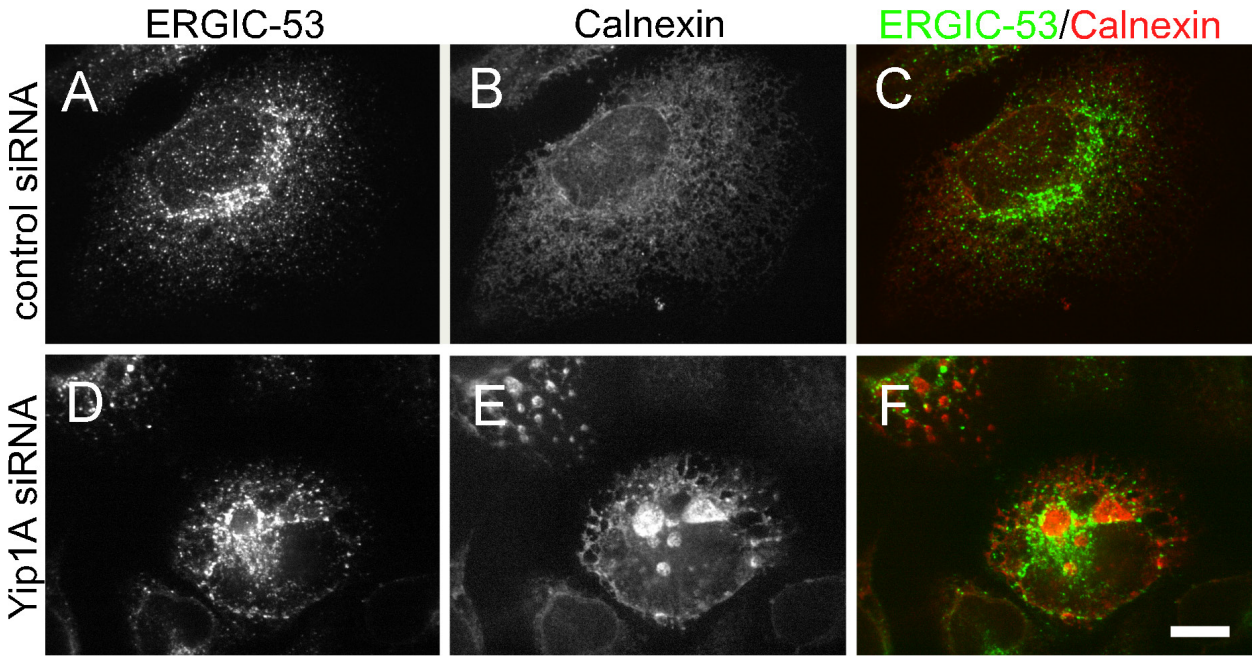

Figure 2-7: ERGIC-53 remains largely separate from the whorled ER in cells lacking Yip1A.

Cells treated with a control siRNA (A-C) or Yip1A siRNA (D-F) were fixed 72 hrs. later and doubly stained using antibodies against ERGIC-53 (A, D) and Calnexin (B, E). The merge is also shown (C, F). Scale bar, 10 μm.

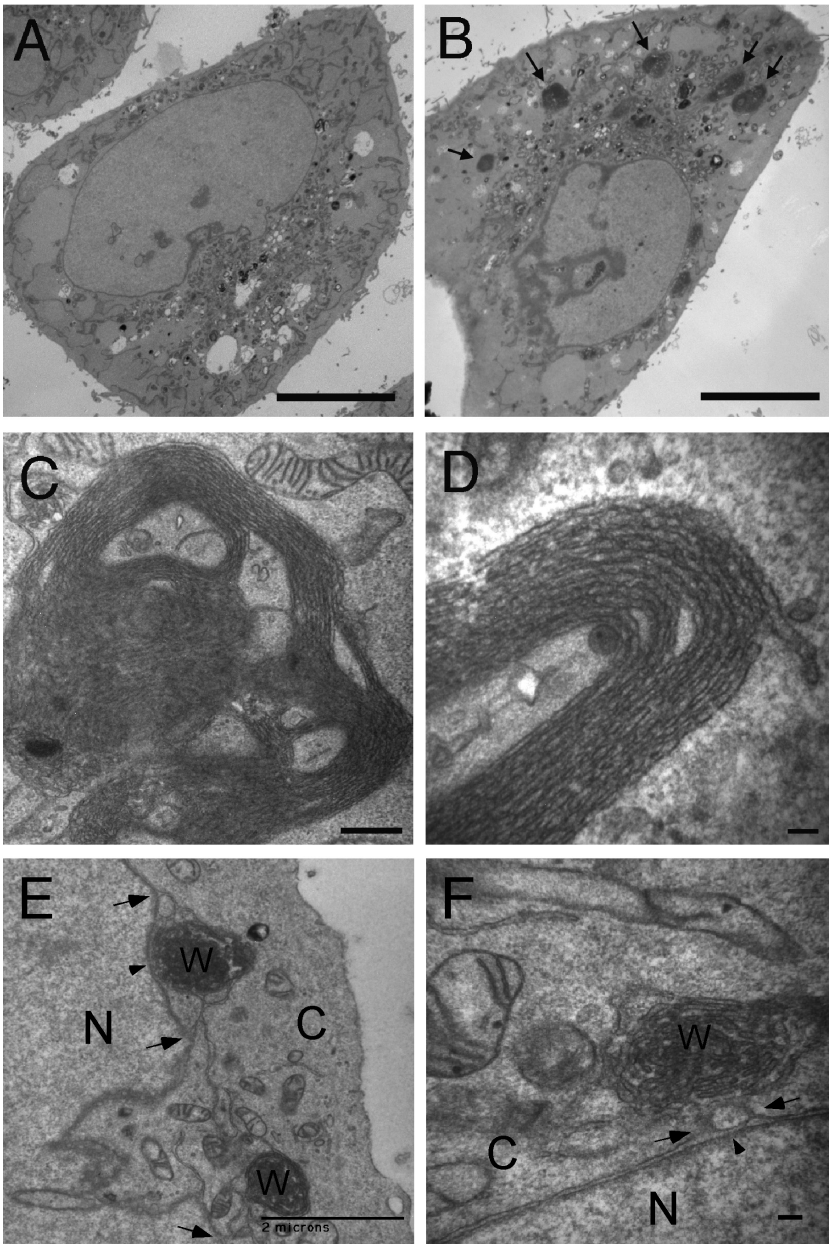

Figure 2-8: Ultra-structural analysis of cells lacking Yip1A.

(A, B) A low magnification thin section transmission EM view of cells treated with a control (A) or Yip1A (B) siRNA. Arrows (B) indicate dense ER membrane aggregates seen only in Yip1A siRNA-treated cells. Scale bar, 10 μm. (C) A higher magnification view of an entire ER whorl. Scale bar, 500 nm. (D) A high magnification view of stacked membranes of a portion of an ER whorl. Scale bar, 100 nm. (E, F) ER whorls are continuous with the nuclear envelope. A low magnification view of two interconnected whorls each connected to the nuclear envelope (E) and a higher magnification view of a whorl exhibiting connections to the outer nuclear envelope (F). Arrowheads (E, F) indicate the nuclear envelope and arrows (E, F) indicate membrane continuities between whorl and nuclear envelope. N=nucleus; C=cytoplasm; W=whorl. Scale bar, 2 μm (E) and 100 nm (F).

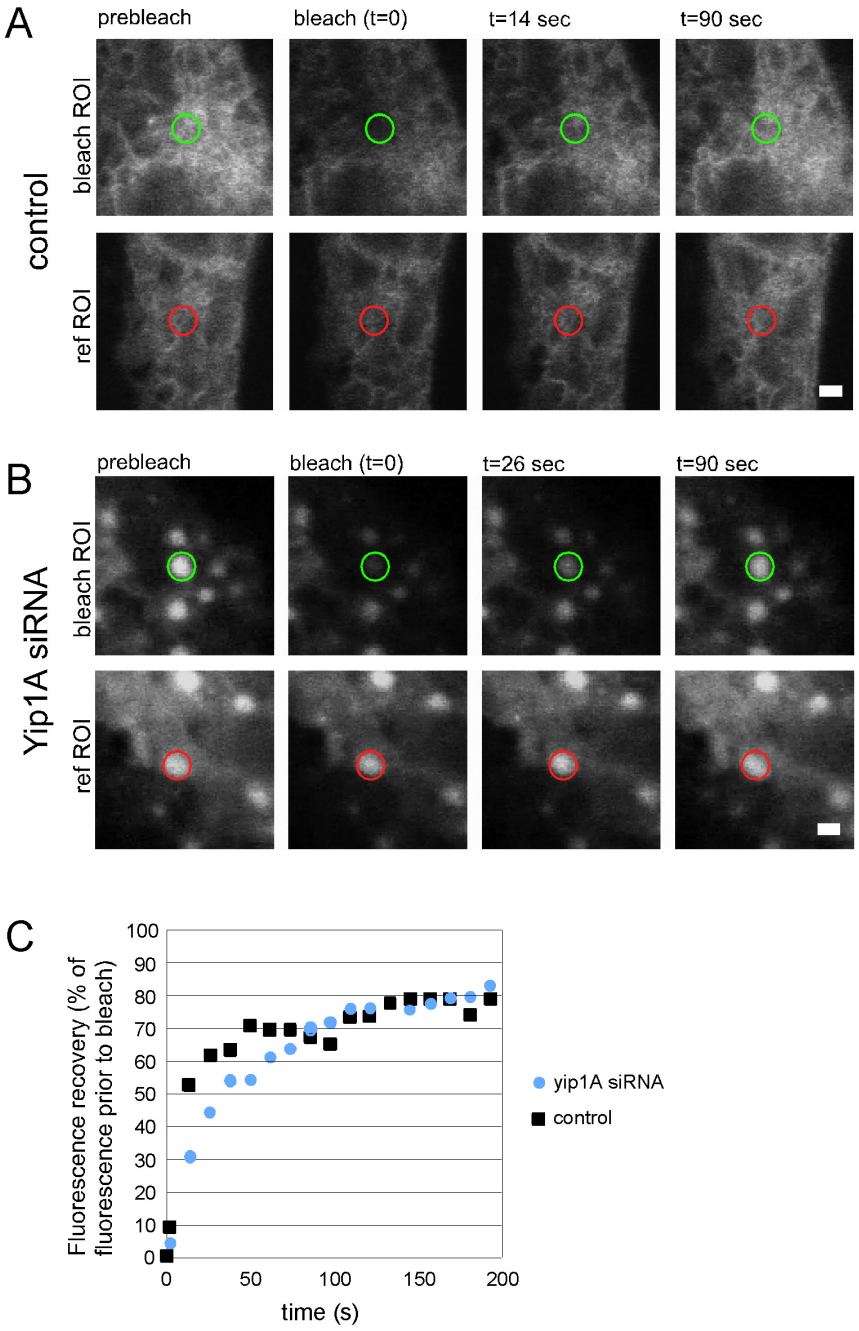

Figure 2-9: Whorls retain continuity with the general ER.

A part of the general ER within cells transfected with mGFP-Sec61g alone (A) or a whorl within cells co-transfected with mGFPSec61γ and Yip1A siRNA (B) were photobleached 48 hrs. after transfection and subsequently monitored for fluorescence recovery after bleaching. Green circles mark the bleached region of interest (ROI) and red circles mark an unbleached reference ROI within the same cells. Scale bar, 1 µm. (C) Normalized fluorescence recovery plot showing rapid diffusion of mGFP-Sec61γ into both the general ER (black squares, t1/2 ~ 10s) and whorled ER (blue circles, t1/2 ~ 20s).

fragmentation seen at the light level.

Three observations suggested that the ER whorls were not a consequence of stress induced ER autophagy. First, a limiting membrane (Bernales et al., 2006; Ogata et al., 2006) was never observed to surround the whorls. Second, immuno-blotting with an antibody against BiP (Munro and Pelham, 1986), an ER chaperone that is up-regulated by ER stress (Ron and Walter, 2007), showed no increase in BiP protein expression (unpublished data). Third, immuno-staining with antibodies against LC3, a marker of autophagy (Kabeya et al., 2000), showed no change in knock down cells (unpublished data). Also, the Tubulin-staining pattern in cells lacking Yip1A was indistinguishable from that in control cells (Fig 2-10), rendering it unlikely that the effect of Yip1A depletion on ER organization was an indirect consequence of perturbation of the MT cytoskeleton (Terasaki et al., 1986).

Serial thin sections prepared from cells relatively early after knock down (48 hrs.) revealed that newly forming ER whorls were likely comprised of flat, sheet-like cisternae, as well as narrow diameter tubules. In many whorls, concentric tubule-like arrays frequently persisted through multiple 100 nm serial sections, suggesting a structure comprised predominantly of stacked sheets (Fig 2-11A-I). However newly forming whorls also contained membranes with more tubule-like morphology. For instance, we observed whorls (Fig 2-11J) containing circular profiles that persisted for more than a single 100 nm section (Fig 2-11J, i and i') as well as tubular profiles that did not persist for more than a single 100 nm section (Fig 2-11J, ii and ii' and Fig 2-11J, iii and iii'). Both were indicative of a tubular morphology. Thus it appeared that the ER generally, both flat sheets and curved tubules, was transformed into a stacked and concentrically whorled arrangement upon Yip1A loss.

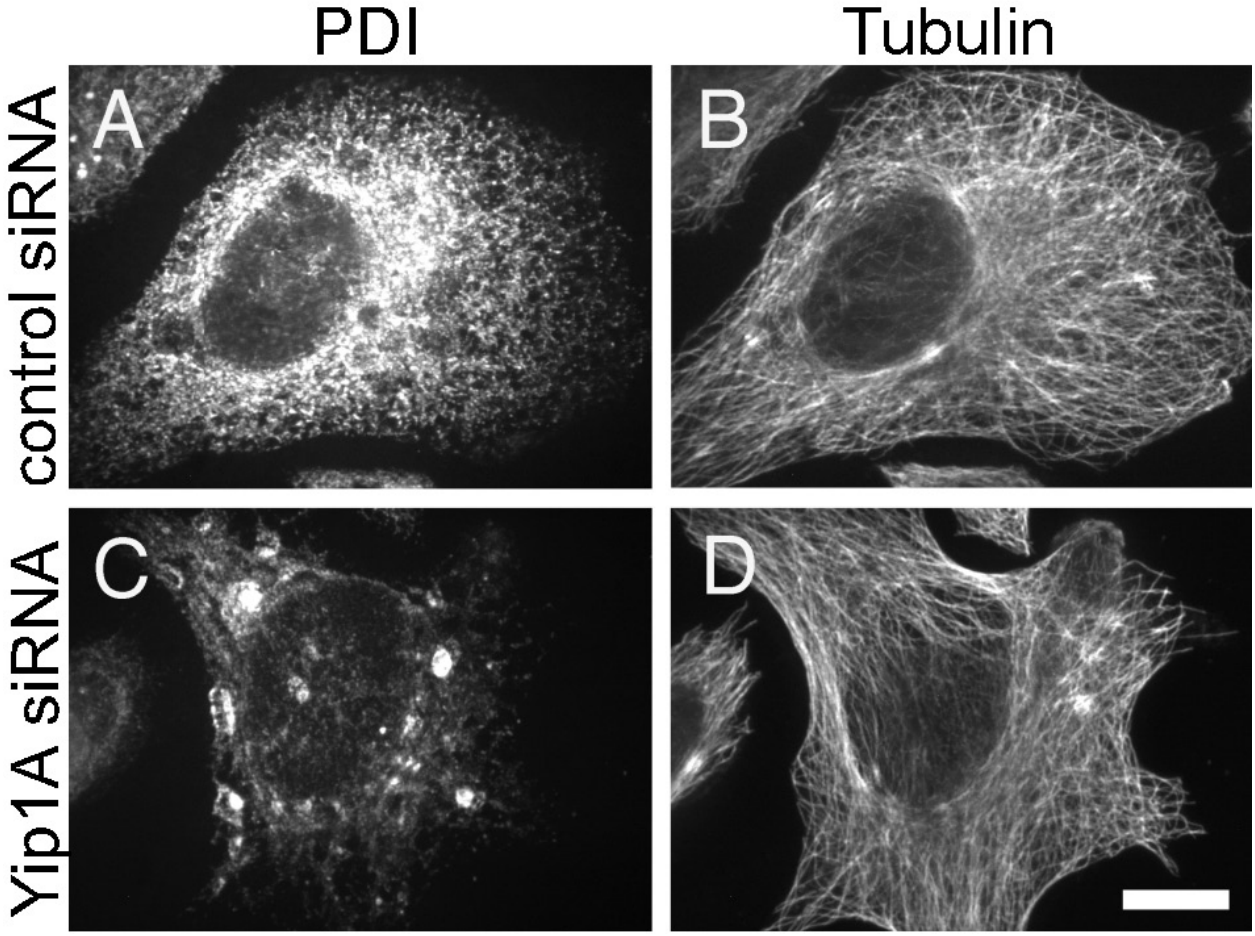

Figure 2-10: Yip1A knockdown has no apparent effect on the microtubule cytoskeleton.

Cells transfected with a control siRNA (A, B) or Yip1A siRNA (C, D) were fixed 72 hrs. later and doubly stained with antibodies against PDI (A, C) and Tubulin (B, D). Scale bar, 10 μm.

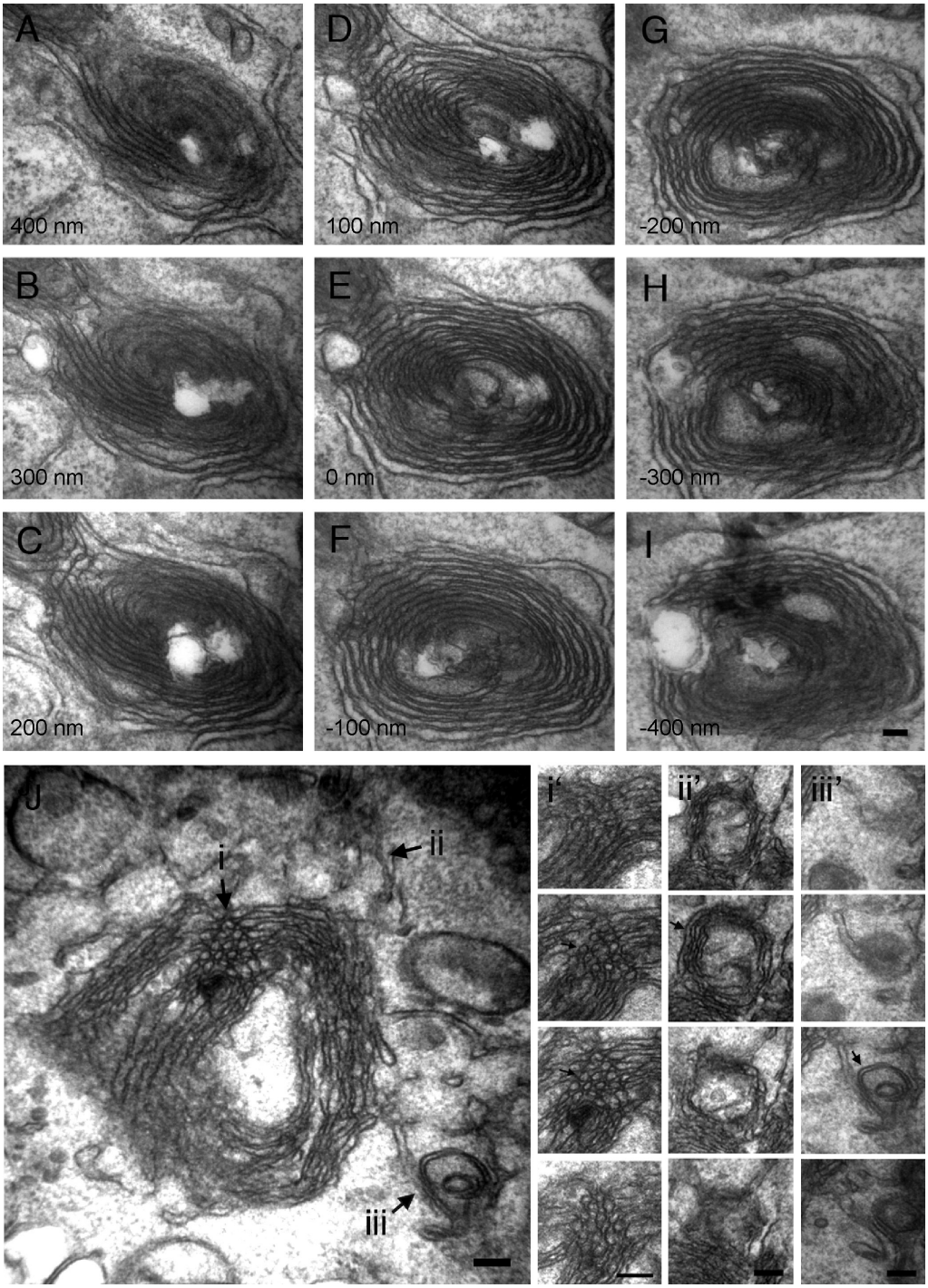

Figure 2-11: Early ER whorls consist of both sheets and tubules.

(A-I) Serial (100 nm) transmission EM thin sections through an ER whorl 48 hrs. after Yip1A siRNA treatment. Scale bar, 100 nm. (J) A thin section micrograph through a different ER whorl 48 hrs. after Yip1A siRNA treatment. Arrows (i, ii, iii) indicate three different examples of tubular morphology. Serial 100 nm thin sections through the corresponding regions (i, ii, iii) of the whorl in (J) are shown in i', ii' and iii'.

A CONSERVED RESIDUE IN THE CYTOPLASMIC DOMAIN OF YIP1A IS REQUIRED FOR THE ER STRUCTURING FUNCTION

To ascertain that the large-scale reorganization of the ER network into whorls was due specifically to Yip1A depletion, a siRNA-immune Flag-Yip1A rescue construct was generated and co-transfected into cells along with the siRNA. Under these conditions, 66±4% (3 independent experiments of >50 cells per experiment) of cells expressing a control Sec13-Myc construct (Fig 2-12A) displayed the whorled ER phenotype (marked by single asterisks in Fig 2-12B, quantified in 2-12G). In contrast, virtually no cells expressing the Flag-Yip1A rescue construct displayed whorled ER. That is, every cell expressing the Flag-Yip1A rescue construct (Fig 2-12C) exhibited a normal dispersed, tubular-reticular ER network morphology (marked by double asterisk in Fig 2-12D, quantified in 2-12G). This result confirmed that the large-scale reorganization of the ER network observed upon treatment with Yip1A siRNA was indeed a specific consequence of Yip1A loss.

To determine whether the ER structuring function of Yip1A might depend on conserved and essential residues, we took advantage of a previously published mutagenesis study of yeast Yip1 wherein charged Yip1 residues conserved between yeast and mammals were individually altered and tested for effects on growth (Chen et al., 2004). Because a charge reversal of a specific Glu residue to Lys (E76K) in the N-terminal cytoplasmic domain of Yip1 rendered the protein nonfunctional for restoring growth even though the protein was stably expressed (Chen et al., 2004), we chose to test this version for its ability to structure the ER. Strikingly, 64+1% of cells expressing Flag-Yip1A (E95K) displayed the whorled ER phenotype despite the properly localized expression of protein (marked by single asterisks in Fig 2-12E, F, quantified in G). Thus the Yip1A (E95K) construct was no better than the negative control Sec13-Myc construct

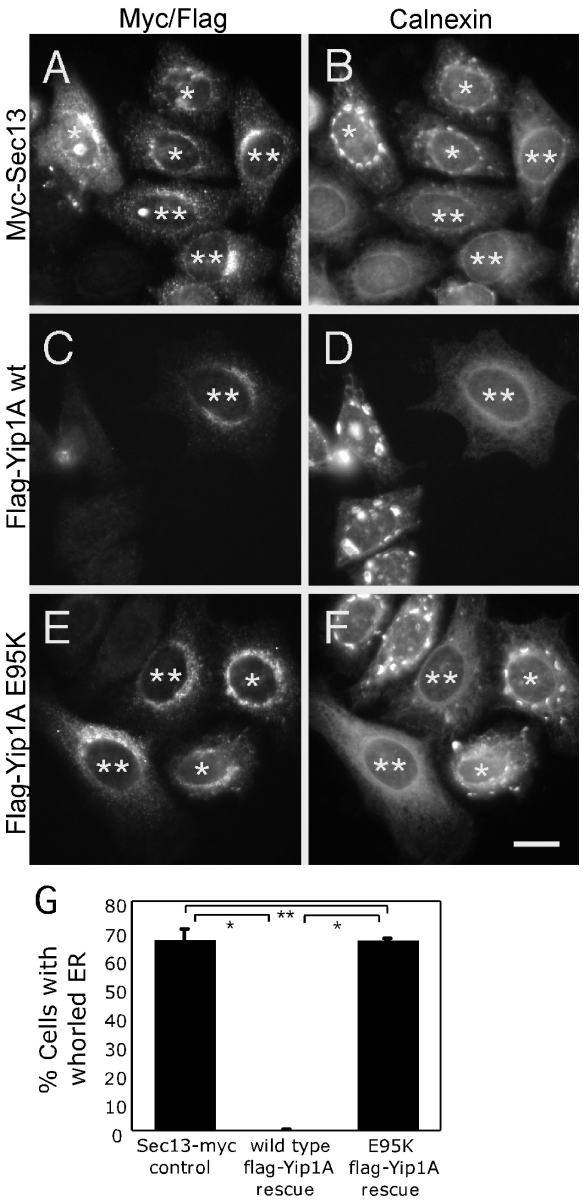

Figure 2-12: The whorled ER phenotype is rescued by a wild type but not mutant siRNA-immune Yip1A construct.

Cells co-transfected with Yip1A siRNA-2 and either a control Sec13-Myc construct (A, B) a siRNA-immune wild type Flag-Yip1A construct (C, D) or a siRNA-immune mutant (E95K) Flag-Yip1A construct (E, F) were fixed 72 hrs. later and doubly stained with antibodies against the Myc epitope (A) and Calnexin (B) or the Flag epitope (C,E) and Calnexin (D, F). Single asterisks (A-F) indicate expressing cells that exhibit ER whorls. Double asterisks (A-F) indicate expressing cells that do not exhibit ER whorls. Scale bar, 10 μm. (G) Quantitation of the percent of Sec13-Myc or wild type or mutant (E95K) Flag-Yip1A expressing cells displaying the whorled ER phenotype from 3 independent experiments (>50 cells per experiment), +/- S.D. Single asterisks indicate $p<0.0001$ (student's t-test). Double asterisk indicates no statistically significant difference.

in its ability to rescue the whorled ER phenotype. This result indicates that the ER structuring function of Yip1A in mammals depends critically on a conserved, cytoplasmic residue.

YIP1A INTERACTS WITH THE ER STRUCTURING PROTEIN DP1

We reasoned that the inability of Yip1A (E95K) to fulfill its ER structuring function might stem from its inability to interact with a critical binding partner. Among the several Yip1 binding proteins identified in yeast (Matern et al., 2000; Calero et al., 2001; Chen et al., 2004; Heidtman et al., 2005), the ER integral membrane protein Yop1 stands out as a potential candidate for mediating the ER structuring function of Yip1. Deletion of Yop1 along with the structurally related Rtn1/Rtn2 in yeast resulted in a loss of cortical ER tubules (Voeltz et al., 2006); and purified Yop1 reconstituted into synthetic liposomes was sufficient to induce liposome tabulation (Hu et al., 2008). Further, Yip1 over-expression in yeast suppressed lethality due to Yop1 overexpression, suggesting an antagonistic relationship between the two proteins (Calero et al., 2001). These observations prompted us to test whether DP1 (Voeltz et al., 2006), the mammalian homologue of Yop1, binds Yip1A. For this, Yip1A immunoprecipitation was performed on detergent-solubilized lysates from cells transfected with Myc-DP1. Indeed, both Myc-DP1 and the related Myc-DP1L1 (50% identical) were recovered on Yip1A antibody beads but not on control antibody beads (Fig 2-13A).

To next assess whether the inability of Yip1A (E95K) to structure the ER might be due to an inability to bind DP1, an antibody against the Flag epitope tag was used to immunoprecipitate Flag-Yip1A from cells co-transfected with Myc-DP1 and either wild type Flag-Yip1A or Flag-Yip1A (E95K). As shown (Fig 2-13B), Myc-DP1 was recovered in association with both the wild type and the E95K variant of Flag-Yip1A. Therefore, the inability of Yip1A (E95K) to maintain a dispersed ER network cannot be attributed simply to its failure to bind the ER

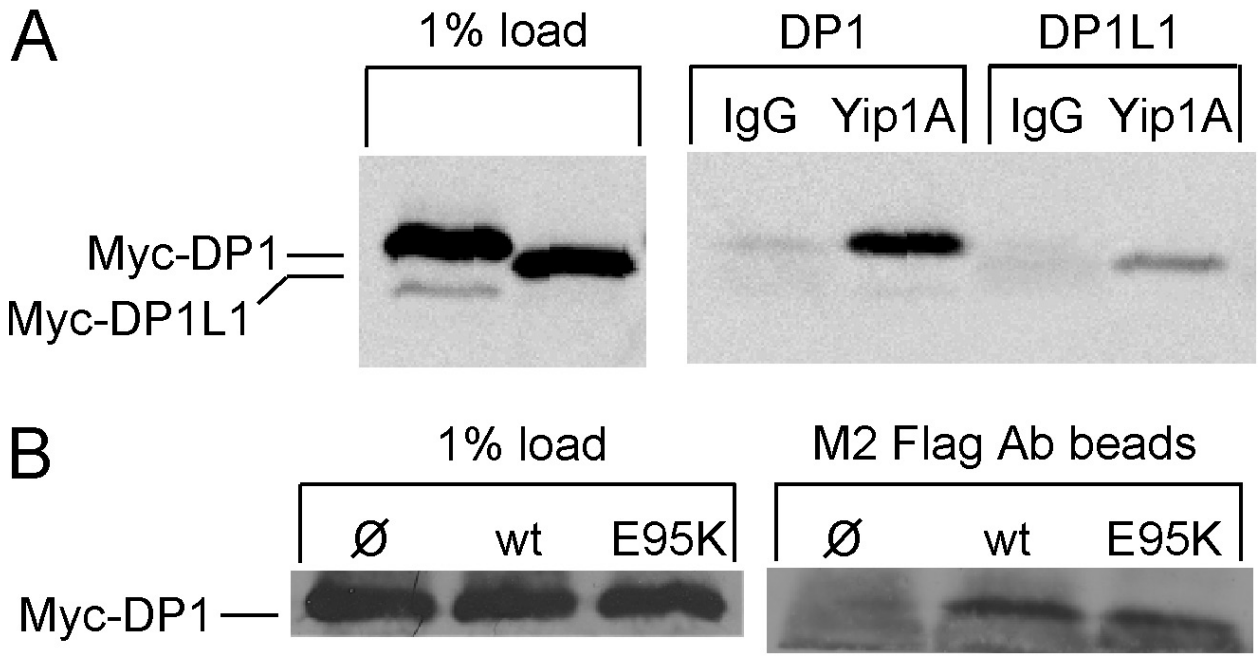

Figure 2-13: Both wild type and E95K Yip1A bind to DP1.

(A) HeLa cells transfected with either Myc-DP1 or Myc-DP1L1 were solubilized in 1% Triton-X-100 and subjected to immunoprecipitation with either a control antibody (IgG) or Yip1A antibody. Bound protein was subjected to immunoblotting with an antibody against the Myc epitope. (B) HeLa cells cotransfected with Myc-DP1 and either wild type Flag-Yip1A or Flag-Yip1A (E95K) were solubilized in 1% Triton-X-100 and subjected to immunoprecipitation with M2 Flag antibody beads. Bound protein was subjected to immunoblotting with the Myc epitope antibody. As a control, the Myc-DP1 recovered on M2 beads in the absence of Flag-Yip1A is also shown.

structuring protein DP1. Further work will be required to elucidate the functional relevance of the Yip1A-DP1 interaction for ER structuring.

YIP1A DEPLETION SLOWS VSVG EXPORT FROM THE ER WITHOUT AFFECTING COPII RECRUITMENT

Our results thus far indicated that Yip1A was required specifically to maintain a dispersed tubular-reticular ER network. Because previous studies in yeast had implicated Yip1 in COPII-mediated ER export, we next compared the kinetics of ts045 VSV-G ER export (Kreis and Lodish, 1986; Presley et al., 1997) in the presence and absence of Yip1A. For this, cells were co-transfected with either Myc-tagged ts045 VSV-G and a control siRNA, or Myc-ts045 VSV-G and Yip1A siRNA. 48 hrs. after transfection, cells were placed at 40°C, the non-permissive temperature for ER export of ts045 VSV-G, to accumulate VSV-G in the ER. Following a 24 hr. incubation at the non-permissive temperature, cells were shifted to the permissive temperature of 32°C for 0, 20, 60 or 120 min. As expected, VSV-G moved synchronously from the ER (Fig 2-14A) to the Golgi (Fig 2-14B) by 20 min and to the surface (Fig 2-14C) by 60 min in control siRNA-treated cells (quantified in Fig 2-14G). In Yip1A knock down cells, VSVG also accumulated in the ER at the non-permissive temperature (Fig 2-14D). Indeed, staining for Myc-VSV-G in these cells allowed ready visualization of the whorls induced by Yip1A loss. In contrast to the control cells however, a significant fraction of Yip1A knock down cells retained VSV-G in the ER at 20 min (Fig 2-14E). Cells lacking Yip1A function were identified by the presence of whorled ER structures after doubly staining with Calnexin antibodies. By 20 min, VSV-G had moved out of the ER in only ~20% of cells displaying whorled ER membranes (Fig 2-14G). In the remaining 80% of Yip1A knock down cells, VSV-G was clearly retained in whorled ER membranes (Fig 2-14E, quantified in Fig 2-14G). By 60 min, the fraction of cells

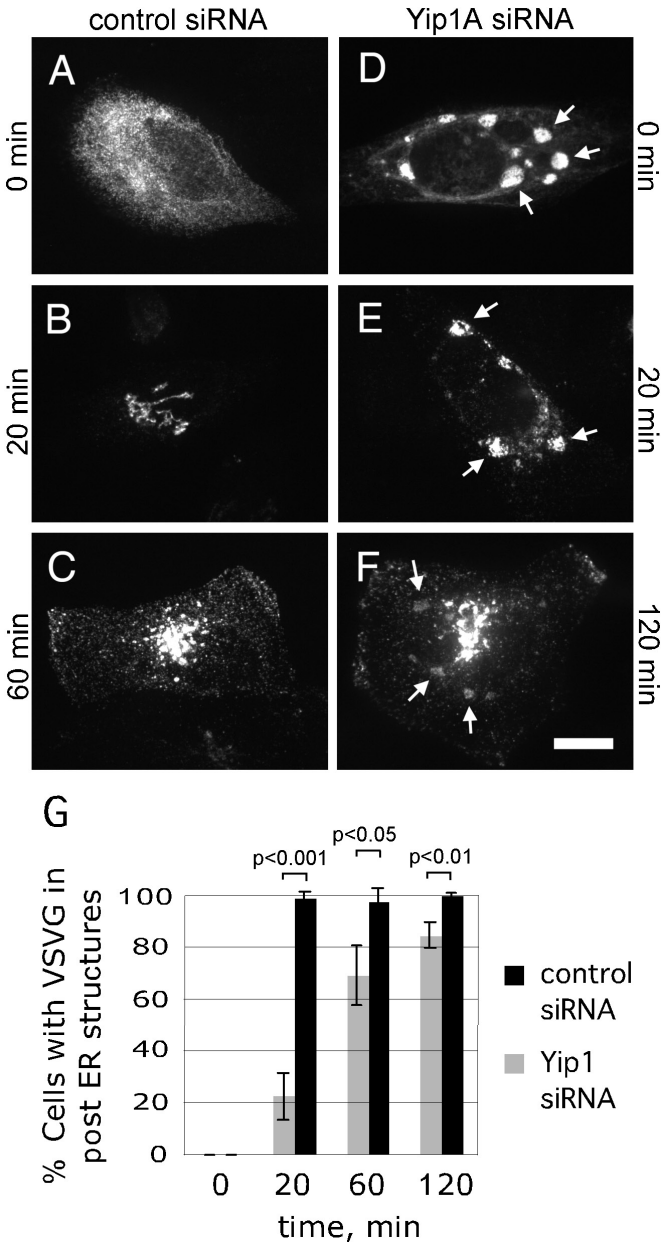

Figure 2-14: Export of ts045 VSV-G from the ER is slowed by ER whorling.

(A-F) Cells cotransfected with Myc-ts045 VSV-G and either a control siRNA (A-C) or Yip1A siRNA-2 (D-F) were shifted 48 hrs. post transfection to 40°C to accumulate VSV-G in the ER. After an additional 24 hrs., cells were shifted to 32°C for 0 (A, D), 20 (B, E), 60 (C) or 120 (F) min to allow ER export. Cells were fixed and doubly stained with antibodies against the Myc epitope and Calnexin (only the Myc staining is shown). Arrows (D-F) indicate the positions of ER whorls as marked by Calnexin staining. Scale bar, 10 μm. (G) Quantitation of the percent of cells expressing Myc-ts045 VSV-G with the protein in post-ER structures. For cells transfected with Yip1A siRNA, only cells with whorled ER, as marked by Calnexin staining, were quantified. Shown are the averages from 3 independent experiments, +/- S.D (p-values obtained using the student's t-test).

with VSV-G in whorled ER declined to ~30% and VSV-G was detected in the Golgi and/or surface in ~70% of cells (quantified in 2-14G). By 120 min, ER export of VSV-G had occurred in >80% of cells displaying whorled ER (Fig 2-14F, quantified in G). Thus ER export was significantly delayed, though not altogether blocked, in the absence of Yip1A. The marked slowing of ER export upon loss of Yip1A function was in agreement with studies in yeast (Heidtman et al., 2003).

To determine whether the slowing of ER export might be due to defects in the recruitment and assembly of COPII subunits to ER exit sites, the steady state distribution of the COPII subunit Sec13 was examined in cells with and without Yip1A. For this, cells were cotransfected with Sec13-Myc and either a control siRNA or Yip1A siRNA. As expected, control cells exhibited a robust Sec13-Myc distribution consistent with an ER exit site pattern (Fig 2-15A). Assembled COPII structures were distributed throughout the dispersed ER (Fig 2-15B, merge in 2-15C). Surprisingly, Yip1A knock down cells also exhibited a robust Sec13-Myc distribution (Fig 2-15D), even in cells with extensive ER whorling (Fig 2-15E). Notably, Sec13 positive structures appeared to be largely excluded from the whorled ER (arrows in merge in Fig 2-15F). This result suggested that Yip1A was not required for the recruitment of COPII subunits to presumptive ER exit sites, though the exit sites formed in its absence appeared altered in their distribution.

To further assess the ability of cells lacking Yip1A to recruit COPII proteins to the ER, an in vitro COPII assembly assay was also performed. To ensure that most of the Yip1A siRNA-treated cells utilized in the assembly assay were depleted of Yip1A, a double sequential knock down was performed. Then to confirm efficient depletion, cells were stained with antibodies against Calnexin 24 hrs. prior to the assembly assay. At this time >95% of the doubly transfected

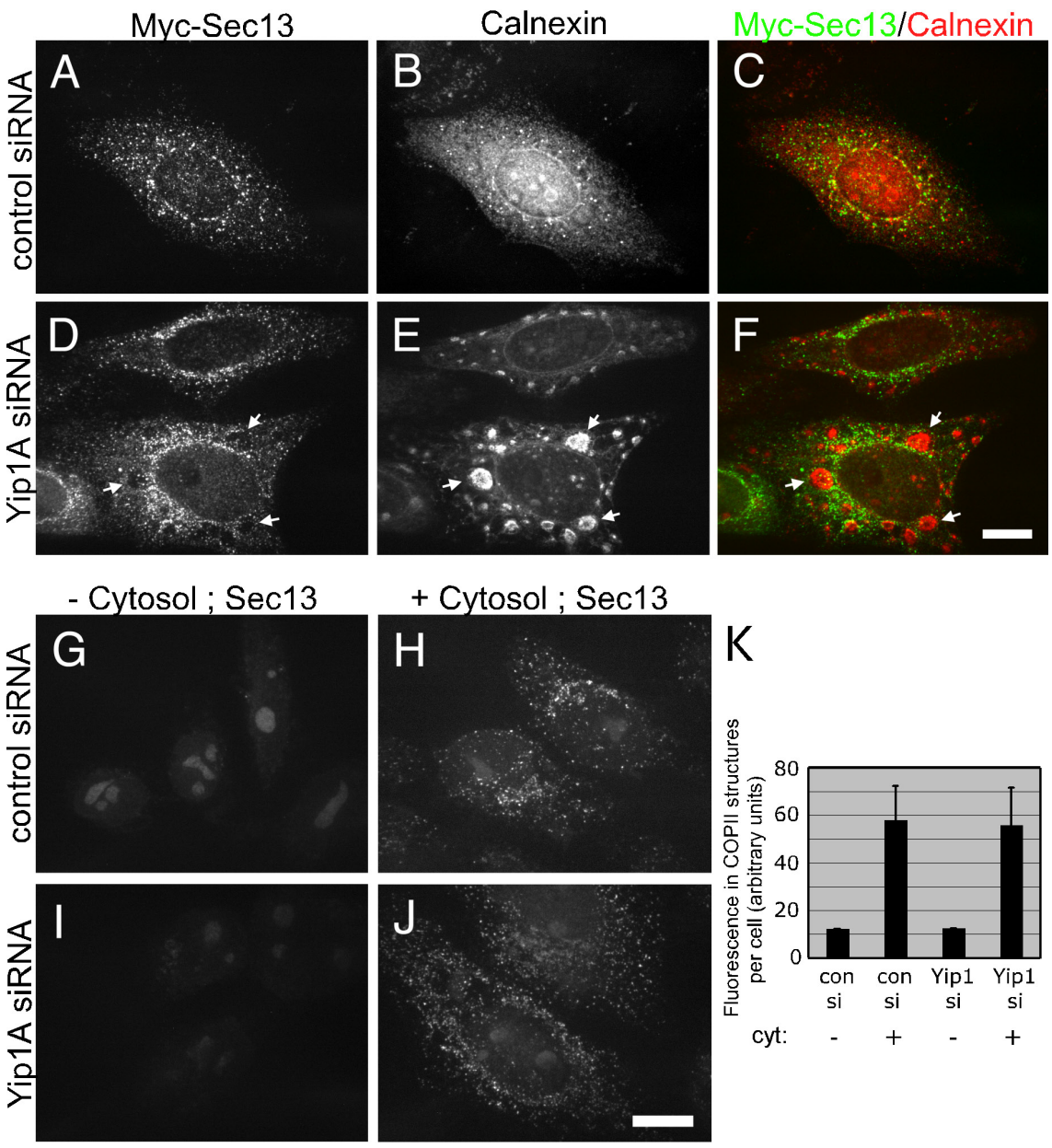

Figure 2-15: COPII recruitment is not blocked in cells lacking Yip1A.

(A-F) Cells co-transfected with Sec13-Myc and either a control siRNA (A-C) or Yip1A siRNA-2 (D-F) were fixed 72 hrs. later and doubly stained with antibodies against the Myc epitope (A, D) and Calnexin (B, E). The merge is also shown (C, F). Arrows (D-F) indicate the lack of Sec13-Myc in ER whorls. Scale bar, 10 µm. (G-K) Cytosol dependent COPII assembly does not require Yip1A. Cells doubly transfected with a control (G, H) or Yip1A siRNA-2 (I, J) were permeabilized with 30 µg/ml digitonin 72 hrs. after the second transfection and incubated with an ATP regenerating system and GTPγ S in the absence (G,I) or presence (H,J) of 4 mg/ml rat liver cytosol. After 20 min at 37°C, cells were fixed and stained with antibodies against Sec13. Scale bar, 10 µm. (K) Quantitation of the total fluorescence in Sec13-positive structures under the indicated conditions is shown, 3 independent experiments, +/- S.D.

Yip1A knock down cells displayed the whorled ER morphology, confirming efficient Yip1A depletion. To monitor the ability of the ER to support COPII assembly in the absence or near complete absence of Yip1A, cells were subsequently permeabilized with digitonin to extract endogenous COPII proteins (Kapetanovich et al., 2005). The permeabilized cells were then incubated in the presence or absence of rat liver cytosol. As expected, COPII assembly did not occur in the absence of added cytosol (Fig 2-15G) but was robust in the presence of added cytosol (Fig 2-15H) in control siRNA-treated cells. Also as expected, cells depleted of Yip1A were incapable of supporting COPII assembly in the absence of added cytosol (Fig 2-15I). However, assembly was again surprisingly robust in the presence of added cytosol (Fig 2-15J, quantified in Fig 2-15K). Thus, although COPII-mediated ER export was significantly delayed in the absence of Yip1A, the delay appeared not to be a simple consequence of inhibition of coat protein recruitment to ER membranes.

BLOCKING ER EXPORT DOES NOT INDUCE ER STACKING

Two straightforward models could account for both the loss of normal ER network morphology and the slowing of ER export in response to Yip1A loss: 1) Yip1A is required primarily for COPII vesicle biogenesis but the inhibition of COPII function resulting from Yip1A loss secondarily cause changes in ER structure. 2) Yip1A is required primarily for ER morphogenesis but the structural rearrangements resulting from Yip1A depletion secondarily inhibit COPII function. To distinguish between these models, we first asked whether an ER export delay similar to that caused by Yip1A loss, but induced by independent means, would lead to ER organizational changes such as those seen in Yip1A knockdown cells. ER export blockade was imposed by two independent means. In the first, cells were treated with siRNAs targeting both Sar1a and Sar1b (Kuge et al., 1994), a GTPase required for COPII assembly and

vesicle formation (Nakano and Muramatsu, 1989). After confirming a block in ER export in Sar1a/b double knock down cells (Fig 2-16A), ER morphology was assessed. As expected, the ER network in control cells with normal levels of assembled Sec13 (Fig 2-16B) was typically dispersed (Fig 2-16C). Significantly, cells with only background levels of assembled Sec13 (Fig 2-16D) also had a relatively normal dispersed ER network morphology (Fig 2-16E). Similar results were obtained when COPII assembly was blocked by another means, this time by treatment with the protein kinase inhibitor H89 (Aridor and Balch, 2000; Lee and Linstedt, 2000). Treatment of cells with H89 caused a rapid redistribution of ERGIC-53 from its typical ERGIC localization (Fig 2-16F) to an ER-like pattern (Fig 2-16H), indicating efficient ER export blockade by H89. Nonetheless, the morphology of the ER, as marked by PDI staining, was similar in both untreated (Fig 2-16G) and H89-treated (Fig 2-16I) cells. Thus neither of two independent means of blocking ER export yielded an ER morphological resembling that obtained by Yip1A depletion. Therefore, the whorled ER phenotype observed upon Yip1A depletion was unlikely to have occurred as a secondary consequence of inhibiting ER export.

ER STACKING IS SUFFICIENT TO SLOW ER EXPORT

We next considered the alternate model, that ER membrane stacking caused by Yip1A loss might be sufficient to delay ER export and account for the diminishment of COPII function in cells lacking Yip1 function. In support of this hypothesis, membrane stacking induced by an unrelated method has previously been shown to delay VSV-G export from the ER (Amarilio et al., 2005). In that case, over-expression of the integral ER membrane anchored VAP-B/Nir2 complex was suggested to lead to membrane stacking through trans-dimerization of VAP-B/Nir2 complexes on opposing membranes, leading to a membrane zippering effect (Amarilio et al., 2005). One caveat however, is that VAP-B, like Yip1A, has also been suggested to function in

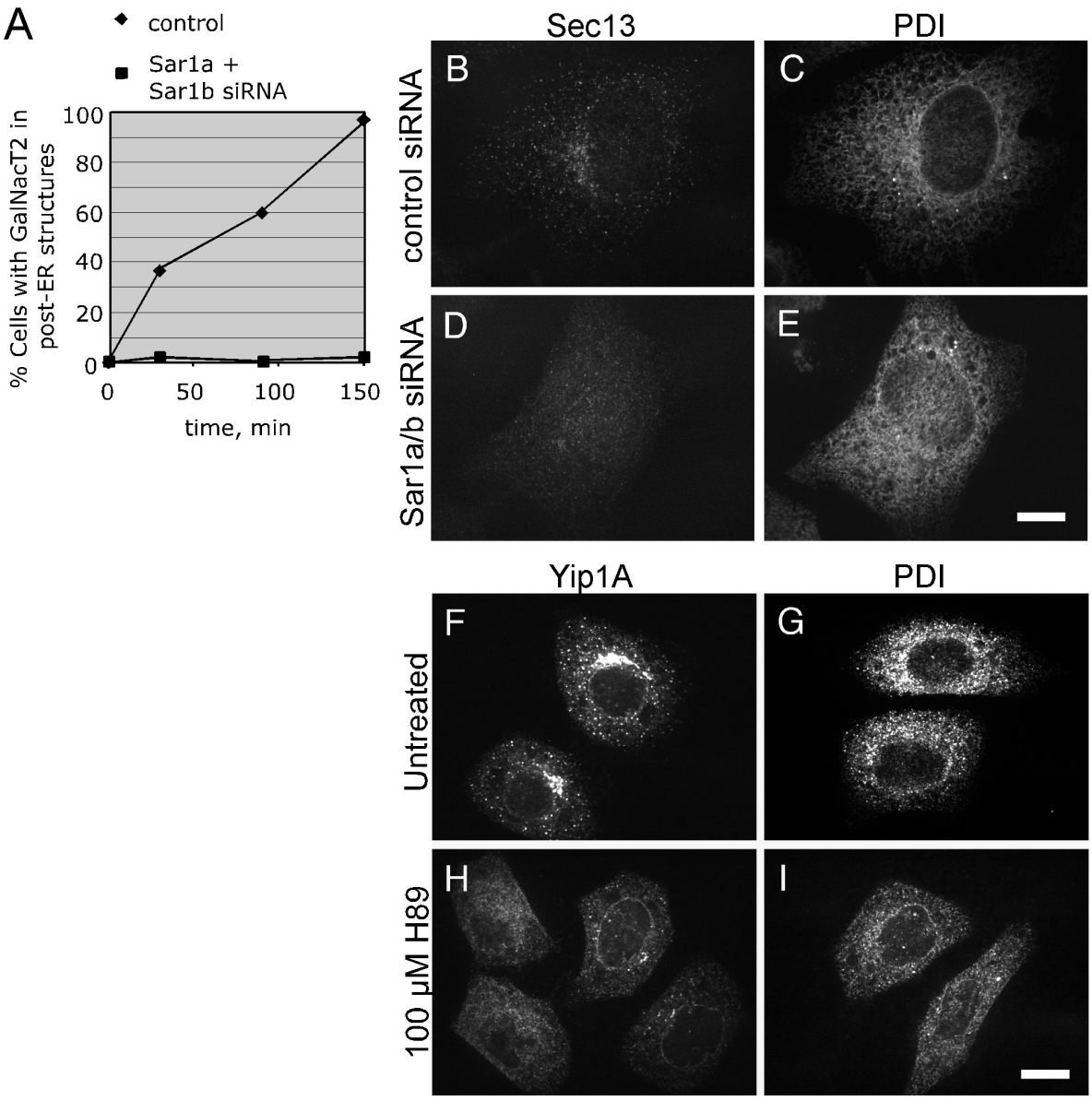

Figure 2-16: ER export blockade is not sufficient to cause ER whorling.

(A-E). (A) Sar1 knockdown blocks ER export. HeLa cells expressing the Golgi marker GFP-GalNacT2 and transfected with a control siRNA or siRNAs targeting both Sar1a and Sar1b isoforms were treated with 2.5 µg/ml BFA for 30 min to redistribute GFP-GalNacT2 to the ER and subsequently incubated without drug to allow ER export. At the indicated times, cells were fixed and the percent of cells with GFP-GalNacT2 in post-ER structures counted. (B-E) ER export blockade by Sar1 knock down does not affect ER morphology. Control (B, C) or Sar1 knock down cells (D, E) were fixed 72 hrs. post transfection and doubly stained with antibodies against Sec13 (B, D) and PDI (C, E). Scale bar, 10 µm. (F-I) ER export blockade by H89 treatment does not affect ER morphology. Untreated cells (F, G) or cells treated for 20 min with 100 µM H89 (H, I) were fixed and stained singly for ERGIC-53 (F, H) or PDI (G, I). Scale bar, 10 µm.

ER-to-Golgi trafficking (Soussan et al., 1999). Thus it remained possible that the delay in ER export induced by VAP-B/Nir2 over-expression could be attributed to a direct role for VAP-B in ER-to-Golgi trafficking. To address this caveat, we sought a means of inducing ER stacking that was unlikely to impact ER export directly. For this, we took advantage of an earlier study demonstrating that over-expression of a dimerizing GFP-Sec61ϒ fusion protein (dGFP-Sec61γ) could drive ER stacking through head-to-head interactions between ER membrane anchored GFP monomers on opposing ER membranes (Snapp et al., 2003). Because neither Sec61γ nor GFP have any role in COPII function, we reasoned that this method of inducing ER membrane stacking provided a way of testing whether ER membrane stacking per se might be sufficient to delay ER export.

To assess ER export efficiency, the time course of VSV-G ER export in cells expressing dGFP-Sec61γ was compared to that in cells expressing mGFP-Sec61γ, a variant incapable of inducing ER stacking due to a mutation in a residue required for GFP dimerization (Snapp et al., 2003). As anticipated, cells expressing dGFP-Sec61γ exhibited compacted ER structures (Fig 2-17B, E, H, K) previously shown to correspond to stacked and whorled ER membranes by EM (Snapp et al., 2003). Also as anticipated, Myc-ts045 VSV-G was predominantly in the compacted ER structures prior to shift to the permissive temperature (Fig 2-17A-C). Even 20 min after the shift, at a time when VSV-G had exited the ER in nearly all cells expressing the control mGFP-Sec61γ construct (Fig 2-17M), nearly 80% of cells with compacted ER retained VSV-G in the compacted ER structures (Fig 2-17D-F, quantified in M). Therefore, the export of VSV-G from the ER was slowed markedly by ER membrane stacking. Export was not blocked though, as VSV-G reached post-ER structures in ~50% of cells with stacked ER by 60 min (Fig 2-17G-I, M), and the number increased further to ~70% at the 120 min time point (Fig 2-17J-L,

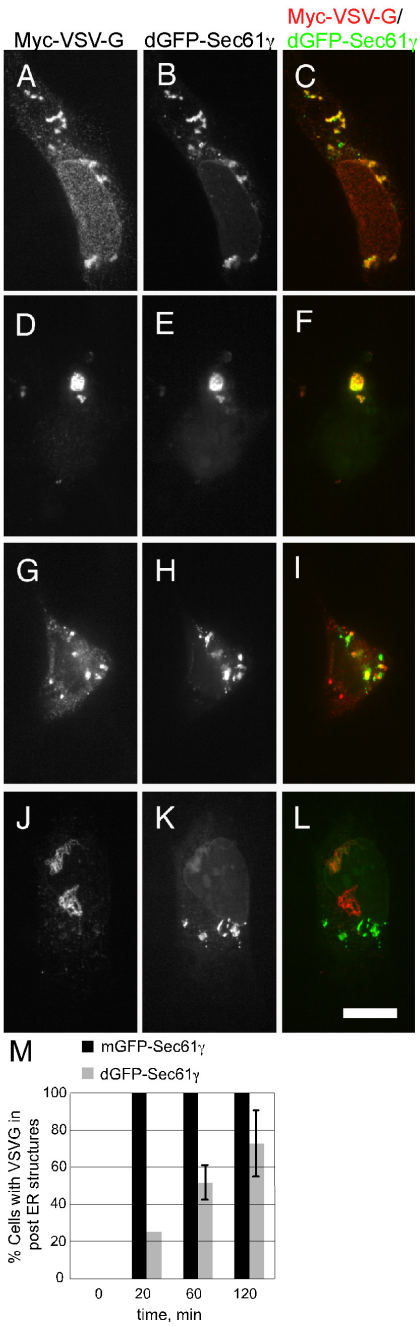

Figure 2-17: ER membrane stacking is sufficient to slow ER export.

Cells co-transfected with Mycts045 VSV-G and either a control mGFP-Sec61γ construct (not shown but quantified in M) or the ER stack-inducing dGFP-Sec61γ construct were shifted to 40°C to accumulate VSV-G in the ER. Thereafter, cells were shifted to 32°C for 0 (A-C), 20 (D-F), 60 (G-I) or 120 (J-L) min. At the indicated times, cells were fixed and stained with Myc epitope antibodies. The corresponding VSV-G (A, D, G, J) and GFP-Sec61γ (B, E, H, K) as well as merged images (C, F, I, L) are shown. Scale bar, 10 μm. (M) Quantitation of the kinetics of VSV-G export under each condition, the average of two independent experiments, +/- S.D. is shown.

M). Interestingly the kinetics with which VSV-G exited the ER in these cells mirrored closely the kinetics with which it exited the ER in Yip1A knock down cells. The results support the notion that membrane stacking per se is sufficient to reduce ER export kinetics. Altogether, the results described herein suggest that Yip1A plays a novel ER network dispersal function. ER network dispersal by Yip1A in turn is required for rapid ER export.

DISCUSSION

Yip1A depletion in mammalian cells led to dramatic alterations in ER network organization unlike any previously documented for a specific loss of function perturbation. Based on the combined data, we hypothesize that Yip1A plays a role in maintaining a dispersed ER network. In its absence, ER membranes undergo a stacking and whorl formation reaction that in turn slows protein export. Our results also provide experimental support for the notion that a general change in the organization of the ER network can significantly impact rates of protein export from the organelle. Further, they suggest the possibility that certain specialized cells might use large scale ER reorganization to elicit transient changes in the secretory capacity of the ER.

Previous studies have reported variable degrees of Golgi fragmentation but no ER morphological change or delay in ER-to-Golgi trafficking after Yip1A RNAi (Yoshida et al., 2008; Kano et al., 2009). A potential underlying explanation for the observed differences in the knockdown phenotype is the extent of Yip1A depletion obtained with distinct siRNAs. Indeed, we have observed a strong correlation between ER morphology and the level of residual Yip1A protein remaining after knockdown. Cells without detectable Yip1A almost always displayed the whorled ER phenotype, whereas cells with residual Yip1A did not, suggesting that low levels of Yip1A are able to maintain a relatively dispersed ER network.

THE BASIS FOR INHIBITION OF ER EXPORT BY ER MEMBRANE STACKING AND WHORLING

Why does ER membrane stacking and whorling delay COPII-mediated protein export? COPII proteins were recruited efficiently to presumptive ER exit sites even in the absence of

Yip1A, and yet ER export of VSVG was markedly slowed. One potential explanation is that reorganization of a large fraction of the ER into stacked whorls sequesters cargo molecules away from cytoplasmic coat proteins, thereby reducing the efficiency of cargo capture by the COPII coat. Thus COPII vesicle formation per se might proceed in the absence of Yip1A, but the resulting vesicles might contain reduced amounts of cargo. While our FRAP data suggests that the diffusion of mGFP-Sec61γ into and presumably out of whorls is relatively unrestricted (Fig 2-9), the diffusional mobility of VSV-G has not yet been examined and may be preferentially hindered. An alternative possibility is that a late step in COPII vesicle biogenesis, subsequent to the initial steps of Sar1 activation and coat protein recruitment, is sensitive to the membrane morphological changes associated with ER stacking and whorling. Generation of either positive or negative membrane curvature or the mixing of phospholipids ultimately required for vesicle budding may comprise this late step.

YIP1A MAY REGULATE THE ABILITY OF ONE OR MORE ER PROTEINS TO INTERACT IN-*TRANS*

Although the MT cytoskeleton and associated motor proteins are acknowledged to play a key role in extending ER tubules towards the cell periphery (Waterman-Storer and Salmon, 1998), they are unlikely to account for all of the observed variations in ER morphology. Indeed, ER membrane stacking is readily experimentally inducible without perturbation of the MT cytoskeleton. High-level expression of several distinct ER membrane anchored proteins including HMG-CoA reductase (Chin et al., 1982), microsomal aldehyde dehydrogenase (Yamamoto et al., 1996), cytochrome b(5) (Pedrazzini et al., 2000), the inositol 1,4,5-triphosphate receptor (Takei et al., 1994), and the ER anchored VAP-B along with its binding partner Nir2 (Amarilio et al., 2005) have each been shown to drive ER stacking. In many if not

all cases, membrane stacking appears to be driven by the ability of the cytoplasmic domain of the over-expressed protein to interact with itself in-trans, in effect 'zippering' apposing membranes together. Even low affinity (100 μM) interactions between membrane-anchored GFP monomers were sufficient to drive formation of stacked structures as long as the monomers were expressed at high enough concentrations to drive the head-to-head binding reaction (Snapp et al., 2003). Thus it appears that the ER network has an inherent propensity to undergo stacking. As such, a general mechanism for preventing undesired stacking reactions might contribute significantly to the morphogenesis of a dispersed ER network. Conversely, down-regulation of a factor such as Yip1A that promotes network dispersal might provide a mechanism for generating stacked and whorled membranes in accordance with a physiological need, for instance, to transiently slow the export of lipid and protein from the ER.

NETWORK DISPERSAL BY YIP1A MAY INVOLVE DP1

Although trans-interactions between ER membrane proteins may underlie ER stacking and whorled ER formation in Yip1A knock down cells, alternate mechanisms can be envisioned. In this regard, several putative Yip1 binding partners have been reported in yeast (Calero et al., 2001; Heidtman et al., 2003; Chen et al., 2004; Heidtman et al., 2005). Among the group, the conserved integral ER membrane protein Yop1 (DP1 in mammalian cells) is unique in its steady state localization to the ER as well as its previously proposed role in tubulating ER membranes (Voeltz et al., 2006). Moreover, an antagonistic relationship between Yip1 and Yop1 has been established in yeast (Calero et al., 2001). As such, DP1 stands out as a possible mediator of Yip1A function in ER network dispersal. Indeed, we have observed that both DP1 and the related DP1L1 protein can be co-immunoprecipitated with mammalian Yip1A. Further, DP1 is present in ER membrane whorls (Fig 2-18). However, assessing the functional significance of

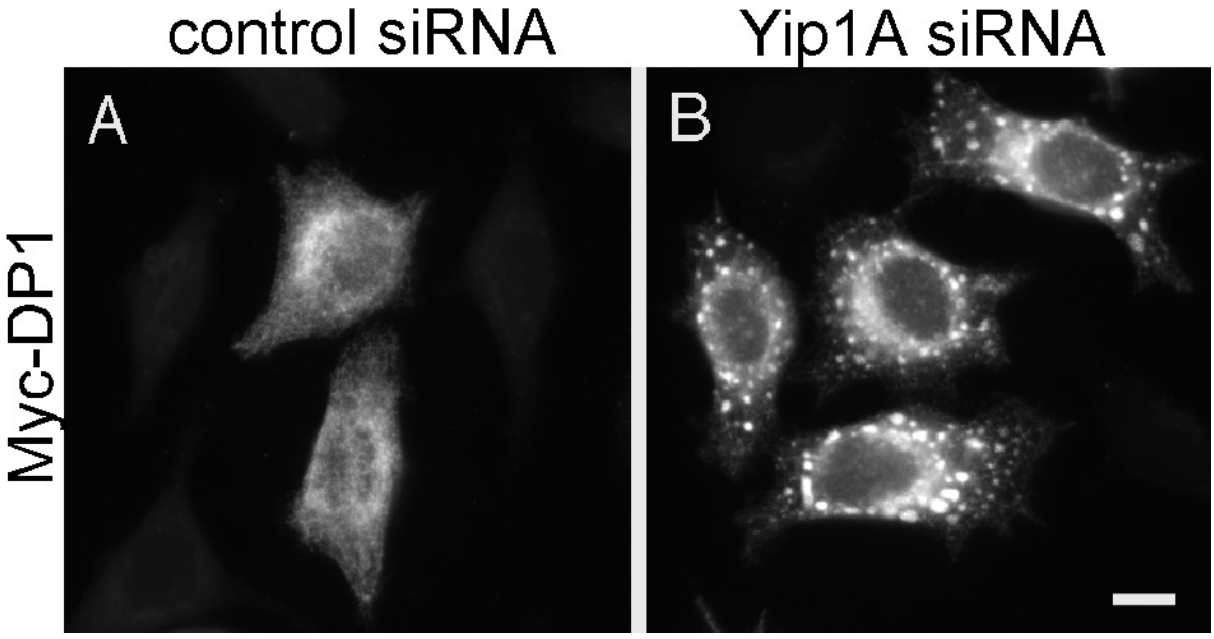

Figure 2-18: DP1 is in ER whorls.

Cells co-transfected with Myc-DP1 and either a control siRNA (A) or Yip1A siRNA (B) were fixed 72 hrs. later and stained with antibodies against the Myc epitope. Scale bar, 10 μm.

the interaction will require mapping the DP1 binding determinant in Yip1A and testing whether the binding interaction is required for the network dispersal function of Yip1A. If indeed the ER dispersal function of Yip1A were to involve DP1, it would be of interest to determine whether the underlying mechanism of network dispersal involves the proposed membrane curvature-inducing activity of DP1 (Voeltz et al., 2006; Hu et al., 2008). For instance, Yip1A might be envisioned to negatively regulate DP1, perhaps through competitive inhibition of the homo-oligomerization of DP1 that has been suggested to tubulate ER membranes. In the absence of Yip1A, excessive oligomerization of DP1 would lead to excessive tubulation of the ER, resulting in ER whorls.

ADDITIONAL ROLES FOR YIP1A

While our results indicate a novel role for Yip1A in ER membrane morphogenesis, Yip1A may play additional roles in the early secretory pathway. Indeed, while a significant pool of Yip1 is in the ER at steady state (Lorente-Rodríguez et al., 2009), it also appears to cycle rapidly between the ER and Golgi (Heidtman et al., 2003; Yoshida et al., 2008). Therefore Yip1A appears to exit the ER at a significant rate and may travel as far as the early Golgi before being retrieved back to the ER. Interestingly, Yip1A knock down has been reported to lead to a reduction in membrane-associated Rab6, suggesting that Yip1A somehow stabilizes Rab6 on membranes (Kano et al., 2009). The loss of membrane-bound Rab6 in turn was associated with a slowing of Shiga toxin trafficking from the Golgi to the ER, suggesting a possible role for Yip1A in Rab6-mediated retrograde trafficking (Sun et al., 2007; Kano et al., 2009). Consistent perhaps with those observations, we have detected a delay in the retrograde redistribution of ERGIC53 to the ER upon ER export blockade in Yip1A knock down cells (unpublished data). Thus there may be an additional role for Yip1A in ERGIC-to-ER retrograde transport that might help to

explain the Golgi fragmentation observed in Yip1A knock down cells. Indeed additional roles for the protein as it cycles through post-ER compartments may account for the ability of Yip1A to interact with specific proteins within the early Golgi. Further work will be required to elucidate these other potential roles of Yip1A. Nonetheless, it is important to note that the ER structuring defects observed herein are unlikely to occur as a consequence of Rab6 membrane dissociation or a block in retrograde transport, as previous studies have shown that targeted Rab6 (Sun et al., 2007) and COPI (Guo et al., 2008) knockdown has no obvious effect on ER network morphology.

ER WHORLING IS REVERSIBLE AND REGULATED

Concentrically whorled and stacked ER membranes have been documented in a surprising number and variety of normal tissues, though the functional significance of the membrane whorls remains largely unknown (Carr and Carr, 1962; Nickerson and Curtis, 1969; King et al., 1974). Intriguingly, the majority of the tissues in which ER whorls have been documented serve to secrete either peptide or steroid hormones (King et al., 1974). In the case of GnRH-secreting hypothalamic arcuate neurons, ER whorls peak during the diestrus phase of the estrous cycle, diminishing during the proestrus, when an increase in GnRH secretion signals the pituitary to release leutinizing hormone (King et al., 1974). Thus ER whorling is a reversible process that is regulated by specific signaling pathways. It is tempting to speculate that rearrangement of the ER into whorls may serve to reversibly regulate hormone secretion. Finally, whether the Yip1A-dependent ER dispersal/ER whorling pathway might provide a regulatory mechanism contributing to the formation of such structures is an intriguing possibility that remains to be explored.

MATERIALS AND METHODS

CELL CULTURE, CONSTRUCTS AND TRANSFECTIONS

HeLa cells were maintained in MEM (Sigma-Aldrich) containing 10% fetal bovine serum (Atlanta Biological) and 100 IU/ml of penicillin and streptomycin (Mediatech) at 37ºC in a 5% CO2 incubator. Knockdown of HeLa cells stably expressing GalNacT2-GFP (Storrie et al., 1998) was performed with Oligofectamine (Invitrogen) as described previously, using 40 nM siRNA (Kapetanovich et al., 2005), with the exception that a single transfection was sufficient for knockdown. The siRNAs were synthesized using the siRNA construction kit from Ambion. The two siRNAs (-1, -2) used against Yip1A were made against the following target sequences, respectively: AAGTTACAGCATCGATGATCA and AATGGTTTTTTGCCTTGCTTT. The siRNA target sequence for Sar1a was AACCACTCTTCTTCACATGCT and AAGAACTGACCATTGCTGGCA for Sar1b. The control siRNA used throughout this study targeted bovine p115 and does not affect p115 in HeLa cells as described previously (Puthenveedu and Linstedt, 2004).

Transient co-transfection of HeLa cells with both plasmid DNA and siRNA was performed with Lipofectamine 2000 (Invitrogen) according to manufacturer's specifications using 150 ng DNA and 10 pmol siRNA per 0.5 ml. Yip1A was cloned out of a HeLa cDNA library using PCR and inserted into the pCS2-MT vector (Turner and Weintraub, 1994) using the EcoRI and XbaI sites. The Flag-tagged Yip1A construct was generated by cutting out the myc-epitope using the BamHI and EcoRI sites, followed by the addition of a single Flag epitope using a PCR based loop-in modification of the QuikChange protocol (Stratagene). The Yip1A rescue construct was generated by introducing silent mutations into the siRNA-2 target sequence using QuikChange (AATGGTCTTCTGTCTTGCTTT). The E95K mutation in the rescue construct

was also generated by QuikChange using the sequence GAGCCACCTTTATTAGAAAAGTTAGGTATCAATTTTGACCAC. The Myc-tagged Sec13 control construct was cloned by PCR amplification from HeLa cDNA and inserting the PCR product into the pCS2-MT vector using BamHI and ClaI. The Myc-ts045 VSV-G construct was cloned using PCR to amplify ts045 VSV-G and inserting the product into the pCS2-MT vector at the BamHI site. Myc-tagged DP1 and DP1L1 were generated by PCR amplification from HeLa cDNA and insertion into EcoRI and XbaI sites in pCS2-MT. Sec61γ -GFP (both monomeric mGFP or a dimerizing dGFP) was kindly provided by Dr. E. Snapp (Albert Einstein University).

ANTIBODIES AND OTHER REAGENTS

Antibodies used include mouse mAb against PDI (Abcam), a rabbit pAb against Calnexin (Abcam), a rabbit pAb against BiP (ABCAM), a rabbit pAb against LC3 (Cell Signaling), a rabbit pAb against Tubulin (Abcam), rabbit pAbs against Giantin, GM130 and GRASP65 (kindly provided by Dr. A. Linstedt, Carnegie Mellon University), a mouse mAb against ERGIC-53 (kindly provided by Dr. H.P. Hauri, Biozentrum, University of Basel), the M2 mouse mAb against the FLAG epitope (Sigma-Aldrich), and a mouse mAb against the Myc epitope from the 9E10 cell line. Fluorophore-conjugated secondary antibodies were from Zymed/Invitrogen. A rabbit pAb was raised against a 6His-Yip1A (aa 1-89) fusion protein as antigen (Covance), and was affinity purified on Affi-Gel 15 beads (Bio-Rad) coupled with a GSTYip1A N-terminal fusion protein. A rabbit pAb was raised against GST-Sec13 (Covance) and affinity purified on Affi-Gel 10 beads (Bio-Rad) coupled with 6His-Sec13. H89 was from Toronto Research Chemicals and BFA was from Sigma-Aldrich.

IMMUNOFLUORESCENCE AND IMMUNOBLOT ASSAYS

siRNA transfections were analyzed 48-72 hours post transfection as indicated.

Immunofluorescence procedures were as described previously (Kapetanovich et al., 2005) except that a 20 min ice-cold methanol fixation was substituted for PFA. Immunoblotting using our affinity-purified Yip1A antibody, as well as rabbit pAbs against Calnexin and Tubulin (Abcam), was performed on siRNA-treated cells harvested from 60 mm dishes as described previously (Kapetanovich et al., 2005).

LIGHT MICROSCOPY AND PHOTOBLEACHING EXPERIMENTS

All static images with the exception of those in Fig 4 were obtained using a Yokagawa spinning disk confocal scanhead (PerkinElmer) mounted on a Zeiss Axiovert 200 microscope with a 100x 1.4 NA objective (Carl Zeiss, Inc) and acquired using a 12-bit Orca ER digital camera (Hamamatsu Photonics). Maximum value projections of sections at 0.3 μm spacing (4-6 per cell) were acquired using Imaging Suite software (PerkinElmer). Quantitation of COPII assembly was carried out using ImageJ (NIH) as previously described (Kapetanovich et al., 2005). The wide field images in Fig 4 were obtained with a 63x 1.3 NA objective on a Zeiss Axioplan microscope and acquired with QED software and a 12-bit Orca ER digital camera (Hamamatsu Photonics).

FRAP analyses were performed on a Zeiss 510 Meta/UV Duoscan Spectral Confocal with LSM Zen 2007 software using a 100x 1.4 NA objective. Regions of interest were subjected to photobleaching with repeated pulses at 100% laser power with the pinhole wide open to obtain maximal depth of field. Recovery after photobleaching was monitored with attenuated laser power. To generate the fluorescence recovery curves, fluorescence within the photobleached region of interest at each time point was first normalized to that of a non-bleached reference region to account for general loss of fluorescence due to image acquisition. Recovery curves were then generated by setting the fluorescence intensity prior to bleaching to 100% and the

intensity after the last bleach pulse to 0%.

ELECTRON MICROSCOPY

35 mm dishes of HeLa cells treated with control and Yip1A siRNA were fixed 48 or 72 hrs. post-transfection with 2% glutaraldehyde/PBS for 30 min at room temperature. After 3 washes in PBS, cells were further fixed in 2% potassium permanganate/H2O for 45 min, washed 3 times in dH2O, followed by dehydration in an ascending series of ethanol (10-100%). Samples were then infiltrated in a 1:1 mixture of Epon-Araldite and 100% ethanol. After 30 minutes, the mixture was exchanged with 100% Epon-Araldite and held in a desiccator for 60 hrs. Samples were then transferred for 24 hrs. each at 30°C, 40°C, 50°C and 60°C. Epoxy disks were removed from the dishes, and areas of the disk with cells were cut out and glued onto a blank embedding capsule with two-part epoxy. Thin (100nm) sections were cut using a DDK diamond knife on a Reichert-Jung Ultracut E Ultramicrotome and stained with lead citrate for 2 minutes. The grids were viewed on a Hitachi H-7100 transmission electron microscope (Hitachi High Technologies America, 5100 Franklin Drive, Pleasanton, CA, 94588) operating at 75 kV. Digital images were obtained using an AMT Advantage 10 CCD Camera System (Advanced Microscopy Techniques Corporation, 3 Electronics Ave., Danvers, MA, 01923) and NIH Image.

CO-IMMUNOPRECIPITATION ASSAY

For the pull down of DP1 and DP1L1 with endogenous Yip1A, a 10 cm plate of HeLa cells was transfected with either Myc-DP1 or Myc-DP1L1 using CaPO4. After 72 hours, cells were washed with cold PBS, then scraped and solubilized for 30 min at 4°C for in HKT lysis buffer (100mM KCl, 1% TritonX-100, 20 mM KHEPES, pH 7.2, protease inhibitors). The lysate was then passed five times through a 25-gauge needle then centrifuged for 20 min at 14,000 x *g*. The lysates were then incubated with 5 µl of antibody (IgG or Yip1A) bound to 15 µl Protein A

Sepharose beads (GE Healthcare) that had been washed in lysis buffer. After a two-hour incubation at 4°C, the beads were washed 3x with lysis buffer. The beads were then boiled for 10 min in 50 µl 2X RSB and resolved on a 10% SDS gel. Immunoblotting was performed using anti-Myc antibodies.

For the pull down of DP1 using the Flag-Yip1A constructs, 2 x10 cm plates of HeLa cells were transfected with either Myc-DP1 only, Flag-Yip1A-wt and Myc-DP1, or Flag-Yip1A-E95K and Myc-DP1 using jetPEI (Polyplus-Transfection Inc., New York) according to manufacturer's specifications. The immunoprecipitation was performed as described above, however the lysates were incubated with anti-Flag M2 agarose beads (Sigma-Aldrich).

TS045-VSV-G TRANSPORT ASSAY

To assay ER export in Yip1A knock down cells, HeLa cells were co-transfected with either Myc-ts045 VSV-G and a control siRNA, or Myc-ts045 VSV-G and Yip1A siRNA using Lipofectamine 2000 (Invitrogen). 48 hrs. after transfection, cells were placed at 40°C, the non-permissive temperature for ER export of ts045 VSVG, to accumulate VSVG in the ER. Following a 24 hr. incubation at the non-permissive temperature, cells were shifted to the permissive temperature of 32°C for varying times. To assay ER export in cells expressing GFPSec61γ, HeLa cells were co-transfected with Myc-ts045 VSV-G and either dGFP-Sec61γ or mGFP-Sec61γ. 24 hrs. after transfection, cells were shifted to 40°C and processed for the trafficking assay as described just above.

IN VITRO COPII ASSEMBLY ASSAY IN YIP1A KNOCK DOWN CELLS

Cells in a 10 cm dish were transfected with either control or Yip1A siRNA using Oligofectamine (Invitrogen) and passaged onto coverslips after 24 hrs. After an additional 24 hrs., a second siRNA transfection was performed. Knockdown was monitored 48 hrs. following

the second transfection by immunostaining with Calnexin antibodies. At this time, the whorled ER phenotype was confirmed in >95% of cells. The COPII assembly assay was performed precisely as previously described (Lee and Linstedt, 2000) 72 hrs. after the second transfection.

This chapter appeared as an article in the journal Molecular Biology of the Cell:

Dykstra, K.M., Pokusa, J.E., Suhan, J., and Lee, T.H. (2010). Yip1A structures the mammalian endoplasmic reticulum. Mol. Biol. Cell *21*, 1556–1568.

CHAPTER 3

IDENTIFICATION OF DISCRETE SITES IN YIP1A NECESSARY FOR REGULATION OF ENDOPLASMIC RETICULUM STRUCTURE

INTRODUCTION

The ER is a singular and essential organelle with a complex three-dimensional structure. The organelle consists of both flattened sheet-like cisternal membranes and highly curved tubules that are interconnected at hundreds of three-way junctions (Voeltz et al., 2002). In most cell types, ER membranes are widely distributed throughout the cell cytoplasm, extending from the outer nuclear envelope to the cell periphery (Terasaki et al., 1986; Lee et al., 1989; Baumann and Walz, 2001).

Many essential processes, including protein and lipid biosynthesis, drug detoxification and calcium regulation, occur within sub-domains of the ER (Baumann and Walz, 2001). In response to specific developmental cues, select sub-domains of the ER undergo dramatic expansion, presumably reflecting physiological changes in demand for certain ER functions over others (Wiest et al., 1990). The ER can also undergo major changes in overall organization, suggesting that organelle organization also impacts function. For instance, in professional secretory pancreatic acinar cells, flattened sheets of ribosome-studded rough ER membranes are organized into highly regular parallel arrays (Rajasekaran et al., 1993; Baumann and Walz, 2001). In other specialized cell types that secrete either peptide or steroid hormones, rough or

smooth ER membranes undergo reversible reorganization into concentric ribbon-like whorls (Carr and Carr, 1962; Nickerson and Curtis, 1969; King et al., 1974). In most cases, neither the mechanisms that alter ER organization, nor the functional consequences on organelle function, are well understood.

We previously identified the ER-to-Golgi cycling protein Yip1A as a regulator of ER network structure and organization. RNAi mediated knockdown of Yip1A in HeLa cells resulted in a remarkable transformation of the typically dispersed ER network into tightly stacked, micrometer sized concentric membrane whorls (Dykstra et al., 2010). Importantly, the ER whorl phenotype, somewhat reminiscent of the ribbon-like concentric whorls seen in specialized cells (Carr and Carr, 1962; Nickerson and Curtis, 1969; King et al., 1974), was specific to the loss of Yip1A, as it was rescued by the expression of a siRNA immune Yip1A construct (Dykstra et al., 2010).

Our identification of Yip1A as an apparent ER structuring protein was surprising in many respects. First, although as much as half the protein is present in the ER at any given time (Heidtman et al., 2005), Yip1A undergoes constant ER exit and depends on retrieval from post-ER compartments to achieve its steady state ER exit site localization (Heidtman et al., 2003; Yoshida et al., 2008). Second, Yip1A was initially discovered in yeast as a protein required for vesicle trafficking rather than organelle structuring. In one set of studies yeast Yip1p was implicated in COPII-mediated vesicle biogenesis (Heidtman et al., 2003); while in another, Yip1p was implicated in fusion of ER-derived COPII vesicles with the Golgi (Barrowman et al., 2003). Additionally, Yip1A has been shown to bind the Sec23/24 subunit of the COPII coat (Tang et al., 2001). Stable binding partners of Yip1p have been identified in Yif1p (Matern et al., 2000) and Yos1p (Heidtman et al., 2005), also ER-to-Golgi cycling proteins. Additional

transient interacting partners have been found in Yop1p (Calero et al., 2001) and the Ypt1p/Ypt31p sub-class of Rab GTPases (Yang et al., 1998; Chen et al., 2004). In yet another set of studies, mammalian Yip1A was found to be required for COPI-independent retrograde trafficking to the ER (Kano et al., 2009). Consistent with earlier observations that Yip1p/Yip1A is required for proper trafficking between the ER and Golgi, our work also revealed a marked delay of COPII-mediated protein export from the ER in HeLa cells depleted of Yip1A (Dykstra et al., 2010). However, the delay could also be attributed to a secondary consequence of ER whorl formation, as whorl formation through an entirely independent means (Snapp et al., 2003) was also sufficient to delay ER export (Dykstra et al., 2010).

In this study, we wished to gain insight into the molecular mechanism by which Yip1A regulates ER structure. Taking advantage of the ability of a siRNA-immune Yip1A transgene to rescue the whorled ER phenotype in knockdown cells (Dykstra et al., 2010), we carried out a systematic mutational analysis of nearly all residues in the protein; our goal being to determine those residues most important for its ER structural maintenance role. Our analysis revealed two discrete sites (E95 and K146) clearly important for Yip1A function. Strikingly, the identified sites correspond precisely to two sites in the yeast homologue Yip1p previously shown to be essential for maintaining yeast viability. In contrast, a third site (E89), also shown to be essential in yeast, was dispensable for Yip1A function in regulating ER whorl formation. Significantly, the site dispensable for control of whorl formation (E89) was previously shown to be necessary for interaction of Yip1p with its established binding partners Yif1p and Ypt1p/Ypt31, whereas the sites essential for ER structural maintenance by Yip1A were previously shown to be dispensable for binding Yif1p and Ypt1p/Ypt31p. Collectively, these results suggest that the two sites in Yip1A identified herein likely mediate regulation of ER membrane whorl formation

independently of its established binding partners. Consistent with a lack of requirement for Yif1p/Yif1A in regulating ER structure, its knockdown did not cause ER whorls.

RESULTS

BOTH THE CYTOPLASMIC AND TRANSMEMBRANE DOMAINS OF YIP1A ARE REQUIRED FOR ER STRUCTURAL MAINTENANCE

We began by testing the cytoplasmic and multi-pass transmembrane (TM) domains of Yip1A independently for their ability to regulate ER whorls. We generated two constructs based on the siRNA-immune HA-Yip1A parent rescue construct (schematized in Fig 3-1C). One replaced the C-terminal TM domain of Yip1A with the single pass C-terminally anchored TM domain of Sec61β (Kalies et al., 1998) so as to maintain ER membrane targeting of the cytoplasmic domain (HA-Yip1AN/Sec61β TM; schematized in Fig 3-1F). The other truncated the entire N-terminal cytoplasmic domain (HA-Yip1A Δ1-118; schematized in Fig 3-1I). Each construct was transiently co-transfected into HeLa cells with the Yip1A siRNA and processed 3 days later for immunofluorescence using antibodies against HA and the integral ER membrane marker calnexin (Ahluwalia et al., 1992). Similar to our previous report (Dykstra et al., 2010), 68 ±3% of cells expressing the negative control construct Myc-Sec61β had ER whorls; whereas virtually none expressing wild type HA-Yip1A (Fig 3-1A,B) displayed whorls; this was as expected for full rescue by the wild type transgene. For ease of comparison across experiments, we present the data from hereon in terms of rescue efficiency (calculated as detailed in Experimental Procedures), with 1 representing full rescue as exhibited by wild type Yip1A and 0 representing non-rescue as exhibited by the negative control Myc-Sec61β. Notably, neither HA-Yip1AN/Sec61TM (Fig 3-1D,E; quantified in J) nor HA-Yip1A Δ1-118 (Fig 3-1G,H; quantified in J) were able to rescue the ER whorl phenotype; rather they were both indistinguishable from

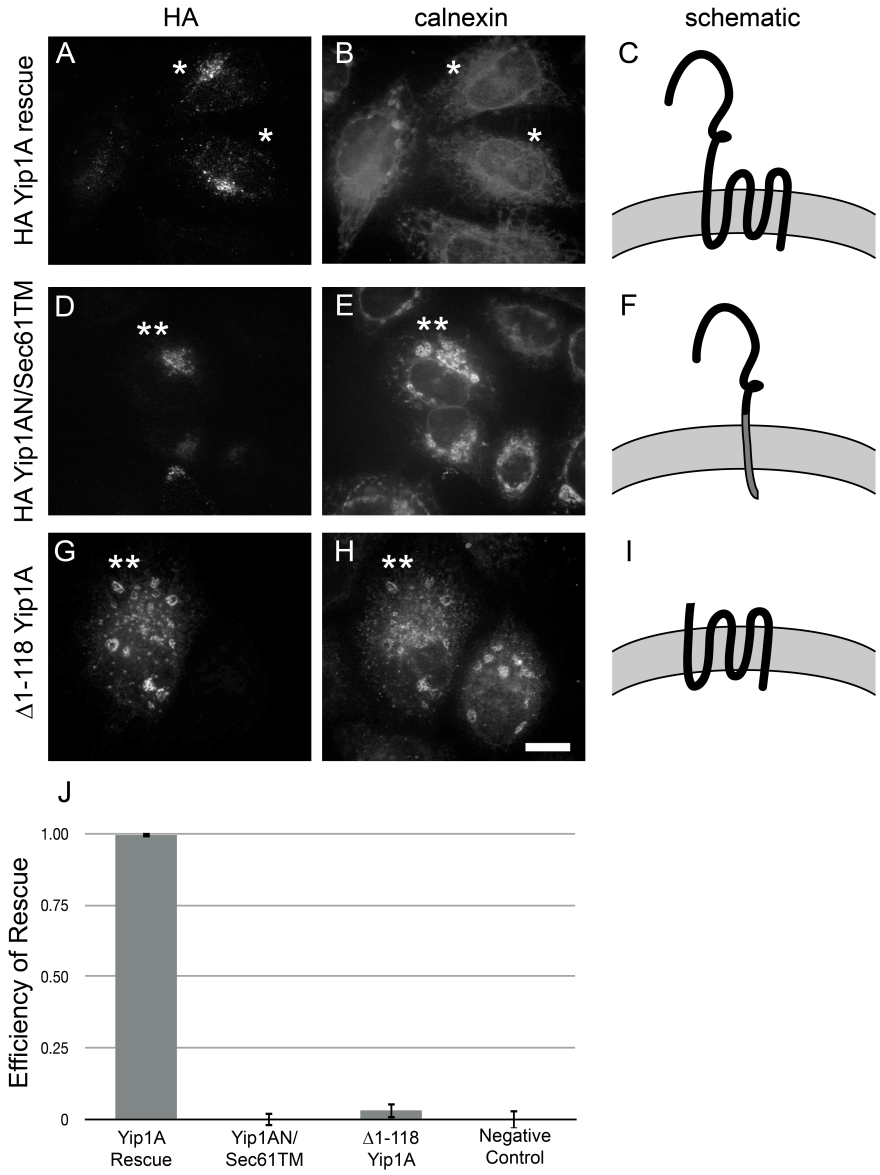

Figure 3-1: Both the cytoplasmic and TM domains of Yip1A are required to maintain a dispersed ER.

HeLa cells were co-transfected with Yip1A siRNA and either a negative control myc-Sec61β construct (not shown), a wild-type HA-Yip1A rescue construct (A-C), a chimeric construct (HA-Yip1AN/Sec61TM) with the N-terminus of Yip1A fused to the TM helix of Sec61β (D-F), or a Yip1A truncation construct (HA-Yip1A Δ1-118) lacking the entire cytoplasmic domain (G-I). Cells were fixed 72 h after transfection and co-stained with antibodies against HA (A, D, G) or Myc (not shown) and calnexin (B, E, H). Single asterisks mark cells expressing the indicated construct that do not exhibit ER whorls; whereas double asterisks mark expressing cells that do exhibit ER whorls. Scale bar, 10 μm. The constructs are schematized (C, F, I). (J) Quantification of the efficiency of rescue by wild type HA-Yip1A, HA-Yip1AN/Sec61TM, HAYip1A Δ1-118 or the Myc-Sec61β negative control (as detailed in Experimental Procedures). Data were from 3 independent experiments (>100 cells per experiment), ±SD.

the negative control. Thus Yip1A depends on both its cytoplasmic and TM domains for function.

ONLY A FEW KEY RESIDUES COMPRISING A SINGLE SITE IN THE CYTOPLASMIC DOMAIN ARE REQUIRED

Given that the cytoplasmic and TM domains of Yip1A were both required for function, we sought to define the necessary elements in each half, starting with the cytoplasmic domain. We previously showed that a conserved Glu residue (E95) required for Yip1p-dependent viability in yeast (Chen et al., 2004) was also required for the ER structuring function of Yip1A in HeLa cells (Dykstra et al., 2010). However, we wanted to extend our prior analysis by determining if the Yip1A cytoplasmic domain contained any other residues essential for function. We began by performing progressive truncations from the N-terminus of the protein, testing each truncated version for function. Deletion of the first 83 amino acids had no observable effect on function, with virtually all cells expressing the truncated protein having a normal dispersed ER morphology (Fig 3-2A,B and quantified in C). This suggested that the first 83 amino acids are dispensable for the ER structuring function of Yip1A. These results were consistent with an earlier observation that the first 65 residues of the yeast homolog Yip1p are dispensable for yeast viability (Chen et al., 2004). However, as indicated above, further truncation to residue 118 (the end of the cytoplasmic domain) resulted in a non-functional, though stably expressed protein (Fig 3-1G,H; quantified in J), narrowing the required elements in the cytoplasmic domain to between residues 83 and 118.

An alignment between the yeast and human Yip1 sequences revealed a highly conserved block of residues between the human residues 89 and 113 (Fig 3-2D). We proceeded to replace either individual or pairs of residues in the conserved block with Ala (unless otherwise indicated

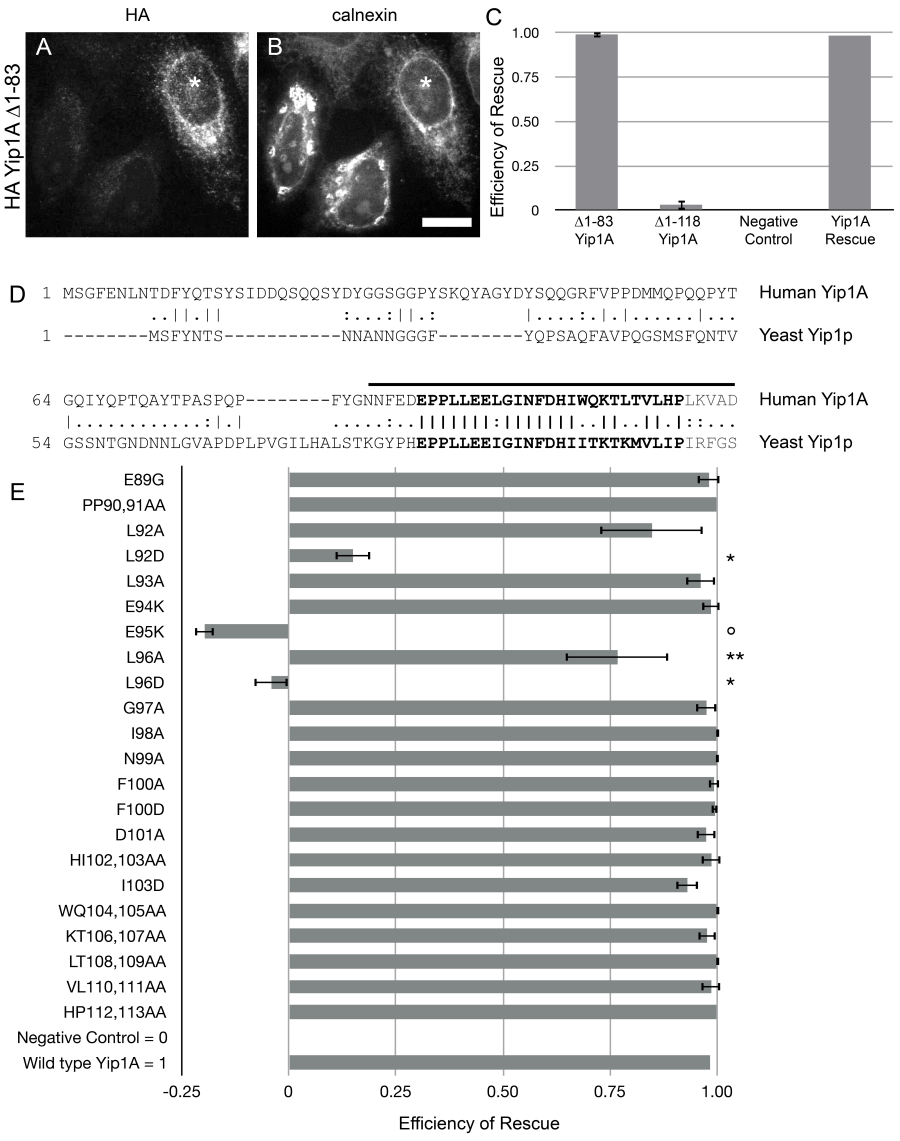

Figure 3-2: Only a few highly conserved residues in the Yip1A cytoplasmic domain are required for function.

Cells co-transfected with Yip1A siRNA and HA-Yip1A ’1-83 were fixed after 72 h and co-stained with antibodies against HA (A) and calnexin (B). The asterisk (A and B) indicates an expressing cell that does not exhibit ER whorls. Scale bar, 10 μm. (C) Quantification of the efficiency of rescue by HA-Yip1A Δ1-83, HA-Yip1A Δ1-118 and the negative control Myc-Sec61β. Data were from 3 independent experiments (>100 cells per experiment), ±SD. (D) An alignment of the cytoplasmic domains of human Yip1A with yeast Yip1p. Residues 83-118 are bracketed, with the highly conserved block highlighted in bold. (E) Bolded residues (in D) were mutated as indicated and tested for rescue. Data from 3 independent experiments (>100 cells per experiment) ±SD are quantified. Single asterisk, p-value <0.001; double asterisk, p<0.05 (Student’s t-test). The open circle indicates the previously identified nonfunctional variant E95K (Dykstra et al., 2010).

in Fig 3-2E) and tested for function. The results of this analysis are quantified in Fig 3-2E. Significantly, the E89G mutation, corresponding to the lethal *yip1-41* allele in yeast (E70G in Yip1p) and previously shown to abolish binding of Yip1p to Yif1p as well as to Ypt1p and Ypt31p (Chen et al., 2004), was fully functional for ER structural maintenance by Yip1A. This was somewhat surprising and suggested that the control of ER whorl formation by Yip1A might not require binding to either Yif1A or the Rab GTPases. On the other hand, the previously identified Glu residue mutated to Lys (E95K) proved to be most disruptive to function. This mutation corresponds to another lethal allele of Yip1p, *yip1-6* (E76K in Yip1p); though in contrast to *yip1-41*, this mutation had only minor effects on binding of Yip1p to either Yif1p or Ypt1p/Ypt31p (Chen et al., 2004). Collectively, these data can be interpreted as an indication that the ability of Yip1A to regulate ER structure does not correlate with its ability to bind either Yif1A or Rab GTPases.

Interestingly, we saw a mild loss of function when two Leu residues (L92 and L96) surrounding the essential E95 residue were replaced with Ala. Because a Leu to Ala substitution is a relatively conservative change, we further tested the effect of replacing L92 or L96 with a charged residue. Indeed, both L92D and L96D yielded essentially nonfunctional proteins, indicating the importance of the uncharged character of those residues for function (Fig 3-2E). On the other hand, a similar substitution of other nearby conserved nonpolar residues such as F100D or I103D had no effect on function (Fig 3-2E). This selectivity underscores the importance of L92 and L96 in addition to E95. L92, E95 and L96 are predicted to lie on the same face of a predicted short alpha helix; therefore it is tempting to speculate that the three residues comprise a single crucial binding site on Yip1A.

ALA/LEU REPLACEMENTS OF TRANSMEMBRANE SEGMENTS REVEAL CRUCIAL RESIDUES

For dissecting the required regions of the TM domain, we relied on both secondary structure and TM domain prediction algorithms (schematized in Fig 3-3B) to make truncations of individual TM helices and loops so as to minimize perturbation of overall membrane topology. Unfortunately, none of the resulting deletion constructs led to stably expressing protein (data not shown). To bypass this issue, we proceeded by replacing segments of predicted TM helices with Ala residues interspersed with Leu so as to maintain their stability in the membrane (Hessa et al., 2007); similarly, predicted luminal and cytoplasmic loops were replaced with stretches of Ala. In the case of charged residues, charge reversal mutations were made to maximize the potential effect of the mutation. All of the constructs made were expressed, except for those with substitutions in TM3 and TM4. Curiously, even single amino acid substitutions within TM3 and TM4 led to poorly expressed protein, precluding their analysis. Nonetheless all other TM helices and loops were amenable to substitutions, allowing a dissection of the remainder of the TM domain. Each expressing construct was tested in our knockdown replacement assay and the results are quantified in Fig 3-3A and schematized in Fig 3-3B. (A full table of mutations and results is included in Supplemental Table 1.) The analysis revealed substantial stretches where residue identity was seemingly not important for function, such as all of TM1 and Loop2; however for others, such as TM2 and Loop1, substitutions of 7-10 amino acid stretches disrupted function. To further refine the required residues, we constructed point mutations within the seemingly required regions. Somewhat surprisingly, when variants with individual amino acid substitutions were produced, it became clear that only two point mutations, K146E and V152L,

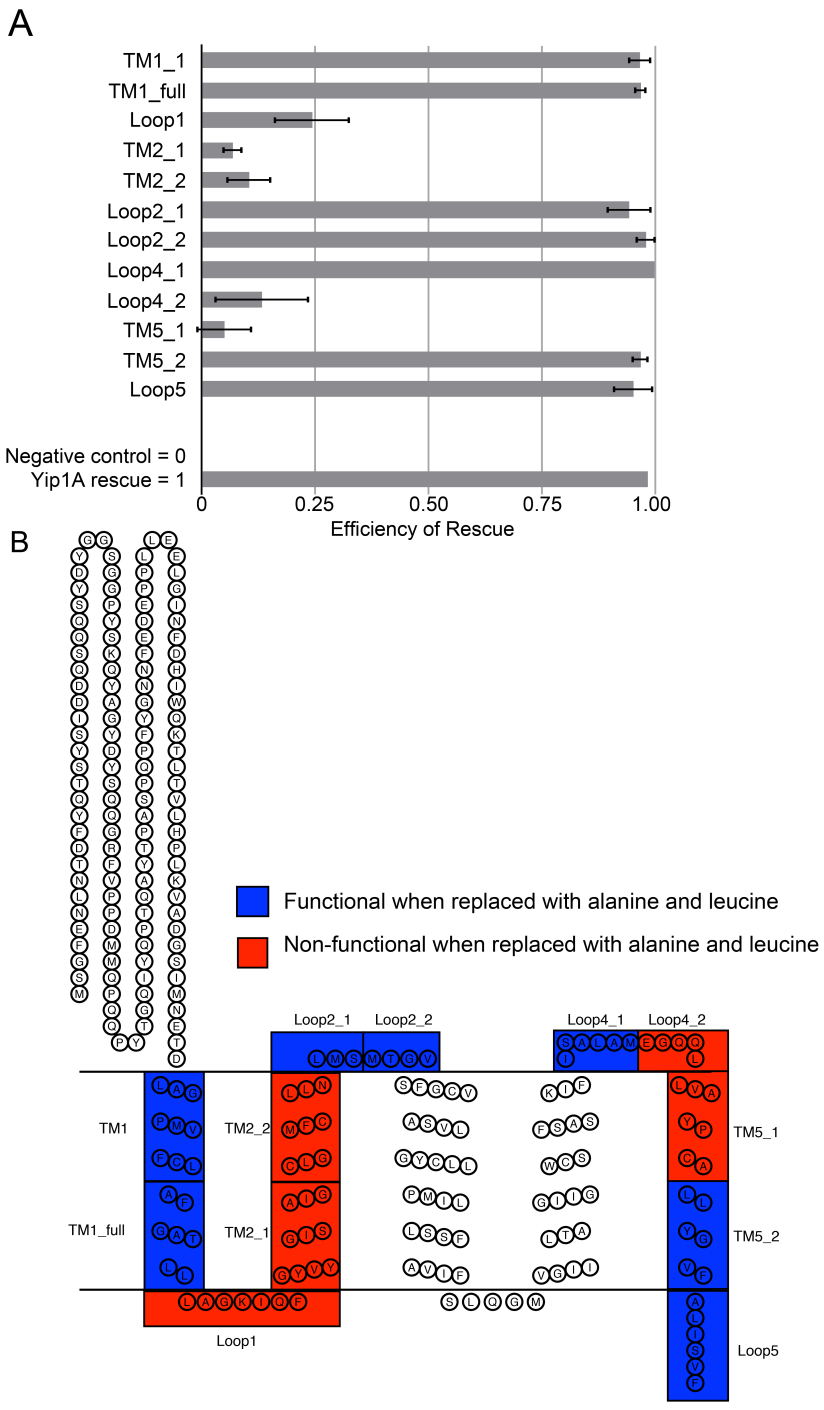

Figure 3-3. Regions of the Yip1A TM domain required for ER structuring.

(A) Quantification of rescue in cells that were co-transfected with Yip1A siRNA and mutated HA-Yip1A constructs. Data were from 3 independent experiments (>100 cells per experiment), ±SD. (B) A schematic representation of the predicted topology of Yip1A. The results from (A) are represented on the schematic. Residues highlighted in blue were functional and red were nonfunctional when replaced with Ala/Leu.

resulted in loss of function, though the loss was modest (Fig 3-4A,D). Because the individual substitutions led to a clear, albeit partial, disruption of function, and given their proximity to one another, we also tested the effect of combining the two substitutions. Notably, the double mutant variant K146E/V152L was completely nonfunctional (Fig 3-4B, C and quantified in D), suggesting that the two residues might work in a cooperative fashion to support Yip1A function. This result was also intriguing given that the yeast mutant counterpart of K146E (K130E) was similarly disruptive to Yip1p function when combined with another mutation (Chen et al., 2004). In sum, though multiple large-scale substitutions within the TM domain of Yip1A were disruptive, the identity of only a few individual residues, namely K146 in the first luminal loop, and V152 - a nearby residue at the start of the second TM helix - were critical.

Required residues in Yip1A may control ER whorl formation independently of its established binding partners Yif1A/Yif1p and the Ypt1p/Ypt31p subclass of GTPases

It was initially surprising that our unbiased analysis revealed only two discrete sites crucial for the ER structural maintenance function of Yip1A (E95 and K146). However it was also satisfying that the sites corresponded precisely to two sites previously identified as essential for Yip1p-dependent viability in yeast (E76 and K130). More surprising was our finding that a third site previously shown to be essential for Yip1p function in yeast was completely dispensable for the control of ER whorl formation by Yip1A. This surprising finding suggested that Yip1A/Yip1p might possess two separate functions. One function, supported by E95 (E76) and K146 (K130), that is required for ER structural maintenance; and another, supported by E89 (E70), that is dispensable for ER structural maintenance. Furthermore, the ability of Yip1p to

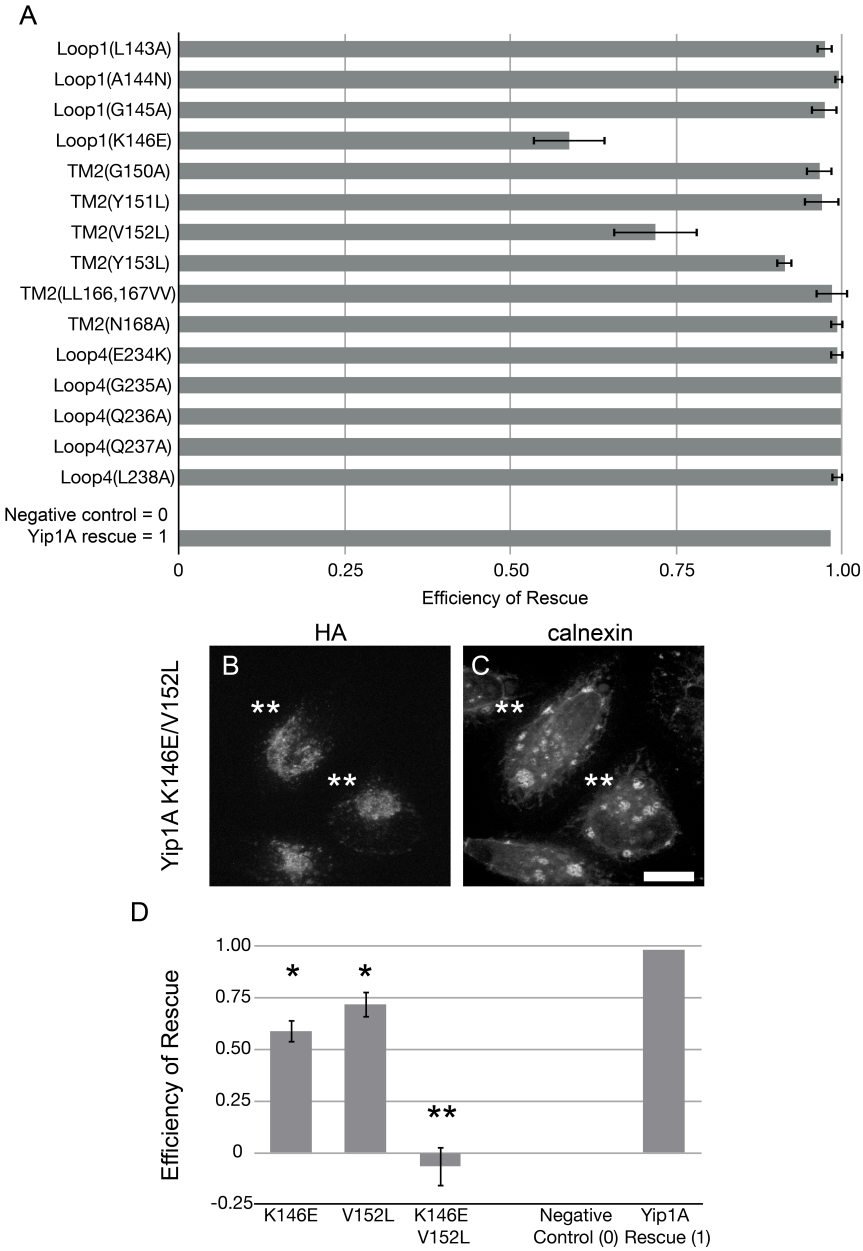

Figure 3-4: Two residues in the Yip1A TM domain are essential for the ER structuring function of Yip1A.

(A) Quantification of cells that were co-transfected with the indicated HA-Yip1A mutated constructs and Yip1A siRNA. Data were from 3 independent experiments (>100 cells per experiment), ±SD. (B, C) Cells co-transfected with Yip1A siRNA and HA-Yip1A K146E and V152L single or double mutant variant constructs were fixed after 72 h and costained with HA (B) and calnexin (C) antibodies. Double asterisks indicate expressing cells that exhibit ER whorls. Scale bar, 10 µm. (D) Quantification of the efficiency of rescue for (B) and (C) from three independent experiments (>100 cells per experiment) ±SD. Single asterisk, $p<0.02$ and double asterisk, $p<0.0001$.

bind its established binding partners Yif1p and Ypt1p/Ypt31p, mapped to E70 (Chen et al., 2004), the residue dispensable for control for ER whorl formation by Yip1A. Thus it seemed that the ER structuring function of Yip1A/Yip1p might operate independently of either Yif1A/Yif1p or the Ypt1p/Ypt31p category of Rab GTPases. Of relevance to this hypothesis, RNAi-mediated Yif1A knockdown was previously reported to cause a fragmentation of the Golgi apparatus, consistent with an ER-to-Golgi trafficking defect, but no ER phenotype was reported (Yoshida et al., 2008). To confirm our suspicion that Yip1A-mediated control of ER whorl formation does not depend on Yif1A, we reproduced the previously published Yif1A knockdown but with eye towards revealing any potential ER phenotypes. Consistent with a lack of requirement for Yif1A in ER structural maintenance, we observed no ER whorls in cells depleted of Yif1A, even though Golgi fragmentation was clearly and frequently observed (Fig 3-5).

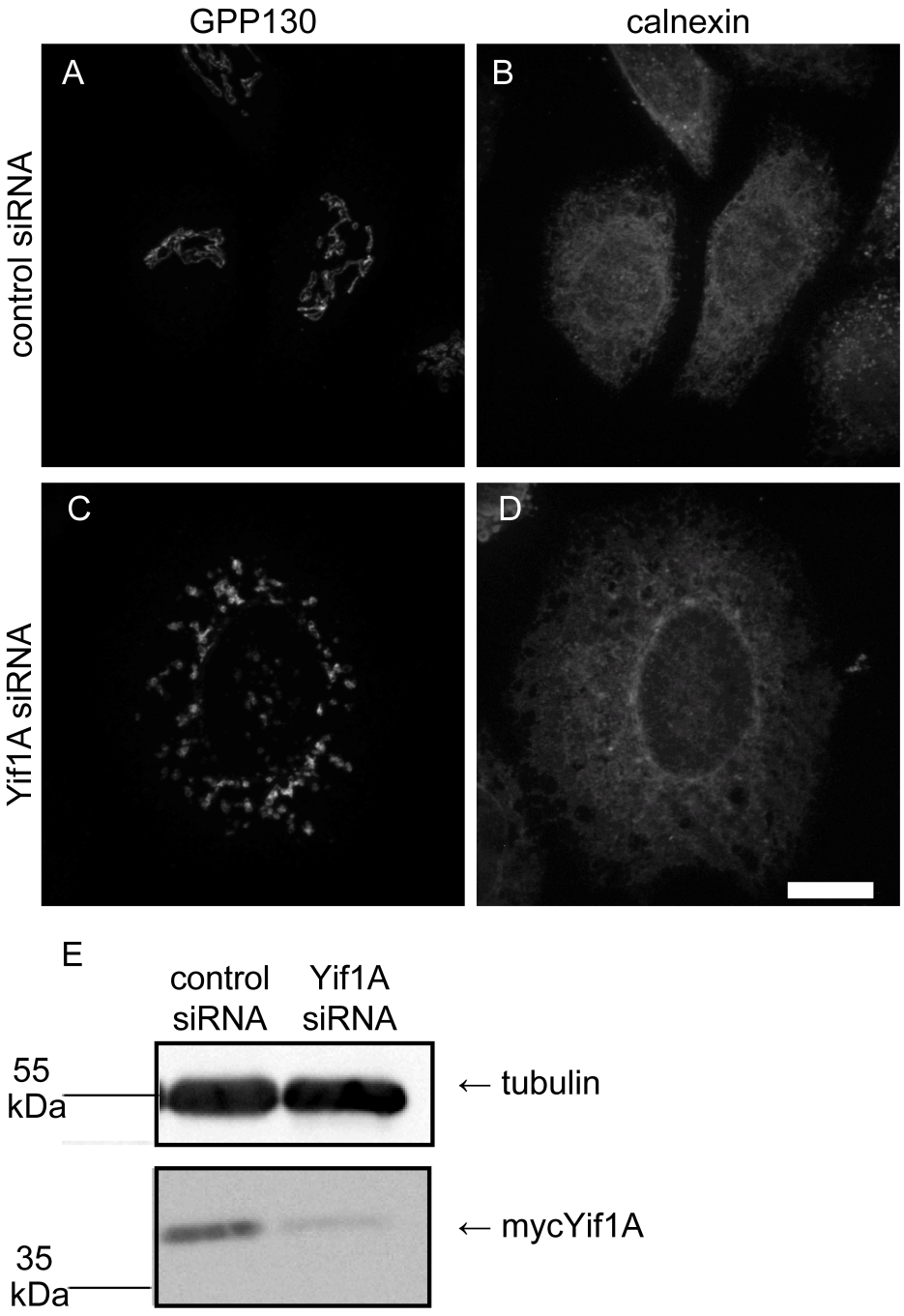

Figure 3-5: Yif1A knockdown does not result in a whorled ER phenotype.

HeLa cells were transfected with either a negative control siRNA (A and B) or siRNA against Yif1A (C and D) and were fixed after 72 h and costained with antibodies against GPP130 (A and C) and calnexin (B and D). (E) HeLa cells were co-transfected with mycYif1A and either a control siRNA or Yif1A siRNA, harvested after 72 h and then immunoblotted using antibodies against tubulin and the myc-epitope.

DISCUSSION

THE RESIDUE IDENTITY OF SURPRISINGLY FEW AMINO ACIDS TESTED ARE IMPORTANT FOR THE MECHANISM OF YIP1A FUNCTION

As shown previously for its yeast counterpart in a viability assay (Chen et al., 2004), the vast majority of the cytoplasmic domain of Yip1A was dispensable for its ER structural maintenance function. This dispensable portion has no predicted secondary structure and therefore is unlikely to aid in the folding of Yip1A. Yet its persistence through evolution suggests a role, perhaps regulatory, under conditions yet-to-be assessed. In contrast to the cytoplasmic domain, we found that the membrane-spanning domain of Yip1A was extremely sensitive to deletional mutagenesis. This was especially the case for TM3 and TM4, where even a few amino acid substitutions severely compromised protein stability. We speculate that the five predicted TM helices pack together to adopt a stable tertiary structure, with TM3/4 at the core. As we were unable to generate any stably expressing variants within TM3/4, it is unclear whether individual residues within this region are required specifically for the structural maintenance function of Yip1A, or whether they might simply play a scaffolding role for Yip1A protein folding and stability.

A comprehensive scan of the remainder of the Yip1A membrane spanning domain as well as its cytoplasmic domain revealed only a surprisingly few amino acids whose identity was critical for function: residues predicted to lie on one face of a predicted short alpha helix in the cytoplasmic domain (L92, E95, L96) and those within the first luminal loop and adjacent TM2 helix (K146 and V152). As Yip1A lacks any identifiable structural motifs indicative of function, we can only speculate at present that these residues interface either with a crucial protein-binding partner and/or directly with the phospholipid bilayer to regulate ER whorl formation.

CONTROL OF ER STRUCTURE BY YIP1A IS LIKELY INDEPENDENT OF ITS ESTABLISHED BINDING PARTNERS

It is revealing that a mutation (E89 in human and E70 in yeast), that abolishes Yip1p binding to either Yif1p or Ypt1p/Ypt31p GTPases (Chen et al., 2004) had no impact on the ability of Yip1A to regulate ER whorl formation; whereas mutations (E95 and K146 in human and E76 and K130 in yeast) that have minor if any effects on Yip1p binding to either Yif1p or Ypt1p/Ypt31p (Chen et al., 2004) yet completely disrupted the control of ER structure by Yip1A. As both sets of mutations are lethal for yeast, it seems reasonable to speculate that Yip1p/Yip1A has at least two distinct essential functions: one that depends on Yif1p and Ypt1p/Ypt31p binding; and a separate function in regulating ER structure that does not depend on binding the same partners.

HOW MIGHT YIP1A CONTROL ER WHORL FORMATION?

Candidate Yip1A/Yip1p binding partners additional to Yif1A/Yif1p and Ypt1p/Ypt31p GTPases (Yang et al., 1998; Matern et al., 2000) include the curvature-inducing integral ER membrane protein Yop1p/DP1 (Calero et al., 2001; Voeltz et al., 2006). We previously reported that the nonfunctional E95K mutant variant of Yip1A retains binding to DP1 (Dykstra et al., 2010), the mammalian homologue of Yop1p (Voeltz et al., 2006). Thus, none of the previously identified Yip1A/Yip1p binding partners are obvious candidates for mediating the ER structural maintenance role of Yip1A. Though, a definitive test of this hypothesis awaits fine mapping and mutagenesis of each of the binding sites on Yip1A for each of its binding partners. A final intriguing possibility is that Yip1A could be affecting ER membrane morphology through a direct lipid interaction. As little is understood about how local lipid composition contributes to

the structure of the ER, it seems plausible that Yip1A might directly bind and sort lipids thereby maintaining an ER membrane composition that is conducive to a dispersed, rather than stacked, membrane network. Alternatively, Yip1A could be directing localized lipid synthesis by binding and regulating a lipid-modifying enzyme. Intriguingly, Got1p, a high copy suppressor of a temperature sensitive Yip1p mutant in yeast has been proposed to affect lipid composition (Lorente-Rodríguez et al., 2009). These possibilities have yet to be explored, and the identification of two crucial functional determinants in this study will be useful for future mechanistic studies of the control of ER whorl formation by Yip1A.

MATERIALS AND METHODS

CELL CULTURE AND TRANSFECTIONS

HeLa cells stably expressing a GalNacT2-green fluorescent protein (GFP) (Storrie et al., 1998) were maintained in minimal essential medium (Sigma-Aldrich, St. Louis, MO) containing 10% fetal bovine serum (Atlanta Biologicals, Norcross, GA) and 100 IU/ml penicillin and streptomycin (Mediatech, Herndon, VA) at 37°C in a 5% CO_2 incubator. Transient plasmid DNA transfection of HeLa cells was performed with jetPEI™ (Polyplus transfection, Illkirch, France), according to the manufacturer's specifications using 0.5 μg DNA per 1 mL media. Transient co-transfection of HeLa cells with both plasmid DNA and siRNA was performed with jetPRIME™ (Polyplus transfection) according to the manufacturer's specifications by using 150 ng of DNA and 10 pmol siRNA per 0.5 mL media. Transient siRNA transfections of siRNAs against Yif1A were performed using jetPRIME™ (Polyplus transfection) using 20 pmol siRNA per 0.5 mL media.

QUANTIFICATION OF EFFICIENCY OF RESCUE

For each of our transgene replacement experiments, 100 cells were counted in three individual experiments and the data was calculated as the percentage of cells expressing the transgene that display ER whorls. In order to compare the different constructs over multiple sets of experiments, this percentage was normalized to the negative control for that experiment using the following formula: Efficiency = 1 – (fraction cells expressing transgene with ER whorls / fraction cells expressing negative control with ER whorls). An efficiency of 1 reflects full rescue and 0 is a complete non-rescue.

CONSTRUCTS

The siRNAs used against Yip1A were described previously (Dykstra et al., 2010) and synthesized by Ambion (Austin, TX). The myc-tagged Sec61β was subcloned from GFP-Sec61 β (kindly provided by Dr. Gia Voeltz, University of Colorado, Boulder) into the EcoRI and XbaI sites of the pCS2-MT vector. The myc-tagged Yif1A construct was cloned by PCR amplification from HeLa cDNA (Qiagen, Hilden, Germany) and inserting the PCR product into the pCS2-MT vector using EcoRI and XbaI sites. The HA-Yip1A rescue construct was created by replacing the FLAG epitope from the FLAG-Yip1A construct (Dykstra et al., 2010) with the HA epitope (YPYDVPDYA) using a PCR-based loop-out/loop-in modification of the QuikChange protocol (Stratagene, La Jolla, CA) and was the parent construct for all further HA-Yip1A mutations. The HA-Yip1AN/Sec61β TM was created by first using a PCR-based loop-out technique (Stratagene) to remove the TM domain region (AA 126-257) of the Yip1A construct and the TM domain from Myc- Sec61β (AA 61-97) was subcloned into the XbaI site at the C-terminus. The HA-Yip1A Δ1-83 and Δ1-118 constructs were created using the PCR-based loop-out technique (Stratagene). All additional HA-Yip1A mutant constructs were created using QuikChange site directed mutagenesis PCR (Stratagene). siRNAs directed against Yif1A were created using a siRNA construction kit (Ambion) and previously published target sequences (Yoshida et al., 2008). The control siRNA used in this study targets bovine p115 and does not affect p115 in HeLa cells (Puthenveedu and Linstedt, 2004).

ANTIBODIES, IMMUNOFLUORESCENCE AND IMMUNOBLOTTING

Antibodies used include mouse monoclonal antibody (mAb) against the HA-epitope (Sigma-Aldrich, St. Louis, MO); a rabbit polyclonal antibody (pAb) against Calnexin (Abcam,

Cambridge, MA); a mouse mAb against the myc epitope from the 9E10 cell line; a mouse mAb against GPP130 (kindly provided by Dr. A. Linstedt, Carnegie Mellon University, Pittsburgh, PA) and a rabbit pAb against tubulin (Abcam). Fluorophore-conjugated secondary antibodies were from Zymed Laboratories (South San Francisco, CA)/Invitrogen (Carlsbad, CA). HeLa cells were analyzed 72 h post-transfection. Immunofluorescence procedures were as described previously (Dykstra et al., 2010). Immunoblotting using a mouse mAb against the myc-epitope and a rabbit pAb against tubulin (Abcam), was performed on cells co-transfected with Yif1A siRNA and myc-Yif1A harvested from 60-mm dishes as described previously (Kapetanovich et al., 2005).

FLUORESCENCE MICROSCOPY

All images were obtained using a Yokagawa spinning disk confocal scanhead (Perkin Elmer Life and Analytical Sciences, Boston MA) mounted on an Axiovert 200 microscope (Carl Zeiss, Jena, Germany) with a 100X 1.4 numerical aperture (NA) objective (Carl Zeiss) and acquired using a 12-bit Orca ER digital camera (Hamamatsu Photonics, Hamamatsu City, Japan). Maximal value projections of sections at 0.3-μm spacing (5-8/cell) were acquired using ImageJ (National Institutes of Health, Bethesda, MD).

CHAPTER 4

CONCLUSIONS AND FUTURE DIRECTIONS

While the propensity of the ER to undergo a dramatic transformation from a dispersed fenestrated network into concentric membranous whorls is not unprecedented through over-expression of certain proteins, the results presented in this thesis are the first documented observation of these ER whorls forming as a result of siRNA knockdown of a protein. Using a knockdown/*trans*-gene replacement approach, we were able to show this knockdown phenotype was due specifically to knockdown of Yip1A, given that an siRNA-immune variant of the protein was able to rescue the ER whorl phenotype. Thus, Yip1A is crucial for maintaining proper ER network dispersal and preventing the formation of ER whorls.

ER whorls have been observed in a variety of specialized cells types, specifically those involved in peptide or steroid hormone secretion, however their regulation and functional relevance to cargo export is unknown (King et al., 1974). A marked delay in COPII-mediated cargo export was observed in Yip1A depleted cells displaying ER whorls, consistent with studies of Yip1p in yeast implicating Yip1p in COPII vesicle biogenesis (Heidtman et al., 2003), however in contrast we observed no COPII recruitment defect. Additionally, ER whorls induced exogenously by a protein with no role in COPII vesicle biogenesis also resulted in a delay with very similar kinetics, indicating that a dispersed ER network is important for proper COPII-mediated export. Determining the basis of how ER whorling inhibits protein export will be an important next step towards understanding the relationship between ER structure and function. It

will also be interesting to see if the specialized cells exhibiting ER whorls use these changes in ER structure to regulate cargo export.

The mechanism by which Yip1A mediates ER network dispersal remains elusive. Mutational analysis of the protein revealed relatively few residues critical for its ER structuring function, both in the cytoplasmic domain and transmembrane domain of the protein. Two of the five residues identified (E95, K146) corresponded to conserved residues in yeast (E76, K130) that were also found to be necessary for cell viability (Chen et al., 2004). Interestingly, a conserved residue from yeast (E70) that was needed for cell viability was not found to be required for maintaining proper ER structure in mammalian cells (E89) (Chen et al., 2004). In yeast two-hybrid studies performed with the yeast proteins, mutations of the E76K and K130E residues did not disrupt binding to known Yip1p interacting partners Ypt1/Ypt31 Rab GTPases as well as Yif1p, whereas mutations of E70G could not bind (Chen et al., 2004). This combined with our mutation corresponding to E70G being able to function in maintaining ER structure, is highly suggestive that Yif1A and Rab binding is not required for the ER structuring function of Yip1A. These interactions may be critical for other Yip1A functions in the cell. Finding how residues E95, K146 and the other essential amino acids identified contribute to Yip1A function will be an important next step. Most likely, these residues are mediating a novel Yip1A interaction. Now that we have a library of Yip1A residues critical for the ER structuring function of Yip1A, these can be utilized in screens for finding interacting partners following further refinement of Yip1A interaction assays.

The Yip1A protein was highly sensitive to mutation. This was particularly true of the third and fourth transmembrane domains, where even replacement of single amino acids led to an unstable protein product. While this unfortunately meant these domains could not be tested

for function, we speculate that these domains may be of importance, either for stabilizing the tertiary structure of the protein or perhaps a function of the protein that depends on maintaining the proper protein structure. While the Yip1A protein is predicted to have a cytoplasmic N-terminus followed by five transmembrane domains, the exact orientation of these transmembrane domains in the membrane is unknown. Efforts at mapping their orientation have revealed that the last predicted TM helix points towards the lumen of the ER, but further information regarding the topology of the second to fourth helices has been difficult to obtain. This is due to the sensitivity of Yip1A to mutation as well as its aberrant migration on SDS-PAGE making traditional approaches to probing membrane topology such as internal epitope tagging, introduction of N-glycosylation sites and cysteine modified maleimide PEGylation infeasible. Determining the orientation of helices 2-4 in the membrane might provide us with important insight into how Yip1A is functioning. One interesting possibility suggested by a number of the secondary structure prediction algorithms is that the third and fourth transmembrane domains are not separated by a luminal loop, but are rather both fully in the membrane. This structure may directly shape the lipid bilayer. Incorporation of the full length Yip1A protein into liposomes may reveal interesting membrane shaping properties of the protein that could inform us about how Yip1A is functioning.

Despite its importance, very few proteins have been identified in maintaining ER structure. The proteins identified relate to either attachment of ER to microtubules or microtubules motors, direct shaping of the membrane or fusion of ER membranes. Yip1A may be involved in one or more of these processes. Another intriguing possibility is that Yip1A may have a novel role in modifying ER structure by regulating the interaction of one or more proteins in *trans*, a known mechanism for ER whorl formation (Snapp et al., 2003). Yip1A may be acting

as a global regulator of ER whorling through *trans*-pairing or it may be preventing specific *trans*-interactions. Proteins that interact in *trans*, such as the VAPB and Nir2 can cause ER whorl formation with concurrent overexpression of both proteins (Amarilio et al., 2005). While initial attempts to detect a Yip1A/VAPB interaction through co-IP gave a negative result, another Yip1 family member, PRA2 has been shown to interact with another VAP family member, VAPA, though only through cross-linking (Gougeon and Ngsee, 2005). Thus a Yip1A/VAPB interaction that prevents uncontrolled VAPB/Nir2 interactions in *trans* is still a possibility.

Although the knockdown ER whorl phenotype was shown to be specific to the knockdown of Yip1A, it is possible that Yip1A knockdown may result in changes in regulation at the transcriptional level. This could alter the expression levels of a wide variety of proteins that effect ER structure. Further studies using difference gel electrophoresis (DIGE) on extracts with and without Yip1A would address this concern. It would also be interesting to perform DIGE experiments on extracts from cell types that exhibit ER whorls that can be regulated to determine protein difference before and after whorl formation.

Yip1A clearly has an important role in maintaining a dispersed ER, whereas it had previously only been thought of as a trafficking protein. These findings introduce a framework for studying Yip1A additionally as a mediator of ER structure. Now that this has been established, further study of Yip1A will be needed to determine whether Yip1A is having direct effects on structuring the ER or if it plays regulatory role in controlling ER whorl formation.

REFERENCES

Ahluwalia, N., Bergeron, J.J., Wada, I., Degen, E., and Williams, D.B. (1992). The p88 molecular chaperone is identical to the endoplasmic reticulum membrane protein, calnexin. J. Biol. Chem. *267*, 10914–10918.

Allan, V.J., and Vale, R.D. (1991). Cell cycle control of microtubule-based membrane transport and tubule formation in vitro. The Journal of Cell Biology *113*, 347–359.

Amarilio, R., Ramachandran, S., Sabanay, H., and Lev, S. (2005). Differential regulation of endoplasmic reticulum structure through VAP-Nir protein interaction. J. Biol. Chem. *280*, 5934–5944.

Anderson, D.J., and Hetzer, M.W. (2008). Reshaping of the endoplasmic reticulum limits the rate for nuclear envelope formation. The Journal of Cell Biology *182*, 911–924.

Anderson, R.G., Orci, L., Brown, M.S., Garcia-Segura, L.M., and Goldstein, J.L. (1983). Ultrastructural analysis of crystalloid endoplasmic reticulum in UT-1 cells and its disappearance in response to cholesterol. Journal of Cell Science *63*, 1–20.

Aridor, M., and Balch, W.E. (2000). Kinase signaling initiates coat complex II (COPII) recruitment and export from the mammalian endoplasmic reticulum. J. Biol. Chem. *275*, 35673–35676.

Aridor, M., Weissman, J., Bannykh, S., Nuoffer, C., and Balch, W.E. (1998). Cargo selection by the COPII budding machinery during export from the ER. The Journal of Cell Biology *141*, 61–70.

Bannykh, S.I., and Balch, W.E. (1997). Membrane dynamics at the endoplasmic reticulum-Golgi interface. The Journal of Cell Biology *138*, 1–4.

Barlowe, C. (1998). COPII and selective export from the endoplasmic reticulum. Biochim. Biophys. Acta *1404*, 67–76.

Barlowe, C., Orci, L., Yeung, T., Hosobuchi, M., Hamamoto, S., Salama, N., Rexach, M.F., Ravazzola, M., Amherdt, M., and Schekman, R. (1994). COPII: a membrane coat formed by Sec proteins that drive vesicle budding from the endoplasmic reticulum. Cell *77*, 895–907.

Barr, F.A., Puype, M., Vandekerckhove, J., and Warren, G. (1997). GRASP65, a protein involved in the stacking of Golgi cisternae. Cell *91*, 253–262.

Barrowman, J., Wang, W., Zhang, Y., and Ferro-Novick, S. (2003). The Yip1p.Yif1p complex is required for the fusion competence of endoplasmic reticulum-derived vesicles. J. Biol. Chem. *278*, 19878–19884.

Baumann, O., and Walz, B. (2001). Endoplasmic reticulum of animal cells and its organization

into structural and functional domains. International Review of Cytology *205*, 149–214.

Bernales, S., McDonald, K.L., and Walter, P. (2006). Autophagy counterbalances endoplasmic reticulum expansion during the unfolded protein response. PLoS Biol. *4*, e423.

Bevis, B.J., Hammond, A.T., Reinke, C.A., and Glick, B.S. (2002). De novo formation of transitional ER sites and Golgi structures in Pichia pastoris. Nat. Cell Biol. *4*, 750–756.

Bi, X., Mancias, J.D., and Goldberg, J. (2007). Insights into COPII coat nucleation from the structure of Sec23.Sar1 complexed with the active fragment of Sec31. Developmental Cell *13*, 635–645.

Bielli, A., Haney, C.J., Gabreski, G., Watkins, S.C., Bannykh, S.I., and Aridor, M. (2005). Regulation of Sar1 NH2 terminus by GTP binding and hydrolysis promotes membrane deformation to control COPII vesicle fission. The Journal of Cell Biology *171*, 919–924.

Blumental-Perry, A., Haney, C.J., Weixel, K.M., Watkins, S.C., Weisz, O.A., and Aridor, M. (2006). Phosphatidylinositol 4-Phosphate Formation at ER Exit Sites Regulates ER Export. Developmental Cell *11*, 671–682.

Borgese, N., Francolini, M., and Snapp, E. (2006). Endoplasmic reticulum architecture: structures in flux. Curr Opin Cell Biol *18*, 358–364.

Budnik, A., and Stephens, D.J. (2009). ER exit sites--localization and control of COPII vesicle formation. FEBS Lett. *583*, 3796–3803.

Calero, M., Chen, C.Z., Zhu, W., Winand, N., Havas, K.A., Gilbert, P.M., Burd, C.G., and Collins, R.N. (2003). Dual prenylation is required for Rab protein localization and function. Mol. Biol. Cell *14*, 1852–1867.

Calero, M., Whittaker, G.R., and Collins, R.N. (2001). Yop1p, the yeast homolog of the polyposis locus protein 1, interacts with Yip1p and negatively regulates cell growth. J. Biol. Chem. *276*, 12100–12112.

Carr, I., and Carr, J. (1962). Membranous whorls in the testicular interstitial cell. Anat. Rec. *144*, 143–147.

Chen, C.Z., and Collins, R.N. (2005). Insights into biological functions across species: examining the role of Rab proteins in YIP1 family function. Biochem. Soc. Trans. *33*, 614–618.

Chen, C.Z., Calero, M., DeRegis, C.J., Heidtman, M., Barlowe, C., and Collins, R.N. (2004). Genetic analysis of yeast Yip1p function reveals a requirement for Golgi-localized rab proteins and rab-Guanine nucleotide dissociation inhibitor. Genetics *168*, 1827–1841.

Chin, D.J., Luskey, K.L., Anderson, R.G., Faust, J.R., Goldstein, J.L., and Brown, M.S. (1982). Appearance of crystalloid endoplasmic reticulum in compactin-resistant Chinese hamster cells with a 500-fold increase in 3-hydroxy-3-methylglutaryl-coenzyme A reductase. Proc. Natl. Acad. Sci. U.S.a. *79*, 1185–1189.

Christensen, A.K., and Fawcett, D.W. (1966). The fine structure of testicular interstitial cells in mice. Am. J. Anat. *118*, 551–571.

Dabora, S.L., and Sheetz, M.P. (1988). The microtubule-dependent formation of a tubulovesicular network with characteristics of the ER from cultured cell extracts. Cell *54*, 27–35.

Dahl, K.N., Ribeiro, A.J.S., and Lammerding, J. (2008). Nuclear shape, mechanics, and mechanotransduction. Circ. Res. *102*, 1307–1318.

Dreier, L., and Rapoport, T.A. (2000). In vitro formation of the endoplasmic reticulum occurs independently of microtubules by a controlled fusion reaction. The Journal of Cell Biology *148*, 883–898.

Du, Y., Ferro-Novick, S., and Novick, P. (2004). Dynamics and inheritance of the endoplasmic reticulum. Journal of Cell Science *117*, 2871–2878.

Dubois, P., and Girod, C. (1971). [Concentric lamellar formations in anterior pituitary cells of the golden hamster]. Z Zellforsch Mikrosk Anat *115*, 196–211.

Dykstra, K.M., Pokusa, J.E., Suhan, J., and Lee, T.H. (2010). Yip1A structures the mammalian endoplasmic reticulum. Mol. Biol. Cell *21*, 1556–1568.

Ellgaard, L., Molinari, M., and Helenius, A. (1999). Setting the standards: quality control in the secretory pathway. Science *286*, 1882–1888.

Espenshade, P., Gimeno, R.E., Holzmacher, E., Teung, P., and Kaiser, C.A. (1995). Yeast SEC16 gene encodes a multidomain vesicle coat protein that interacts with Sec23p. The Journal of Cell Biology *131*, 311–324.

Fath, S., Mancias, J.D., Bi, X., and Goldberg, J. (2007). Structure and organization of coat proteins in the COPII cage. Cell *129*, 1325–1336.

Feinstein, T.N., and Linstedt, A.D. (2008). GRASP55 regulates Golgi ribbon formation. Mol. Biol. Cell *19*, 2696–2707.

Fewell, S.W., Travers, K.J., Weissman, J.S., and Brodsky, J.L. (2001). The action of molecular chaperones in the early secretory pathway. Annu. Rev. Genet. *35*, 149–191.

Fridkin, A., Penkner, A., Jantsch, V., and Gruenbaum, Y. (2009). SUN-domain and KASH-domain proteins during development, meiosis and disease. Cell. Mol. Life Sci. *66*, 1518–1533.

Friedman, J.R., Webster, B.M., Mastronarde, D.N., Verhey, K.J., and Voeltz, G.K. (2010). ER sliding dynamics and ER-mitochondrial contacts occur on acetylated microtubules. The Journal of Cell Biology *190*, 363–375.

Gilmore, R., Blobel, G., and Walter, P. (1982). Protein translocation across the endoplasmic reticulum. I. Detection in the microsomal membrane of a receptor for the signal recognition

particle. The Journal of Cell Biology *95*, 463–469.

Gougeon, P.-Y., and Ngsee, J.K. (2005). Purification and functional properties of prenylated Rab acceptor 2. Meth. Enzymol. *403*, 799–807.

Grigoriev, I., Gouveia, S.M., van der Vaart, B., Demmers, J., Smyth, J.T., Honnappa, S., Splinter, D., Steinmetz, M.O., Putney, J.W., Hoogenraad, C.C., et al. (2008). STIM1 is a MT-plus-end-tracking protein involved in remodeling of the ER. Current Biology *18*, 177–182.

Guo, Y., Punj, V., Sengupta, D., and Linstedt, A.D. (2008). Coat-tether interaction in Golgi organization. Mol. Biol. Cell *19*, 2830–2843.

Heidtman, M., Chen, C.Z., Collins, R.N., and Barlowe, C. (2003). A role for Yip1p in COPII vesicle biogenesis. The Journal of Cell Biology *163*, 57–69.

Heidtman, M., Chen, C.Z., Collins, R.N., and Barlowe, C. (2005). Yos1p is a novel subunit of the Yip1p-Yif1p complex and is required for transport between the endoplasmic reticulum and the Golgi complex. Mol. Biol. Cell *16*, 1673–1683.

Helenius, A., and Aebi, M. (2001). Intracellular functions of N-linked glycans. Science *291*, 2364–2369.

Hessa, T., Meindl-Beinker, N.M., Bernsel, A., Kim, H., Sato, Y., Lerch-Bader, M., Nilsson, I., White, S.H., and Heijne, von, G. (2007). Molecular code for transmembrane-helix recognition by the Sec61 translocon. Nature *450*, 1026–1030.

Hetzer, M.W. (2010). The nuclear envelope. Cold Spring Harb Perspect Biol *2*, a000539.

Hu, F. (1971). Ultrastructural changes in the cell cycle of cultured melanoma cells. Anat. Rec. *170*, 41–55.

Hu, J., Shibata, Y., Voss, C., Shemesh, T., Li, Z., Coughlin, M., Kozlov, M.M., Rapoport, T.A., and Prinz, W.A. (2008). Membrane proteins of the endoplasmic reticulum induce high-curvature tubules. Science *319*, 1247–1250.

Hu, J., Shibata, Y., Zhu, P.-P., Voss, C., Rismanchi, N., Prinz, W.A., Rapoport, T.A., and Blackstone, C. (2009). A class of dynamin-like GTPases involved in the generation of the tubular ER network. Cell *138*, 549–561.

Hughes, H., and Stephens, D.J. (2008). Assembly, organization, and function of the COPII coat. Histochem. Cell Biol. *129*, 129–151.

Hwang, K.M., Yang, L.C., Carrico, C.K., Schulz, R.A., Schenkman, J.B., and Sartorelli, A.C. (1974). Production of membrane whorls in rat liver by some inhibitors of protein synthesis. The Journal of Cell Biology *62*, 20–31.

Jin, C., Zhang, Y., Zhu, H., Ahmed, K., Fu, C., and Yao, X. (2005). Human Yip1A specifies the localization of Yif1 to the Golgi apparatus. Biochem. Biophys. Res. Commun. *334*, 16–22.

Johnson, A.E., and van Waes, M.A. (1999). The translocon: a dynamic gateway at the ER membrane. Annu. Rev. Cell Dev. Biol. *15*, 799–842.

Jones, A.L., and Fawcett, D.W. (1966). Hypertrophy of the agranular endoplasmic reticulum in hamster liver induced by phenobarbital (with a review on the functions of this organelle in liver). J. Histochem. Cytochem. *14*, 215–232.

Kabeya, Y., Mizushima, N., Ueno, T., Yamamoto, A., Kirisako, T., Noda, T., Kominami, E., Ohsumi, Y., and Yoshimori, T. (2000). LC3, a mammalian homologue of yeast Apg8p, is localized in autophagosome membranes after processing. Embo J. *19*, 5720–5728.

Kalies, K.U., Rapoport, T.A., and Hartmann, E. (1998). The beta subunit of the Sec61 complex facilitates cotranslational protein transport and interacts with the signal peptidase during translocation. The Journal of Cell Biology *141*, 887–894.

Kano, F., Yamauchi, S., Yoshida, Y., Watanabe-Takahashi, M., Nishikawa, K., Nakamura, N., and Murata, M. (2009). Yip1A regulates the COPI-independent retrograde transport from the Golgi complex to the ER. Journal of Cell Science *122*, 2218–2227.

Kapetanovich, L., Baughman, C., and Lee, T.H. (2005). Nm23H2 facilitates coat protein complex II assembly and endoplasmic reticulum export in mammalian cells. Mol. Biol. Cell *16*, 835–848.

King, J.C., Williams, T.H., and Gerall, A.A. (1974). Transformations of hypothalamic arcuate neurons. I. Changes associated with stages of the estrous cycle. Cell Tissue Res. *153*, 497–515.

Koning, A.J., Roberts, C.J., and Wright, R.L. (1996). Different subcellular localization of Saccharomyces cerevisiae HMG-CoA reductase isozymes at elevated levels corresponds to distinct endoplasmic reticulum membrane proliferations. Mol. Biol. Cell *7*, 769–789.

Kreis, T.E., and Lodish, H.F. (1986). Oligomerization is essential for transport of vesicular stomatitis viral glycoprotein to the cell surface. Cell *46*, 929–937.

Kuge, O., Dascher, C., Orci, L., Rowe, T., Amherdt, M., Plutner, H., Ravazzola, M., Tanigawa, G., Rothman, J.E., and Balch, W.E. (1994). Sar1 promotes vesicle budding from the endoplasmic reticulum but not Golgi compartments. The Journal of Cell Biology *125*, 51–65.

Lazar, T., Götte, M., and Gallwitz, D. (1997). Vesicular transport: how many Ypt/Rab-GTPases make a eukaryotic cell? Trends Biochem. Sci. *22*, 468–472.

Lee, C., Ferguson, M., and Chen, L.B. (1989). Construction of the endoplasmic reticulum. The Journal of Cell Biology *109*, 2045–2055.

Lee, M.C.S., Orci, L., Hamamoto, S., Futai, E., Ravazzola, M., and Schekman, R. (2005). Sar1p N-terminal helix initiates membrane curvature and completes the fission of a COPII vesicle. Cell *122*, 605–617.

Lee, T.H., and Linstedt, A.D. (2000). Potential role for protein kinases in regulation of

bidirectional endoplasmic reticulum-to-Golgi transport revealed by protein kinase inhibitor H89. Mol. Biol. Cell *11*, 2577–2590.

Lorente-Rodríguez, A., Heidtman, M., and Barlowe, C. (2009). Multicopy suppressor analysis of thermosensitive YIP1 alleles implicates GOT1 in transport from the ER. Journal of Cell Science *122*, 1540–1550.

Matern, H., Yang, X., Andrulis, E., Sternglanz, R., Trepte, H.H., and Gallwitz, D. (2000). A novel Golgi membrane protein is part of a GTPase-binding protein complex involved in vesicle targeting. Embo J. *19*, 4485–4492.

Matsuoka, K., Orci, L., Amherdt, M., Bednarek, S.Y., Hamamoto, S., Schekman, R., and Yeung, T. (1998). COPII-coated vesicle formation reconstituted with purified coat proteins and chemically defined liposomes. Cell *93*, 263–275.

Mazzarella, R.A., Srinivasan, M., Haugejorden, S.M., and Green, M. (1990). ERp72, an abundant luminal endoplasmic reticulum protein, contains three copies of the active site sequences of protein disulfide isomerase. J. Biol. Chem. *265*, 1094–1101.

Mellman, I., and Warren, G. (2000). The road taken: past and future foundations of membrane traffic. Cell *100*, 99–112.

Morin-Leisk, J., Saini, S.G., Meng, X., Makhov, A.M., Zhang, P., and Lee, T.H. (2011). An intramolecular salt bridge drives the soluble domain of GTP-bound atlastin into the postfusion conformation. The Journal of Cell Biology *195*, 605–615.

Munro, S., and Pelham, H.R. (1986). An Hsp70-like protein in the ER: identity with the 78 kd glucose-regulated protein and immunoglobulin heavy chain binding protein. Cell *46*, 291–300.

Nakano, A., and Muramatsu, M. (1989). A novel GTP-binding protein, Sar1p, is involved in transport from the endoplasmic reticulum to the Golgi apparatus. The Journal of Cell Biology *109*, 2677–2691.

Nakano, A., Brada, D., and Schekman, R. (1988). A membrane glycoprotein, Sec12p, required for protein transport from the endoplasmic reticulum to the Golgi apparatus in yeast. The Journal of Cell Biology *107*, 851–863.

Nickerson, P.A., and Curtis, J.C. (1969). Concentric whorls of rough endoplasmic reticulum in adrenocortical cells of the mongolian gerbil. The Journal of Cell Biology *40*, 859–862.

Ogata, M., Hino, S.-I., Saito, A., Morikawa, K., Kondo, S., Kanemoto, S., Murakami, T., Taniguchi, M., Tanii, I., Yoshinaga, K., et al. (2006). Autophagy is activated for cell survival after endoplasmic reticulum stress. Molecular and Cellular Biology *26*, 9220–9231.

Orso, G., Pendin, D., Liu, S., Tosetto, J., Moss, T.J., Faust, J.E., Micaroni, M., Egorova, A., Martinuzzi, A., McNew, J.A., et al. (2009). Homotypic fusion of ER membranes requires the dynamin-like GTPase atlastin. Nature *460*, 978–983.

Palade, G. (1975). Intracellular aspects of the process of protein synthesis. Science *189*, 347–358.

Pathre, P., Shome, K., Blumental-Perry, A., Bielli, A., Haney, C.J., Alber, S., Watkins, S.C., Romero, G., and Aridor, M. (2003). Activation of phospholipase D by the small GTPase Sar1p is required to support COPII assembly and ER export. Embo J. *22*, 4059–4069.

Pedrazzini, E., Villa, A., Longhi, R., Bulbarelli, A., and Borgese, N. (2000). Mechanism of residence of cytochrome b(5), a tail-anchored protein, in the endoplasmic reticulum. The Journal of Cell Biology *148*, 899–914.

Presley, J.F., Cole, N.B., Schroer, T.A., Hirschberg, K., Zaal, K.J., and Lippincott-Schwartz, J. (1997). ER-to-Golgi transport visualized in living cells. Nature *389*, 81–85.

Puri, S., and Linstedt, A.D. (2003). Capacity of the golgi apparatus for biogenesis from the endoplasmic reticulum. Mol. Biol. Cell *14*, 5011–5018.

Puthenveedu, M.A., and Linstedt, A.D. (2004). Gene replacement reveals that p115/SNARE interactions are essential for Golgi biogenesis. Proc. Natl. Acad. Sci. U.S.a. *101*, 1253–1256.

Rajasekaran, A.K., Morimoto, T., Hanzel, D.K., Rodriguez-Boulan, E., and Kreibich, G. (1993). Structural reorganization of the rough endoplasmic reticulum without size expansion accounts for dexamethasone-induced secretory activity in AR42J cells. Journal of Cell Science *105 (Pt 2)*, 333–345.

Rietsch, A., and Beckwith, J. (1998). The genetics of disulfide bond metabolism. Annu. Rev. Genet. *32*, 163–184.

Ron, D., and Walter, P. (2007). Signal integration in the endoplasmic reticulum unfolded protein response. Nat. Rev. Mol. Cell Biol. *8*, 519–529.

Rossi, D., Barone, V., Giacomello, E., Cusimano, V., and Sorrentino, V. (2008). The sarcoplasmic reticulum: an organized patchwork of specialized domains. Traffic *9*, 1044–1049.

Runz, H., Miura, K., Weiss, M., and Pepperkok, R. (2006). Sterols regulate ER-export dynamics of secretory cargo protein ts-O45-G. Embo J. *25*, 2953–2965.

Sato, K., and Nakano, A. (2004). Reconstitution of coat protein complex II (COPII) vesicle formation from cargo-reconstituted proteoliposomes reveals the potential role of GTP hydrolysis by Sar1p in protein sorting. J. Biol. Chem. *279*, 1330–1335.

Schirmer, E.C., and Gerace, L. (2005). The nuclear membrane proteome: extending the envelope. Trends Biochem. Sci. *30*, 551–558.

Schweizer, A., Fransen, J.A., Matter, K., Kreis, T.E., Ginsel, L., and Hauri, H.P. (1990). Identification of an intermediate compartment involved in protein transport from endoplasmic reticulum to Golgi apparatus. Eur. J. Cell Biol. *53*, 185–196.

Sengupta, D., Truschel, S., Bachert, C., and Linstedt, A.D. (2009). Organelle tethering by a homotypic PDZ interaction underlies formation of the Golgi membrane network. The Journal of Cell Biology *186*, 41–55.

Shibata, Y., Shemesh, T., Prinz, W.A., Palazzo, A.F., Kozlov, M.M., and Rapoport, T.A. (2010). Mechanisms determining the morphology of the peripheral ER. Cell *143*, 774–788.

Shibata, Y., Voeltz, G.K., and Rapoport, T.A. (2006). Rough sheets and smooth tubules. Cell *126*, 435–439.

Singer, I.I., Scott, S., Kazazis, D.M., and Huff, J.W. (1988). Lovastatin, an inhibitor of cholesterol synthesis, induces hydroxymethylglutaryl-coenzyme A reductase directly on membranes of expanded smooth endoplasmic reticulum in rat hepatocytes. Proc. Natl. Acad. Sci. U.S.a. *85*, 5264–5268.

Snapp, E.L., Hegde, R.S., Francolini, M., Lombardo, F., Colombo, S., Pedrazzini, E., Borgese, N., and Lippincott-Schwartz, J. (2003). Formation of stacked ER cisternae by low affinity protein interactions. The Journal of Cell Biology *163*, 257–269.

Soussan, L., Burakov, D., Daniels, M.P., Toister-Achituv, M., Porat, A., Yarden, Y., and Elazar, Z. (1999). ERG30, a VAP-33-related protein, functions in protein transport mediated by COPI vesicles. The Journal of Cell Biology *146*, 301–311.

Storrie, B., White, J., Röttger, S., Stelzer, E.H., Suganuma, T., and Nilsson, T. (1998). Recycling of golgi-resident glycosyltransferases through the ER reveals a novel pathway and provides an explanation for nocodazole-induced Golgi scattering. The Journal of Cell Biology *143*, 1505–1521.

Sun, Y., Shestakova, A., Hunt, L., Sehgal, S., Lupashin, V., and Storrie, B. (2007). Rab6 regulates both ZW10/RINT-1 and conserved oligomeric Golgi complex-dependent Golgi trafficking and homeostasis. Mol. Biol. Cell *18*, 4129–4142.

Takei, K., Mignery, G.A., Mugnaini, E., Südhof, T.C., and De Camilli, P. (1994). Inositol 1,4,5-trisphosphate receptor causes formation of ER cisternal stacks in transfected fibroblasts and in cerebellar Purkinje cells. Neuron *12*, 327–342.

Tang, B.L., Ong, Y.S., Huang, B., Wei, S., Wong, E.T., Qi, R., Horstmann, H., and Hong, W. (2001). A membrane protein enriched in endoplasmic reticulum exit sites interacts with COPII. J. Biol. Chem. *276*, 40008–40017.

Terasaki, M., Chen, L.B., and Fujiwara, K. (1986). Microtubules and the endoplasmic reticulum are highly interdependent structures. The Journal of Cell Biology *103*, 1557–1568.

Turner, D.L., and Weintraub, H. (1994). Expression of achaete-scute homolog 3 in Xenopus embryos converts ectodermal cells to a neural fate. Genes Dev. *8*, 1434–1447.

Voeltz, G.K., and Prinz, W.A. (2007). Sheets, ribbons and tubules - how organelles get their shape. Nat. Rev. Mol. Cell Biol. *8*, 258–264.

Voeltz, G.K., Prinz, W.A., Shibata, Y., Rist, J.M., and Rapoport, T.A. (2006). A Class of Membrane Proteins Shaping the Tubular Endoplasmic Reticulum. Cell *124*, 573–586.

Voeltz, G.K., Rolls, M.M., and Rapoport, T.A. (2002). Structural organization of the endoplasmic reticulum. EMBO Rep. *3*, 944–950.

Ward, T.H., Polishchuk, R.S., Caplan, S., Hirschberg, K., and Lippincott-Schwartz, J. (2001). Maintenance of Golgi structure and function depends on the integrity of ER export. The Journal of Cell Biology *155*, 557–570.

Waterman-Storer, C.M., and Salmon, E.D. (1998). Endoplasmic reticulum membrane tubules are distributed by microtubules in living cells using three distinct mechanisms. Current Biology *8*, 798–806.

Waterman-Storer, C.M., Gregory, J., Parsons, S.F., and Salmon, E.D. (1995). Membrane/microtubule tip attachment complexes (TACs) allow the assembly dynamics of plus ends to push and pull membranes into tubulovesicular networks in interphase Xenopus egg extracts. The Journal of Cell Biology *130*, 1161–1169.

Wiest, D.L., Burkhardt, J.K., Hester, S., Hortsch, M., Meyer, D.I., and Argon, Y. (1990). Membrane biogenesis during B cell differentiation: most endoplasmic reticulum proteins are expressed coordinately. The Journal of Cell Biology *110*, 1501–1511.

Yadav, S., Puri, S., and Linstedt, A.D. (2009). A primary role for Golgi positioning in directed secretion, cell polarity, and wound healing. Mol. Biol. Cell *20*, 1728–1736.

Yamamoto, A., Masaki, R., and Tashiro, Y. (1996). Formation of crystalloid endoplasmic reticulum in COS cells upon overexpression of microsomal aldehyde dehydrogenase by cDNA transfection. Journal of Cell Science *109 (Pt 7)*, 1727–1738.

Yang, X., Matern, H.T., and Gallwitz, D. (1998). Specific binding to a novel and essential Golgi membrane protein (Yip1p) functionally links the transport GTPases Ypt1p and Ypt31p. Embo J. *17*, 4954–4963.

Yoshida, Y., Suzuki, K., Yamamoto, A., Sakai, N., Bando, M., Tanimoto, K., Yamaguchi, Y., Sakaguchi, T., Akhter, H., Fujii, G., et al. (2008). YIPF5 and YIF1A recycle between the ER and the Golgi apparatus and are involved in the maintenance of the Golgi structure. Exp. Cell Res. *314*, 3427–3443.

Yoshihisa, T., Barlowe, C., and Schekman, R. (1993). Requirement for a GTPase-activating protein in vesicle budding from the endoplasmic reticulum. Science *259*, 1466–1468.

Zerial, M., and McBride, H. (2001). Rab proteins as membrane organizers. Nat. Rev. Mol. Cell Biol. *2*, 107–117.